Ph.D. Thesis

DURABILITY EVALUATION OF TEXTILE HANGING ROOFS MATERIALS

Krzysztof Żerdzicki

Supervisors:

Paweł Kłosowski, Professor	Gdańsk University of Technology
Krzysztof Woźnica, Professor	INSA Bourges

Gdańsk 2015

The important thing is not to stop questioning…

Albert Einstein

Acknowledgements

PhD research often seems a solitary experience. However, it is impossible to maintain the degree of focus and perseverance required for its completion without the help and support of many people.

First and foremost, I am extremely grateful to prof. Paweł Kłosowski and prof. Krzysztof Woźnica for being my supervisors and mentors. Without their constructive critique, recommendations and unconditional support this thesis would not have been the same. I would like to thank prof. Kłosowski for taking me as a PhD student and creating a space for my scientific growth at Gdańsk University of Technology. For me, you will always be an unattainable ideal of an enthusiastic researcher and a hard-working professional. Special thanks are addressed to prof. Krzysztof Woźnica for the warmly welcoming in Bourges and taking care of me during my temporary residence in France. I have truly benefited from our (sometimes) endless and frequently passionate scientific discussions. I am grateful for your patience, sense of humor and willingness to explain even the very basic issues.

I wish to express my deep gratitude for all the sponsors and financial supporters of my PhD research. Firstly, I would like to acknowledge the French Government that has funded my residence and studies in France through the Bourse du Gouvernement Français for the co-tutelle PhD students. Without this help it would not be possible for me to work with specialists from the PRISME laboratory and University of Orleans, that I consider a great honor. I would also greatly acknowledge the National Science Center, Poland (Grant No. UMO-2011/03/B/ST8/06500). The financial support of the Center has allowed me to design and construct a machine for creep tests that has been used in my research program. I would like to thank the Polish Ministry of Science and Higher Education for sponsoring this study through the scholarship for young Polish researches and PhD students aimed at their scientific and developmental work in the years 2011-2014. The obtained funds have helped me to fully equip my laboratory and to pay for my abroad conferences.

Last but not least, I would like to thank my family and friends for all their faith and support. Special thanks are addressed to my flatmate in Bourges – Paweł. Your advice on my thesis, everyday encouragement and company have really cheered me up in the last, but the toughest period of writing my dissertation. I am also grateful to many loyal friends in Poland and many new friends I have made in France and beyond.

Finally, I would express my deep gratitude to my parents for their love and support. They have given me a true background to develop my various interests and always served as a secure anchor during the hard and easy times. Thank you. I dedicate this work to you both.

Abstract

The durability of building materials has always played a crucial role in engineering design. It guarantees safe exploitation and long life of structures made by man. In the last century both domains the science and design capabilities have moved forward. Powerful computer facilities existing almost everywhere help engineers at each step of creating process, while the invention of new materials allows us to build more and more complicated constructions. One type of the composite materials that revolutionized civil engineering world are without doubts technical fabrics.

This thesis describes the investigation on durability of polyester reinforced PVC coated technical fabrics. It is composed of two main parts. For a start, durability of the roofing membranes materials has been evaluated by the comparative analysis of two differently treated examples of the same VALMEX textile fabric. The first one has been used for almost 20 years on the real construction of the Forest Opera in Sopot (Poland), while the second one from the same production part has been kept as a spare material for making small repairs during the service life of the canopy. Both kinds of architectural fabric have been tested towards their elastic, viscoelastic and finally viscoplastic properties. The constitutive relations of the non-linear piecewise elastic, the Burgers viscoelastic, and the Bodner-Partom viscoplastic models have been identified and compared. The obtained results have shown the very good performance of the material used outdoor and indicated that it could work satisfactorily for the next several years.

The second part of the thesis includes the evaluation of artificial ageing influence on polyester reinforced PVC coated technical fabrics. The AF9032 fabric has been tested here, as it has been planned to cover the new roofing structure of the Forest Opera after its reconstruction in 2010-2012. The accelerated ageing has been performed at elevated temperature of 80°C and 90°C in a thermal chamber for up to 12 weeks. After this thermal treatment, the fabric has been tested concerning its elastic and viscoplastic properties and subsequently the parameters of the non-linear piecewise elastic and the Bodner-Partom viscoplastic models have been found. Evolution of these parameters has shown that both proposed models can be used for the thermal ageing evaluation of polyester textiles.

Furthermore, the comparative analysis between the naturally aged VALMEX material from the first part and the artificially aged AF9032 fabric from the second part has been carried out. Some of the observed tendencies in the mechanical behavior of both aged materials have been similar. Consequently, it has been proven that the isothermal ageing is reasonable for the prediction of the long-lasting mechanical properties of polyester reinforced PVC coated membranes.

The additional contribution of this study is the set of constitutive relations found for naturally and artificially aged materials. The three different material models (nonlinear elastic, viscoelastic

and viscoplastic) have been fully identified. It has been intended, thereby, to give the parameters' basis for the numerical calculations of textile structures including ageing effects.

It should be noted that, although the research has the exploratory character, it can be easily extended to introduce the laboratory tested durability of technical fabrics into the numerical simulations of the civil engineering structures made of textiles.

Contents

Contents..... - 9 -

1 Introduction..... - 13 -

1.1 Foreword..... - 13 -

1.2 Aim and range..... - 13 -

1.3 Hanging roof structures..... - 15 -

1.3.1 The amphitheater of the Forest Opera in Sopot (Poland)..... - 18 -

2 Technical fabrics..... - 21 -

2.1 Structure of technical fabrics..... - 21 -

2.2 Numerical models of technical fabrics..... - 22 -

2.3 Laboratory testing methods..... - 25 -

2.4 Summary..... - 31 -

3 Theoretical background..... - 33 -

3.1 Durability and ageing of building materials..... - 33 -

3.2 Ageing of polymer materials..... - 40 -

3.2.1 Types of polymer ageing..... - 40 -

3.2.2 Description of artificial polymer ageing..... - 42 -

3.2.3 Ageing of PVC and PET materials..... - 47 -

3.3 Summary..... - 50 -

4 Material models for ageing analysis..... - 51 -

4.1 Introduction..... - 51 -

4.2 Piecewise linear model..... - 52 -

4.3 Viscoelastic Burgers model ..... - 53 -

4.3.1 Identification of the Burgers model parameters ..... - 54 -

4.4 Viscoplastic Bodner-Partom model ..... - 55 -

4.4.1 Identification of the Bodner-Partom model parameters ..... - 57 -

4.5 Summary ..... - 60 -

5 Experimental study ..... - 61 -

5.1 Introduction ..... - 61 -

5.2 Laboratory equipment ..... - 61 -

5.3 Samples and tests ..... - 63 -

5.4 Experiments ..... - 66 -

5.4.1 Influence of external environment ..... - 66 -

5.4.1.1 Uniaxial tensile tests ..... - 66 -

5.4.1.2 Biaxial tensile tests ..... - 67 -

5.4.1.3 Load-unload tensile cyclic tests ..... - 68 -

5.4.1.4 Creep tests ..... - 69 -

5.4.2 Artificial thermal ageing ..... - 70 -

5.5 Summary ..... - 72 -

6 Parameters determination and analysis ..... - 75 -

6.1 Introduction ..... - 75 -

6.2 Influence of outdoor environment ..... - 76 -

6.2.1 Strength parameters for uniaxial and biaxial tensile tests ..... - 76 -

6.2.2 Analysis of cyclic load-unload tests ..... - 78 -

6.2.3 Burgers model parameters - Creep tests ..... - 83 -

6.2.4 Bodner-Partom model parameters ..... - 89 -

6.2.4.1 Identification and verification ..... - 89 -

6.2.4.2 Sensitivity analysis of the Bodner-Partom model parameters ..... - 92 -

6.3 Influence of artificial thermal ageing - parameters for AF9032 fabric ..... - 95 -

6.3.1 Strength parameters (piecewise linear model) ..... - 95 -

6.3.2 Bodner-Partom model parameters ..... - 99 -

6.3.3 Arrhenius extrapolation ..... - 102 -

6.4 Summary ..... - 108 -

7 Final summary and conclusions ..... - 110 -

8 References ..... - 117 -

Equation Chapter (Next) Section 1

1 Introduction

1.1 Foreword

The architectural fabrics have surely revolutionized the engineering roofing world in the past three decades. The reinforced coated textile membranes are eagerly used as building materials due to their good strength properties, easy construction due to an off-site manufacturing, flexibility to obtain smooth shapes, low production costs and low weight. The development of cable membrane and tension structures have given architects an opportunity to cover larger areas and to design more sophisticated, aesthetic curvatures of roofing spaces. However, to fulfil still rising designing demands and to guarantee long-term, fully functional and repair free lifetime of a roof, the degradation over time of build-in materials must be taken into account. Here comes the issue of ageing and durability estimation of covering materials. Highly developed roofing membranes must exhibit satisfactory long-term durability towards climate and service stresses, which can be evaluated precisely only during the real-life outdoor exposure studies. However, well prepared accelerated ageing tests can shorten the time necessary for the answer on the foreseen life durability of the particular material and therefore allow one to start a construction assembly earlier. The artificial ageing experimental program should be accompanied by analytical and statistical studies of the carried out ageing. The presented work deals with a macroscopic method of the ageing evaluation of architectural fabrics. It focuses on the description of ageing process by following the parameters variations of constitutive formulations that have been identified for technical fabrics subjected to ageing process. A special attention is drawn to the viscoplastic model of Bodner-Partom, which makes the fabrics analysis under extreme loading conditions possible. Both outdoor and accelerated ageing conditions have been considered. The different experimental tests, model analyses and comparison studies give the field to discuss and to draw conclusions.

1.2 Aim and range

The main purposes of the following study may be summarized in the thesis of the presented dissertation:

The ageing process influences the parameters of constitutive equations identified for polyester reinforced PVC-coated fabrics.

For realization of the above statement the following scope of the work has been proposed:

- The literature review concerning the area of ageing phenomenon for building materials in general and for polymer composite materials particularly, different mathematical and laboratory approaches of ageing modelling, as well as the architectural fabrics structure’s constitutive modelling;

- Formulating and conducting the laboratory accelerated ageing program for selected technical fabrics;
- Creating and executing the research testing program incorporating the experiments on technical fabrics subjected to the natural outdoor ageing and laboratory accelerated ageing process. It should be mentioned that carried out experiments are necessary for the material parameters identification;
- Performing the identification of material parameters for the assumed constitutive models and the verification of the identification results;
- Comparing the obtained results and assessing the influence of different ageing methods on the mechanical properties of technical fabrics;
- The discussion of results and conclusions.

The framework of the presented study is organized into seven chapters, the reference list and 11 annexes.

In the Chapter 1 the literature overview is done and the aims of the research are stated. Firstly, the well-known hanging roof structures are presented and some examples of architectural fabrics used as covering materials are given. Among them, there is the amphitheater of the Forest Opera in Sopot roofed with VALMEX fabric, which forms the basis of this study.

Next, in the Chapter 2, the technical fabrics in the context of building materials are introduced. The composite structure and most common laboratory tests performed for the mechanical properties' identification of technical fabrics are described. The dense net model, which can be used for numerical calculations of hanging roofs structures, is presented in details.

The basic definitions concerning ageing and durability field are explained and the extended presentation of the ageing phenomenon for polymer materials is given in Chapter 3. The fundamental types of ageing are described there and some experimental, as well as mathematical methods necessary for their evaluation are specified. The actual field study of PVC roofing membranes is included in this section as well.

The material models used in this study for the behavior description of the technical fabrics subjected to ageing are presented in the Chapter 4. Mathematical foundations and identification procedures of these models are given in detail.

The Chapter 5 outlines experimental program realized for the purpose of the ageing evaluation. Then, each test is precisely described and some experimental results are presented and discussed.

The chapter 6 contains the selected models' parameters identification. A set of tables and the comparative graphs of the model parameters development give a field for discussion on the ageing phenomenon and the durability of architectural fabrics.

The final summary and conclusions are collected in the Chapter 7. Some comments, suggestions and new ideas for the further work are also specified there.

1.3 Hanging roof structures

According to Otto ([184]) "hanging roof" is a membrane stretched among immovable points, which acts simultaneously as a bearing and covering structure. The main bearing elements, such as steel cables are placed in the covering conveyors and carry tensile normal stresses only. They have negative Gauss curvature. The hanging roof structures are usually supported by some form of compression or bending elements, such as concrete rings, beams, arches or steel masts. The canopy, in turn, is made of wood panels, metal or concrete plates, fabric, foil, PVC, synthetic fluoropolymer, cotton, nylon (polyamide), polyester, aramid, glass or fiberglass.

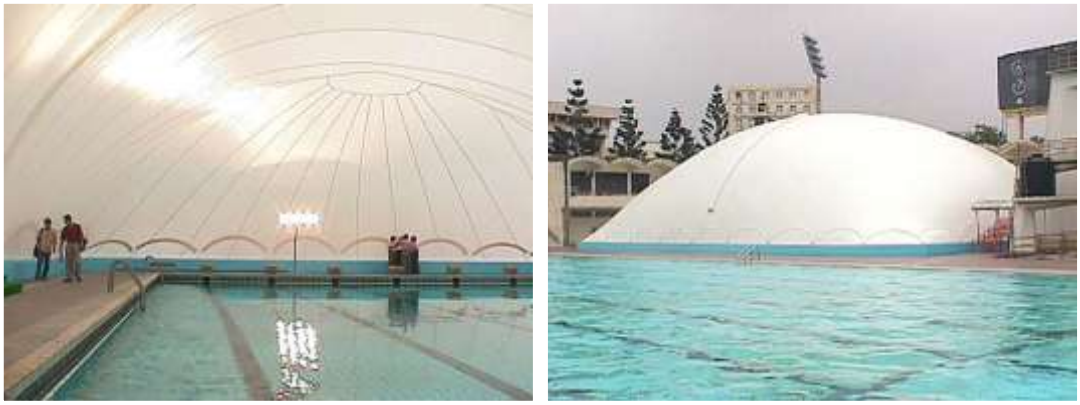

Fig. 1.1. Air dome, China ([109])

A special kind of hanging roofs are membrane structures, which are assumed as being one of the most impressive and demanding among engineering constructions ([152], [222]). They are usually constructed through one of two different techniques ([224]): as air-supported structures (Fig. 1.1) or as tensile cable-membrane structures (Fig. 1.2). The hanging roofs are characterized by geometric non-linearity, which is manifested by the change of the covering original configuration under an applied load. Reconfiguration of the shape is accompanied by the redistribution of the acting forces and occurrence of the wrinkles ([225]). To overcome this problem the form finding analysis must be performed and the initial tensioned configuration of the canopy established. The application of the high strength technical fabrics (reinforced by fibers mats) introduces also the material nonlinearity into the hanging roofs analysis, but allows designers to create various multi-curved forms and span large areas with ease. The membrane structures are used nowadays for covering sports stadiums, entertainments halls (Fig. 1.2), open-air theatres (Fig. 1.3), shopping malls, communication terminals, pavilions etc. (Fig. 1.5). Some advantages of the membrane structures are laid down in [139], where the authors mentioned of light dead weight of a membrane construction, effective usage of high strength materials, low

construction costs and really simple production (prefabrication) followed by the fast montage technology, without boarding or decks.

The biggest hanging roof structure, which has been built so far, is the Millennium Dome in Greenwich, in London, which has been constructed for the celebration of the third millennium beginning in the year 2000 (Fig. 1.2). It is more than one kilometre round and spans more than 80 000 m^2. The technical fabrics area of approximately 90 000 m^2 is supported by about 70 km of steel cables ([112]).

Fig. 1.2. Millennium Dome in London ([110])

Fig. 1.3. Open-air theatres: in Germany (left), in Australia (right) ([109])

The membrane hanging roof structures are becoming more and more popular, not only in large engineering constructions, but also in smaller cubature buildings, like car parks (Fig. 1.4), temporary shelters (Fig. 1.6) or decorative objects (Fig. 1.7). They give designers almost endless possibilities in forming and changing a canopy shape.

Fig. 1.4. Car park covers, UAE ([109])

Fig. 1.5. Cableway station, Malaysia ([109])

Fig. 1.6. Temporary roofing on the sport stadium ([109]) or on the beach ([109])

Fig. 1.7. Decorative and artistic applications of tensioned membranes ([109])

1.3.1 The amphitheater of the Forest Opera in Sopot (Poland)

The Forest Opera is an open-air amphitheatre located in a picturesque forest in Sopot (Poland) ([106]). It is considered as one of the most unique places of its kind and is known for having some of the best acoustic and pleasant surroundings. The official opening of the Forest Opera took place on 11th August 1909 with the show of Conradin Kreutzer's opera "The Night Camp in Granada". After the First World War the theatre won its fame resulting in the organisation of the Wagner festival annually and, then, the Forest Opera started to be called "the second Bayreuth".

Fig. 1.8. Performance of Richard Wagner's "Lohegrin" in 1937 ([106])

In the sixties the stage was, for the first time, covered with technical fabric made of stilon (cotton) fibres and became a home place for the International Song Festival. However, a lot of breakdowns and technical problems resulted in 1969 in rebuilding of the roof structure using TREVIRA fabric composed of polyester fibres coated with PVC. In 1990 the covering was changed for VALMEX fabric also comprising of the polyester fabric and PVC coating.

Fig. 1.9. The Forest Opera in Sopot with roof made of VALMEX fabric

At that time the roof structure was a temporary construction, not designed to carry the snow load, and had to be put down before the winter season and montaged up in the spring each year (Fig. 1.10). During the winter season it was stored under the scene of amphitheater. These actions repeated for many years resulted in the decrease of the roof technical condition and forced the Forest Opera operator to fix still uprising problems with the new covering structure.

Fig. 1.10. Putting down the roofing structure of the Forest Opera in Sopot (Poland) before winter season [81]

In 2009 it was decided to rebuild the whole theatre and set a permanent roof over the scene and the audience. Firstly, the AF9032 fabric (Shelter-Rite, Seaman Corporation) was planned to cover the canopy, but finally the technical fabric Sheerfill I, fabricated by Global Performance Plastics has been selected ([5]). The new structure has been equipped with a multi-task monitoring system, which registers the weather conditions and displacements of the canopy. It allows engineers to follow the changes in the shape of the hanging roof and warns in case of dangerous situations.

Fig. 1.11. The new Forest Opera in Sopot

Although the roof construction has only 2 years, it has not overcome some technical problems. Firstly, during assembly due to exceeded tension, a tear has arisen resulting in dangerous failure in one subpanel of the canopy (Fig. 1.12). The over tension state has probably been induced by wrong installation and by service forces acting on the roof, like wind blow. Besides, after some time, the shackles that join architectural fabric with steel bearing lines had to be replaced by shorter ones due to wrongly calculated compensation of the material in the fill direction. Now, the new monitoring system secures the structure constantly, nevertheless, some additional precautions should be taken. That is the main reason to perform the tests of accelerated ageing

and to evaluate the future behavior of technical fabrics used for large-scale engineering constructions.

Fig. 1.12. Some of the problems with the new canopy covering: tear propagation (left) and a need to change joining shackles (right)

2 Technical fabrics

2.1 Structure of technical fabrics

Architectural fabrics are also known as coated textile membranes, technical fabrics or roofing membranes. They are often montaged as wall coverings or roof structures over large size public gatherings places and for that reason, the durability evaluation of technical fabrics should include not only typical static or dynamic analysis but also the long-lasting creep/relaxation tests and research on ageing of the material.

Architectural fabrics generally consist of the following components ([215]):

- base fabric as reinforcement (e.g. polyester, carbon or glass fiber yarns; more rarely cotton, wool, nylon, polyamide or aramid fiber yarns [104]),
- adhesive coat (e.g. polyurethane),
- exterior coating (e.g. polyvinyl chloride - PVC, polytetrafluoroethylene – PTFE, ethylene propylene diene monomer rubber - EPDM, thermoplastic polyolefin – TPO, silicone [196], [33]),
- top coating (e.g. polyvinylidene fluoride - PVDF, titanium dioxide - TiO2 or polyvinyl fluoride - PVF).

Nowadays, the most common commercially available combinations are PVC-coated polyester fabrics, PTFE-coated glass fiber fabrics and silicone-coated glass fiber fabrics ([196]).

The structure of standard reinforced coated fabric is presented in Fig. 2.1. The base fabric can be produced in two ways giving woven or knitted fabrics. Typical weave patterns include plain, 2/2 twill, leno, mock leno, panama, 4H satin and 8H satin, while knitting patterns contain mainly the warp-knit fill inserted method and raschel knit [2].

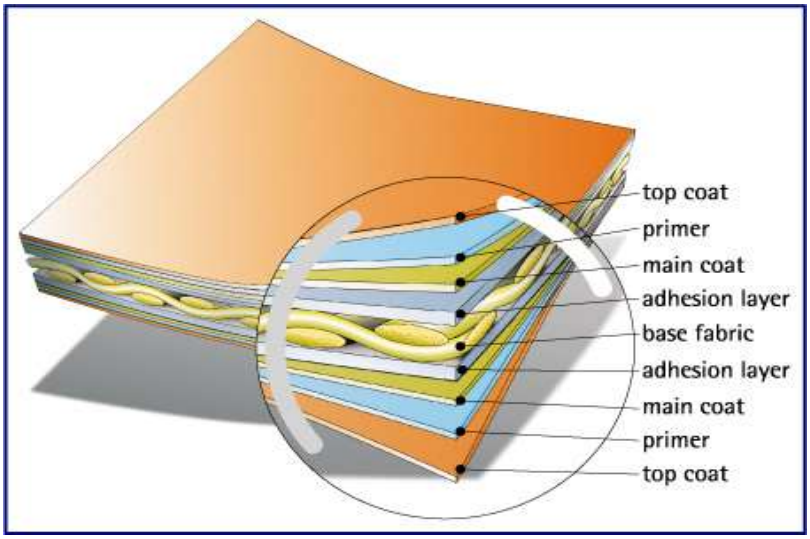

Fig. 2.1. Structure of reinforced coated fabric [172]

The fiber yarns are responsible for the tensile strength of the material, while exterior coating protects yarns from damage, stabilizes weave structure, as well as provides water resistance and shear stiffness. The right level of adhesion guarantees cooperation between the base fabric and coating and, therefore, affects coating delamination, seam strength and tear strength of composite material ([215]). To increase resistance against dirt, biological organisms, UV radiation and to protect surface against degradation special thin films of various compounds are more often introduced forming the top coating of technical fabrics ([196]).

The geometric non-linearity of the twisted fiber structure, complex interactions of orthogonal yarns under the bi-axial in plane stress state (friction, crimp interchange, locking effect) and influence of coating result in the time-dependent, hysteretic and anisotropic material behavior of technical fabrics [49]. Due to these facts, the base fabric threads and exterior coating are most often taken into the mechanical analysis of technical fabrics. The study becomes even more sophisticated when one takes into account the ageing effects. To investigate such behavior and to build the numerical model of textile fabrics performance a set of special laboratory tests as well as numerical simulations are necessary.

2.2 Numerical models of technical fabrics

The coated fabrics mechanical behavior analysis can be carried out at three levels of accuracy ([149]): at macro-, meso- and micro-level. Therefore, the methods used in the finite element modelling of technical fabrics can be divided into the following groups:

- homogenization of the meso-structure behavior and the approximation of the fabric material as an anisotropic continuum with two (or more) preferred material directions ([218], [248], [93], [195]). This concept allows greater computational efficiency and can be straightforwardly integrated into multicomponent, complex system models. However, the identification process of the homogenized parameters is usually difficult.
- mesostructurally based analytical models, which can predict fabric components (yarns, coating) in the specific modes of deformation. These models usually take into account interaction between the warp and fill threads, like friction, crimp interchange and locking effect ([187], [136], [138], [137], [135])
- discrete modelling of each yarn microstructure in the woven material. It results in a very precise description of all mechanisms following fabric deformation ([179], [43], [218]).

A comprehensive summary of fabric models and their development is given in e.g. [10] and [141]. The discrete models and over-detailed continuum approaches require large computational capabilities and are time-consuming. They are not suitable for calculations of large civil

constructions, like roof structures or building facades made of textiles ([141], [248]). Therefore, the homogenized continuum models with the basic comprehension of the meso-structure processes are adequate for civil engineering purpose ([47], [248]). One of them is the dense net model. It has been proposed by Branicki [46] and then extended by Branicki and Kłosowski ([47]), and Kłosowski and Ambroziak ([6]). The model is based on the following assumptions:

- the threads of the fabric work in the uniaxial tensile state,
- for kinematic stability of the woven structure, the initial tension can be put in the threads,
- the force in the particular family of threads depends on the strains in the same family only,
- the influence of the coating is neglected (in the basic formulation),
- the angle between threads families can change during the deformation process.

According to the above assumptions the fabric yarns work in the uniaxial tensile state (the yarns are defined as isotropic separately in the warp and fill direction), while the whole fabric is anisotropic (Fig. 2.2).

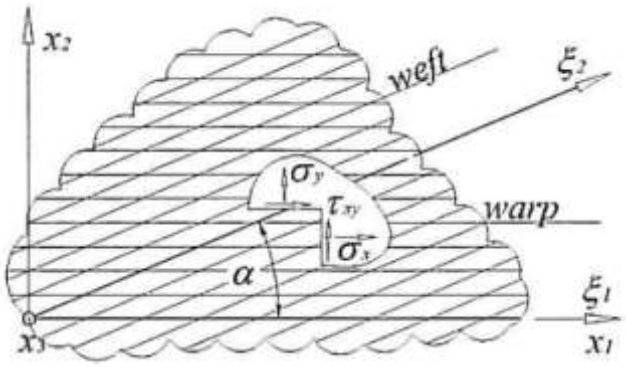

Fig. 2.2. The dense net model [9]

It is assumed, that there is the current coordinate system of threads' families $\left(\xi_j,\ j=1,\ 2\right)$ and the local Cartesian coordinate system of the finite element $\left(x_i,\ \mathrm{i}=1,\ 2\right)$ in the plane stress state. The family threads direction ξ_1 is parallel to axis x_1 of the local Cartesian coordinate system in the current configuration, while the angle between both family thread directions $(\xi_1,\ \xi_2)$ is defined as α. Therefore, the strains $\boldsymbol{\varepsilon}_{\xi}\left(\varepsilon_{\xi_1},\varepsilon_{\xi_2}\right)$ in the direction of threads family ξ_j are expressed by the components of strains in the plane stress state $\boldsymbol{\varepsilon}_x\left(\varepsilon_{x_1},\ \varepsilon_{x_2},\ \gamma_{x_1x_2}\right)$ as follows:

$$\boldsymbol{\varepsilon}_{\xi}=\begin{pmatrix}\varepsilon_{\xi_1}\\ \varepsilon_{\xi_2}\end{pmatrix}=\begin{bmatrix}1 & 0 & 0\\ \cos^2\alpha & \sin^2\alpha & \sin\alpha\cos\alpha\end{bmatrix}\begin{Bmatrix}\varepsilon_{x_1}\\ \varepsilon_{x_1}\\ \gamma_{x_1x_2}\end{Bmatrix}=\mathbf{T}_{x\xi}\boldsymbol{\varepsilon}_x \tag{2.1}$$

As each thread family's stress depends on these family strains only, it is possible to write:

$$\sigma_{\xi} = \begin{Bmatrix} \sigma_{\xi_1} \\ \sigma_{\xi_2} \end{Bmatrix} = \begin{bmatrix} F_1(\xi_1) & 0 \\ 0 & F_2(\xi_2) \end{bmatrix} \begin{Bmatrix} \varepsilon_{\xi_1} \\ \varepsilon_{\xi_2} \end{Bmatrix} = \mathbf{F}\boldsymbol{\varepsilon}_{\xi}, \tag{2.2}$$

where $F_1(\xi_1)$, $F_2(\xi_2)$ are the uniaxial constitutive relations for the warp and fill (marked as weft in Fig. 2.2) direction, respectively. Simple elastic equations, determined from the uniaxial tensile tests, as well as non-linear elastic formulas can be here applied. Rheological effects can also be taken into account when the viscoplastic or viscoelastic forms of uniaxial constitutive equations are used.

From the stress equilibrium equations for basic element of size dx_1, dx_2, the expression for stress components in the plane stress state can be specified as:

$$\boldsymbol{\sigma}_x = \begin{Bmatrix} \sigma_{x_1} \\ \sigma_{x_2} \\ \tau_{x_1x_2} \end{Bmatrix} = \begin{bmatrix} 1 & \cos^2\alpha \\ 0 & \sin^2\alpha \\ 0 & \sin\alpha\cos\alpha \end{bmatrix} \begin{Bmatrix} \sigma_{\xi_1} \\ \sigma_{\xi_2} \end{Bmatrix} = \left(\mathbf{T}_{x\xi}\right)^{\mathrm{T}} \boldsymbol{\sigma}_{\xi} \tag{2.3}$$

Thus, the relation between membrane stresses $\boldsymbol{\sigma}_x$ and strains $\boldsymbol{\varepsilon}_x$ is defined as follows:

$$\boldsymbol{\sigma}_x = \left(\mathbf{T}_{x\xi}\right)^{\mathrm{T}} \mathbf{F}\mathbf{T}_{x\xi}\boldsymbol{\varepsilon}_x = \mathbf{D}_x\boldsymbol{\varepsilon}_x, \tag{2.4}$$

where the elastic matrix $\mathbf{D}_x$ can be written as follows:

$$\mathbf{D}_x = \begin{bmatrix} F_1 + F_2\cos^4\alpha & F_2\sin^2\alpha\cos^2\alpha & F_2\sin\alpha\cos^3\alpha \\ F_2\sin^2\alpha\cos^2\alpha & F_2\sin^4\alpha & F_2\sin^3\alpha\cos\alpha \\ F_2\sin\alpha\cos^3\alpha & F_2\sin^3\alpha\cos\alpha & F_2\sin^2\alpha\cos^2\alpha \end{bmatrix} \tag{2.5}$$

It is assumed that the angle α is constant at particular step of deformation and in a whole finite element, but it can change during deformation. It can be calculated from the formula:

$$\alpha = \operatorname{arctg}\frac{\sigma_{x_2}}{\tau_{x_1x_2}} \tag{2.6}$$

However, the initial value of the angle α must be indicated and is usually provided by manufacturers as a result of weaving technology between the warp and fill threads. In most cases of technical fabrics it is usually set at $\alpha_0 = 90°$.

A more extended variant of the dense net model includes also coating influence ([6]). The technical fabric is assumed then, to be composed of the base woven layer that is symmetrically sandwiched by plastic coating films of small uniform thickness ${}_c t/2$. A woven layer is represented by classical dense net model, whereas the behavior of the coating layers is described by the isotropic material model. In membrane structures, the components of strain tensor $\boldsymbol{\varepsilon}$ do not change values along the thickness. Therefore, the membrane forces in coating layer ${}_c\boldsymbol{\sigma}$ and in the woven layer ${}_n\boldsymbol{\sigma}$ are expressed by separate constitutive equations of the same strains ε:

$$\begin{aligned} {}_c\boldsymbol{\sigma} &= \mathbf{D}_c\varepsilon \\ {}_n\boldsymbol{\sigma} &= \mathbf{D}_x\varepsilon \end{aligned}, \tag{2.7}$$

where $\mathbf{D}_c$ and $\mathbf{D}_x$ are the elasticity matrices for the coating layer and woven fabric, respectively. It is proposed by the authors ([142], [144]) that the elasticity matrix for technical fabric in this model is defined as:

$$\mathbf{D} = {}_c\chi\mathbf{D}_c + {}_n\chi\mathbf{D}_n, \tag{2.8}$$

where ${}_c\chi$ and ${}_n\chi$ are the individual layer's thickness influence parameters, which should also be identified from laboratory tests or estimated by thickness of the particular layers. Consequently, the explicit formulation of the elastic matrix takes the following form:

$$\begin{aligned}\mathbf{D} &= {}_c\chi\mathbf{D}_c + {}_n\chi\mathbf{D}_n = \\ &= \frac{{}_c\chi\,{}_cE}{1-{}_c\nu^2}\begin{bmatrix} 1 & {}_c\nu & 0 \\ {}_c\nu & 1 & 0 \\ 0 & 0 & \dfrac{1-{}_c\nu}{2} \end{bmatrix} + {}_n\chi\begin{bmatrix} E_1+E_2\cos^4\alpha & E_2\sin^2\alpha\cos^2\alpha & E_2\sin\alpha\cos^3\alpha \\ E_2\sin^2\alpha\cos^2\alpha & E_2\sin^4\alpha & E_2\sin^3\alpha\cos\alpha \\ E_2\sin\alpha\cos^3\alpha & E_2\sin^3\alpha\cos\alpha & E_2\sin^2\alpha\cos^2\alpha \end{bmatrix},\end{aligned} \tag{2.9}$$

where ${}_cE$, ${}_c\nu$ are the elastic modulus and Poisson's coefficient for the coating layer, respectively; E_1, E_2 are the elastic moduli identified from laboratory experiments on the warp and fill threads respectively, without the presence of coating; α is the angle between two threads families.

The dense net model allows the use of the different types of constitutive equations describing threads behavior. The model's authors and their co-workers have performed laboratory experiments and identified parameters for several types of technical fabrics accounting for various kinds of constitutive formulations. These have included non-linear elastic piecewise model ([10]), two viscoplastic approaches (Bodner-Partom [144] and Chaboche [146] law) and viscoelastic approach based on the Schapery nonlinear model with two types of transient creep components ([142]). Then, the dense net model with above constitutive relations has been implemented for numerical calculations of different hanging roof structures giving satisfactory results. These results have later been used for designing and engineering of e.g. the Forest Opera in Sopot ([5]).

2.3 Laboratory testing methods

In order to better understand the mechanical performance of architectural fabrics as building materials a set of experimental tests is necessary. Some of the fabrics properties are similar to those of convectional building materials, but most of them are unique due to the flexible nature of fabrics.

The basic mechanical property of all building materials is the tensile strength of a material and its elongation. For technical fabrics two methods of testing tensile strength are recognized: the cut strip test and the grab test. In the first one, material strips of particular width equal to or lower than the width of machine grips are used (Fig. 2.3a). In the grab test, the width of a sample material is far beyond the grips' size (Fig. 2.3b). The test is usually performed with constant

movement of grips, once at the normal environment and then in the elevated humidity conditions. The precise dimensions of samples and grips and other experiment requirements are defined in the national standards, e.g. European EN ISO 13934 ([117]) or American ASTM D-751([24]).

Fig. 2.3. Uniaxial tensile tests of technical fabrics (Gdansk University of Technology): (a) cut strip method; (b) grab test method

Uniaxial tests deliver information about the tensile properties of a material. If one wants to predict a material long-lasting performance the long-term rheological tests are required. There are no standards defining such experiments, but the most widespread approach is to conduct creep and/or relaxation tests depending on the material type loading in a real construction. The creep tests consists in putting particular level of stress to a strip sample and record its elongation for prolonged time, e.g. for several weeks or even months. The examples of creep tests and identification procedure of viscoelastic properties of technical fabrics are presented in [142] and [144].

Biaxial and shear behavior are of the key importance for multidirectional tensioned membrane structures. However, there are no standard requirements in these issues up to now, hence most of producers and designers have developed their own test methods. The most popular biaxial tests are carried out on the cruciform or T-shape samples presented in Fig. 2.4. It is a common practice to perform such tests with different load ratios in perpendicular direction of the warp and fill threads of a fabric. The example of the results obtained by this method is presented in Fig. 2.5. To better catch biaxial properties also biaxial cyclic test becomes more and more widespread approach ([9], [181], [65]).

Shear properties are commonly identified in two ways: the bias test or the picture-frame test. In the bias test a strip specimen is cut at the angle of 45° to warp (fill) direction and then the test is performed likewise the uniaxial tensile strip test. The idea is that if the sample length is at least two times greater than its width, there will be area in the sample that undergoes pure shear effect. The bias test and the particular areas in the sample are shown in Fig. 2.6.

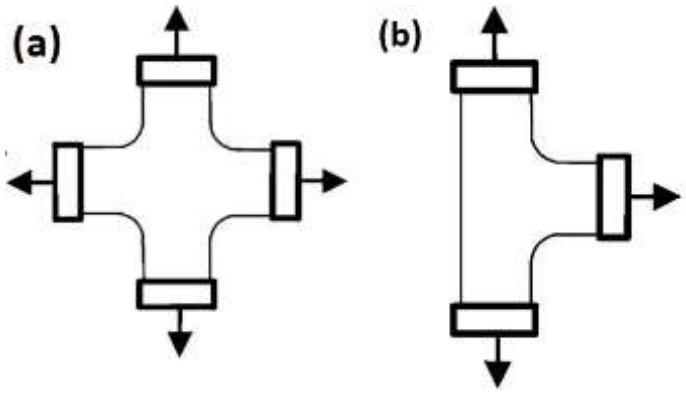

Fig. 2.4. Shape sample used in biaxial tests: (a) cruciform sample; (b) T-shape sample ([9])

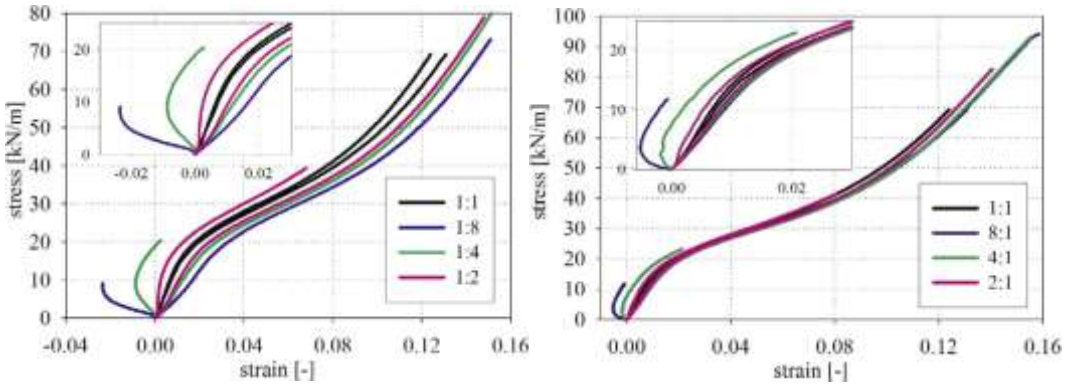

Fig. 2.5.Material response of Precontraint 1202S fabric to biaxial loading with various warp/fill ratios [12] (fill direction – left; warp direction right)

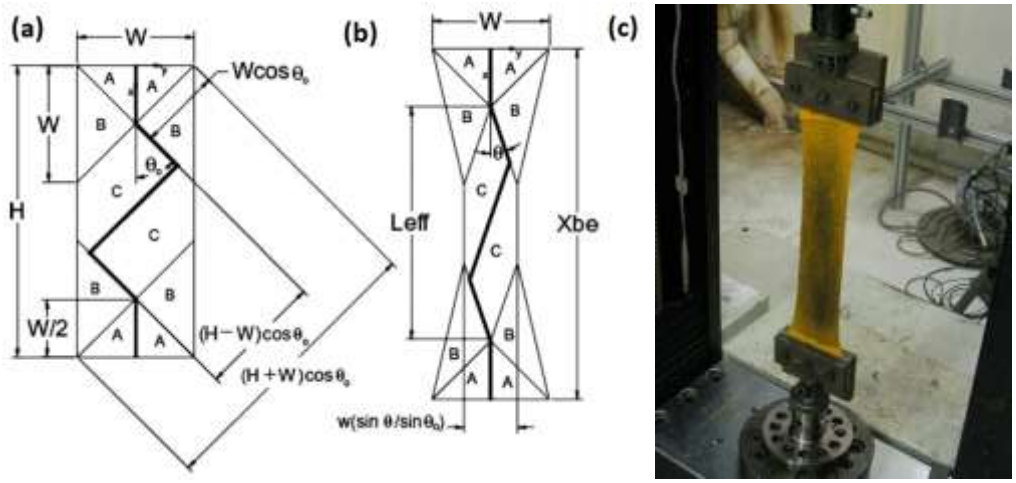

Fig. 2.6. The bias-extension test (PRISME Laboratory at University of Orléans): (a) initial fabric specimen geometry with assumed zones; (b) fabric specimen during the test (zone C – perfect pure shear) ([57]); (c) experimental stand

For the purpose of the picture frame test a special steel device is necessary. It has a shape of square with four pin joints in the corners. It is assembled in the uniaxial strength machine. A force

is applied through diagonally opposing corners of the picture frame causing the device to move from an initially square configuration into a rhomboid one (Fig. 2.7). As a result, the specimen within the picture frame is hypothetically subjected to pure shear forces.

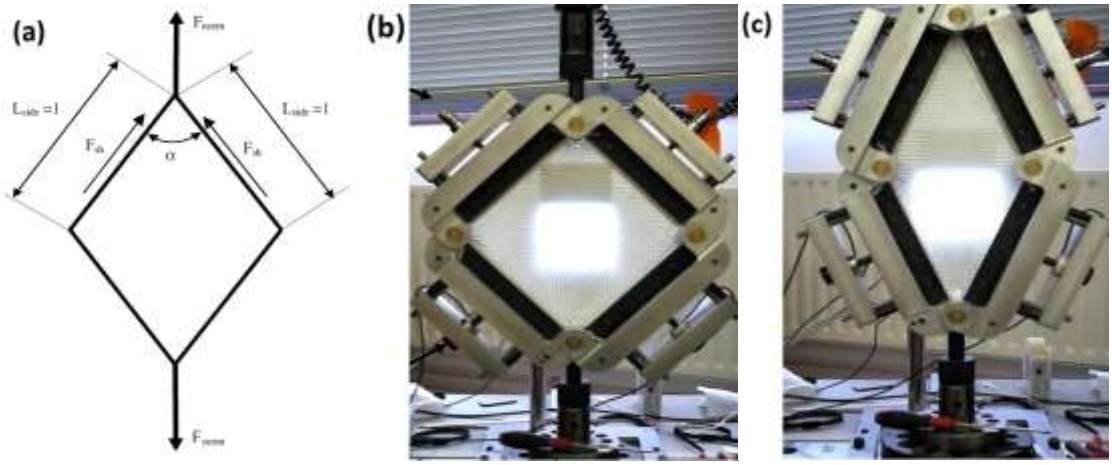

Fig. 2.7. Picture frame test (PRISME Laboratory at University of Orléans): (a) schematic geometry; (b) specimen before the test; (c) specimen during the test ([158])

The following significant feature of architectural fabrics is their tear resistance. It becomes very important when a tensile cable membrane structure get punctured or when there is loss in air pressure in an air supported structure. The problem of this type has occurred on the new roof structure of the Forest Opera in Sopot (see Fig. 1.12). The ASTM standard includes two types of tear tests: the tongue tear method ([24]) and the trapezoid tear method ([22]), while in ISO 13937 there are three tear test types ([119]): the trouser-shaped (Fig. 2.8a), wing-shaped (Fig. 2.8b) and tongue-shaped test (Fig. 2.8c). The concept of all these tests is to prepare a sample (of different shapes indicated in the name of a test) with initial crack or even long cut at which a tear propagation is assumed to start. Then, the uniaxial testing machine is used to introduce tear force.

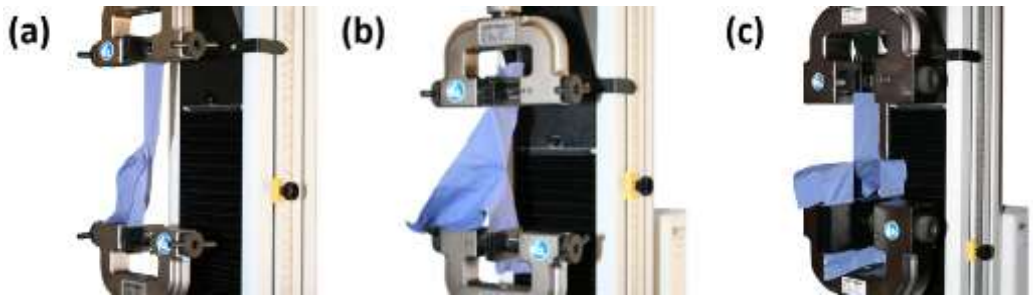

Fig. 2.8. Tear force test according to ISO 13937: (a) trouser-shaped test; (b) wing-shaped test; (c) tongue shape test ([108])

One of the greatest advantages of the PVC polyester coated fabrics is their ability to be welded into large panels. Consequently, a seam that joins two pieces of fabric must have tensile and shear strength at least equal to the bonded pieces of fabric. In the ISO 13935 standard ([118]) the seam

strength tests are very similar to those of uniaxial testing, as there are the cut strip test as well as the grab test. The main difference is a specimen structure that for seam testing is composed of two pieces of fabric welded or glued together. The ASTM D751 ([24]) standard named such test as the peel adhesion test. Additionally, seam tests give the information about the quality of adhesive layer, bonds between fabric and coating layers and finally the correctness of welding process (e.g. the verification of welding temperature).

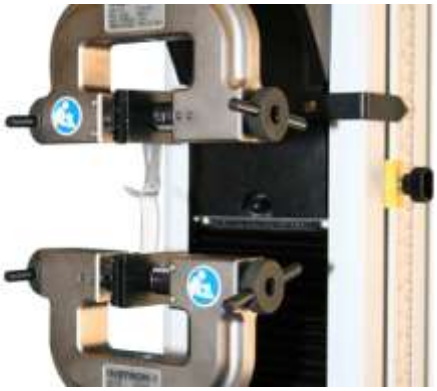

Fig. 2.9. Seam test of two fabric pieces welded together ([108])

The flexibility is a unique membrane property, particularly during the installation phase and a roof maintenance. The flexibility of all types of roofing membranes drops with temperature. For instance, according to the Swiss standard SIA 280 ([219]), flexibility is tested on rectangular samples that are cooled down to a particular temperature and then quickly pressed together so that specimens are bent to a radius of 5mm. The lowest temperature at which no breaks or cracks are observed is recorded.

The flexibility in PVC coated fabrics is guaranteed by the amount and quality of plasticizers and stabilizers that are blended with PVC rigid resin during manufacturing. Plasticizers make up to 35% of the total fabric mass. Thus, it is often desirable to know how fast plasticizers and different additives migrate out or are lost during service. The various methods to evaluate such processes have been widely studied. The Fourier transform infrared (FTIR) spectroscopy allows following the depletion of particular chemical compounds in polymeric materials ([129], [200]), as well as changes of their surface composition ([101], [159]). The Gas Chromatography Mass Spectrometry (GCMS) is used to identify and quantify low molecular weight degradation products, which can migrate from material to the environment ([101], [251]). Concentration of plasticizers, stabilizers and different fillers used in polymers can be determined by the following methods: thermo-gravimetric analysis (TGA) ([129], [251], [99]), supercritical extraction (SFE) ([251], [129]), direct UV spectrophotometry ([99]) and other residual stability methods.

The wheatherability is an ability to resist changes in appearance and function of the exposed surfaces of architectural fabrics. It refers to, for example, retention of color and gloss, chalking, blistering, peeling, flaking and cracking of material. Dirt and air pollution deposition, as well as

microorganisms growth or self-clean ability upon raining falls are also within definition of whetherability. These factors may influence not only the mechanical strength of a fabric, but more importantly its aesthetic worthiness. Therefore, a lot of dedicated tests have been developed over the years for analyzing weatherability. Evaluation of color change is usually measured by spectrocolorimeter ([45]). Transmittance, absorbance and light reflectance is tested by UV-VIS-NIR spectrophotometry, FTIR spectroscopy, direct and diffuse reflected radiation or atomic absorption spectroscopy ([221], [130], [33], [200], [246]). Surface performance is firstly visually studied by low magnification microscopes ([196], [246]), then more precisely by scanning electron microscopes (SEM) ([196]) or transmission electron microscope (TEM) ([130]). If more comprehensive analysis is required the following methods and devices can be introduced: atomic force microscope (AFM), X-ray photoelectron spectroscopy (XPS), fluorescence spectroscopy or Raman spectroscopy ([130]).

Influence of hail hitting the fabrics surface is commonly identified by tests very similar to dynamic puncture, or impact velocity methods ([31], [150], [86], [69], [192]). Generally, the material surface is cooled down with ice and then shot by test projectiles made of polyamide or steel with certain velocity ([219], [20]). Then, the test of watertightness is performed and if there is no leakage the shooting procedure is repeated with higher velocity. The greatest impact velocity not causing leakage is reported.

The dimensional stability characterizes the phenomenon of changing size of a material due to alteration in temperature or humidity. These variations are very important for designing tension membrane structures as fabric patterns are cut before the construction assembly to a given size. There is no specific standards for testing architectural fabrics for dimensional stability, but standards used for e.g. rubber or thermoplastic materials are usually adopted (e.g. ASTM D1204 [19]). All these tests comprise of measuring very precisely the dimensions of the sample before and after maintaining it at different conditions for a short period of time. The scale of observed change is then evaluated.

The water absorption characterizes the level of material wicking. It is tested by drying fabric in an oven for a specific time and then leaving it in a dessicator until it reaches its thermal equilibrium. After that, the material is weighted and then immersed in water for 24 hours at the temperature of 23°C ([23]). Afterwards, it is patted dry with a lint free cloth and weighted again. The water absorption is calculated as an increase in weight percent.

The tests presented above are focused on the strength and stability properties of technical fabrics and are necessary for engineering and designing purposes. Nevertheless, there are several additional features of fabrics that should also be taken into account. One of them is flame resistance. It is mainly tested by measuring time necessary for the self-extinguishing (cessation of glowing or flaming) of a material after exposure to flame, the registration of flame spread with smoke development and melt dripping of a burned material ([233]).

More details of testing technical fabrics can be found in review articles (e.g. [9], [215]).

2.4 Summary

In this chapter the characteristics of technical fabrics have been described. These include composite structure of architectural fabrics and most commonly performed laboratory experiments for identification of fabrics mechanical properties. Special attention has been paid to the dense net material model, which allows the use of the different types of constitutive equations describing threads behavior of technical fabrics. It has been successfully implemented for numerical calculations of different hanging roof structures before (including the forest Opera in Sopot).

3 Theoretical background

3.1 Durability and ageing of building materials

The durability of a material is the potential to maintain its original properties over time ([174]). A durable material is one which can resist erosion coming from various media during its service life ([55]). Building materials are subjected to two types of influence: external environmental conditions and mechanical stresses. Factors coming from the environment are shown in Fig. 3.1 and can be divided into three groups:

- weather factors, including high-low temperature cycles, freeze-and-thaw changes, humidity, UV radiation etc.;
- chemically active particles e.g. oxygen, acid, alkali or salt aqueous solutions causing destruction of material chemical composition (e.g. corrosion of steel, concrete);
- biological acting of fungi, alga and microorgnisms which can molder or rot materials (e.g. decomposition of wood).

Mechanical stresses can be initiated either naturally (e.g. wind blow) or during the service of a material (e.g. during a construction assembly). High stresses cause cracking, delamination and an increase of porosity (e.g. delamination of composite panels).

Overall impact on building materials is obviously a synergic action of all (or of some of) the above components. Owing to various chemical composition and other characteristics, particular materials have different kinds of durability. For instance, stone, concrete, mortar, clay bricks struggle frost, wind, carbonization and wet-and-dry change. Steel is known to exhibit rusting (the formation of iron oxides), while organic materials (asphalt, plastic, rubber) may be destructed by physical ageing ([55], [76]).

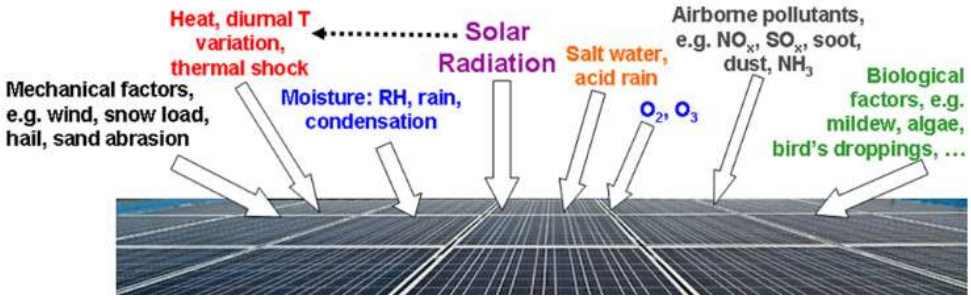

Fig. 3.1. Environmental factors influencing materials used outdoors ([100])

Reliability is a measure of unexpected interruptions during predicted service time of a product ([100]). This engineering discipline uses methods drawn mainly from probability statistics and the theory of stochastic processes. Reliability is assessed in terms of failure rates, cumulative failures, component lifetimes and estimates of product lifetimes. On the contrary, durability takes in the failure mechanisms, kinetics of change or simply the degree of material modification.

Summing up, reliability of a system can be defined as the function of durabilities of its inherent components. Fig. 3.2 illustrates the basic difference between reliability and durability.

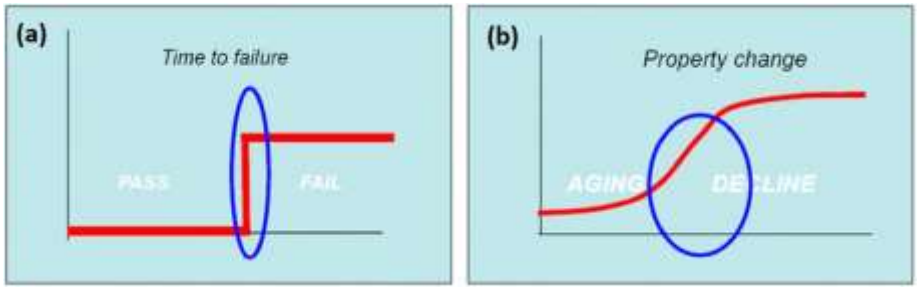

Fig. 3.2. Comparison of reliability (a) and durability (b) criteria ([100])

The service life of a material is defined as the time until replacement of the built-in material is obligatory or when its service function comes to the end (due to, for instance, collapse of the whole building [174]). It is a bit different from the life cycle of a material, which is specified by the ISO-EN-UNE-14.040 standard ([120]) as time spanned from a material acquisition (or generation of natural resources) till its final elimination. As a consequence, the truly durable material should be useful for the period longer than predicted service life. It is closely related to the more and more desirable and important characteristic that is sustainability. In essence, sustainability concerns the endurance of systems and processes remaining diverse, productive and in accordance with the environment. Sustainability in civil engineering demands the usage of renewable energy resources, renewable materials and recycled materials from construction waste as well as an increase in new materials durability and conservation of existing buildings, all with respect to local environment and its natural properties ([174], [77]).

To improve durability of building materials, their ageing process has to be monitored. The term “ageing” is commonly recognized as the phenomenon causing changes (generally unfavorable) of material properties over passing time ([64]). It is usually a complex phenomenon influenced by a lot of physical, chemical, biological and mechanical factors lasting for seconds, days or even years. However, when a new material is designed, there is no time for analyzing its natural ageing process. Instead, the accelerated methods of the ageing process are incorporated to evaluate material durability. They will never give the perfect answer about material’s future behavior, but are still worthwhile and give information of material performance under different ageing conditions ([88]).

To predict the long lasting behavior of materials the various techniques of ageing initiation and acceleration may be introduced. The main point is that artificially established circumstances should reflect as close as possible the environmental and service conditions of a particular material. For example, in the case of naval structures, hydrothermal treatment (combining different temperature level with immersion in natural or synthetic water sea solution) is the sufficient simulation of ageing ([98], [97], [159], [71]), while for electrical cables insulations the

high voltage-stresses must be taken into account ([14],[48]). Another interesting example of accelerated ageing is presented in [238], where Wei et al. checked dynamic properties of rubbers aged at high temperature and simultaneously pre-strained. Ageing by subjecting a material to different stresses in a cyclic sequence (e.g. UV radiation, high/low temperature, salt spray) appears to be the most functional test. Cyclic ageing has been practiced for example by Deflorian et al. [73] on organic coated galvanized steel or by Jakubowicz [128] on commercial PVC. As a result, if classifying various methods of ageing the following techniques of ageing are commonly recognized ([53]): natural ageing (weathering), accelerated natural ageing and artificially (laboratory) accelerated ageing.

Weathering is a phenomenon that every material used outdoor is subjected to ([130], [196]). It includes each aspect of environment influence, but without any service stresses. The stresses can be generated e.g. by wind or hail, but are still a part of natural loading. An example of weathering test is presented in Fig. 3.3. This type of test, however, does not speed up the ageing process at all and therefore can be used in a very limited range for the prediction of a long time material performance. However, if a roofing material is set up on the real structure and undergoes natural weathering test at the same time, its condition can be monitored without taking samples from a building that sometimes is difficult or even impossible.

Fig. 3.3. Example of natural weathering- test racks with fabrics at exposure location on the fifth story of a building in Malaysia [196]

In accelerated natural ageing tests, acting of a particular environmental factor is empowered, but its source still comes from nature. The best example of apparatus used for this test is a sunlight concentrator system. It automatically tracks the sun from morning to night, whereas its special mirrors reflect and concentrate a full spectrum natural sunlight on the test specimens (Fig. 3.4). The efficiency of these machines is often incredible. For instance, the total ultraviolet radiation (TUV) of about 17 000 MJ/m^2 is focused annually on the samples in Phoenix, Arizona ([246]). This result corresponds to the same amount of UV deposited over 60 years of Florida exposure

(16 800 MJ/m^2). For materials which undergo mainly photoageing, this accumulation of radiation really accelerates any studies and the researches of photodegradation process.

Fig. 3.4. Natural sunlight concentrators ([246])

For civil engineering materials, the laboratory non-natural accelerated ageing tests are usually conducted in weather chambers, where particular temperature conditions, atmosphere (air, nitrogen), humidity and UV irradiance are maintained ([128], [124]). In Fig. 3.5, the accelerated climate ageing of wooden samples is presented. In this climate simulator the samples are cyclically exposed to four various surface treatment zones according to Nordtest Method NT Build 495. However, the most common and simple approach is the dry heat method carried out in the dedicated oven with constant air flow ([124], [209], [214], [115]). This procedure often includes performing accelerated tests at various temperature levels and time duration.

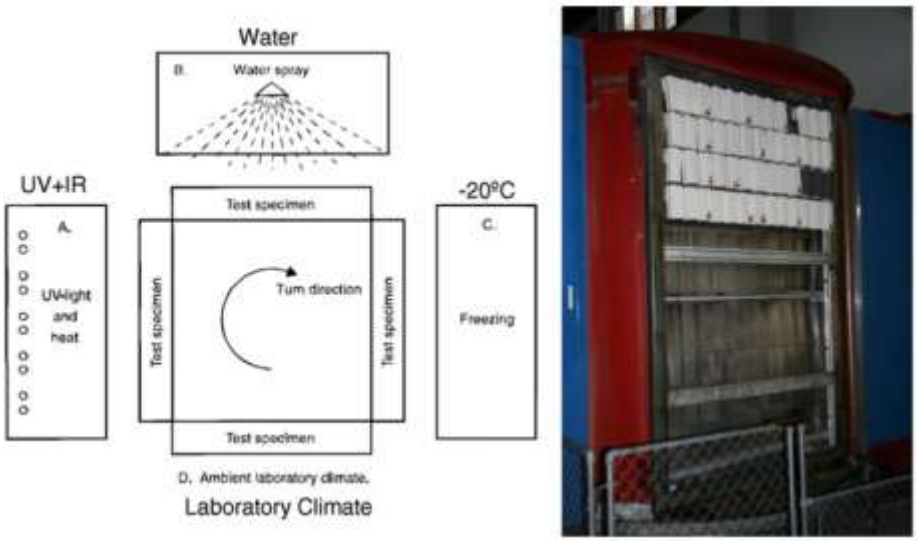

Fig. 3.5. Accelerated climate ageing simulator with various zones treatment ([130])

After being subjected to one of the presented exposure procedures, the material is tested towards particular characteristics. The obtained experimental results should be then mathematically described to qualify and quantify the ageing process. The phenomenon of material ageing is basically defined using a reference test (Fig. 3.6) on a sample before ageing (a) and for the identical sample after waiting for a long or short period (b) ([160]). If the responses (c) to the

tests are the same, there is no ageing and the material can be characterized as stable (over time). Otherwise, the ageing process has taken place.

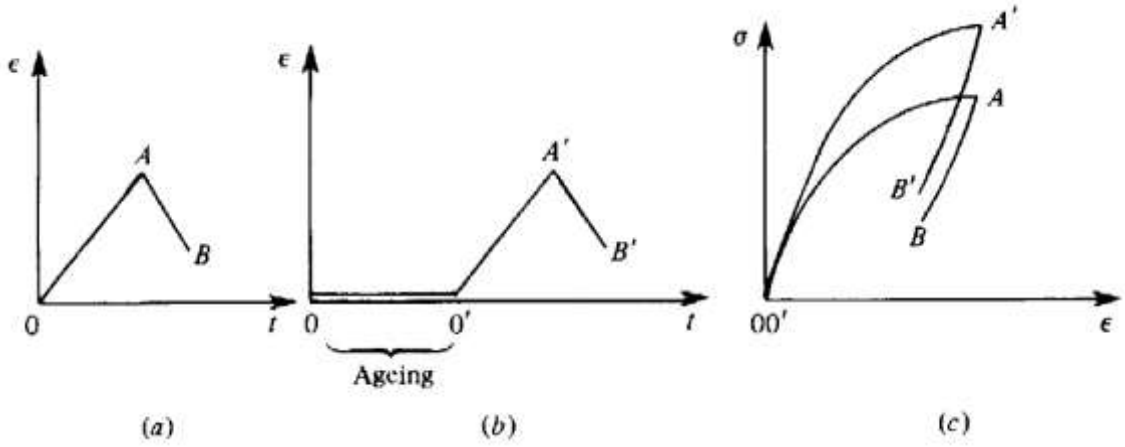

Fig. 3.6. Example of reference test for evaluation of the material ageing: (*a*) before, (*b*) after ageing and (*c*) responses ([160])

The basic and very common approach for material life prediction and mathematical explanation of many processes related to ageing has been offered by Arrhenius. The Arrhenius equation is a simple empirical relationship describing the temperature dependence of chemical reaction rates. It was proposed by Swedish scientist Svante Arrhenius in 1889 ([17], [18]) and based on the work of Dutch chemist Jacobus Henricus van't Hoff on temperature dependence of equilibrium constants ([25], [126]). The Arrhenius law is expressed as the reaction rate constant k ([115], [56])

$$k = k_0 \exp\left(-\frac{E_{act}}{RT}\right), \tag{3.1}$$

where k_0 is the entropy factor, E_{act} is the activation energy in J/mol, $R =\sim 8.314\ \mathrm{J/(mol\ K)}$ is a universal gas constant and T is the absolute temperature in Kelvins. The term of activation energy has been proposed by Arrhenius as the minimum energy that must be brought in a chemical system with potential reactants to cause a particular chemical reaction. This equation states that processes proceed faster under raised temperature, what is commonly used for carrying out the tests of accelerated ageing.

Taking the natural logarithm of the Arrhenius equation (3.1) one gets

$$\ln(k) = \frac{-E_{act}}{R}\frac{1}{T} + \ln(k_0). \tag{3.2}$$

Now, drawing the logarithm of the reaction rate $\ln(k)$ versus inverse temperature $1/\mathrm{T}$ forms the so-called Arrhenius plot. If a process obeys the Arrhenius equation, the plot gives a straight line, which gradient and intercept can be used to determine E_{act} and k_0. It has been observed during tests that in particular conditions (e.g. appropriate range of temperatures) the Arrhenius law can be simplified to so called "10 degree rule", which means that growing ambient temperature by

about 10°C increases the rate of many reactions by the factor of two [115] and can be expressed as

$$f = 2^{\Delta T/10}, \tag{3.3}$$

where $\Delta T = T - T_{ref}$ denotes difference between the ageing temperature T and the service temperature T_{ref} of a material. However, this simplified relation must be introduced with care, as it has been proved that it stays true only below the activation energy of $E_{act} = 120$ Jmol^{-1} ([1]).

The Arrhenius approach is widely applied by many scientists. For example, Boxhammer [45] has confirmed this relation for the dependence between color change and ageing temperature. Mercier et al. ([173]) have observed that the parameter of diffusivity in the Fickian diffusion obeys an Arrhenius type relationship, when analyzing water absorption in epoxy matrix composites reinforced with E-glass fibers. A comprehensive study of the Arrhenius and non-Arrhenius behavior of polymer materials have been presented by Wise et al. ([244]). They have shown that for some macroscopic properties, like tensile elongation, the Arrhenius approach stays proper, while for chemical reactions, like oxygen consumption, it fails. Further research has proven that the energy activation of aged rubber materials depends on a temperature level, thus stays in contrary to the basic assumption of the Arrhenius formulation ([91]). Many other publications suggest that Arrhenius extrapolation methodology is incorrect and should be used with high care ([92], [105]). One of the main drawback of the methodology proposed by Arrhenius is the assumption that chemical mechanisms leading to ageing do not change with temperature. It means that the activation energy does not change in the extrapolation range ([244]). Meantime, the chemical processes in materials tend to be complicated and of a synergic effect of many factors altering due to temperature variations.

The research on durability and its coupled issues require a very comprehensive approach. The crucial one is the analysis of factors influencing the durability of building materials. Then, the laboratory methods of artificial ageing are designed. The field testing of materials in service is done for verification of the accelerated testing protocols, while mathematical descriptions tries to correlate experimental findings with field exposure results. The final step is to achieve unified procedures for durability estimation included in national standards. Most up to date achievements and wide expansion in the durability and ageing of materials used in civil engineering may be found in the series of collective books with the mutual title *"Durability of Building Materials and Components"* ([80]. [76], [79], [78]). Each of this position is the summary of international conference dedicated to the same topic. Many basic problems, new methods and analysis concerning the life prediction of materials such as steel, cement, concrete, glass, wood, masonry, polymers and composite materials are included there. The *"Durability of Building Materials and Components"* series is worth recommendation to get overall insight in the research on the

durability. Moreover, it is the huge database of papers and demonstration of scientific world centers important to get familiar with, when starting studies in this particular area.

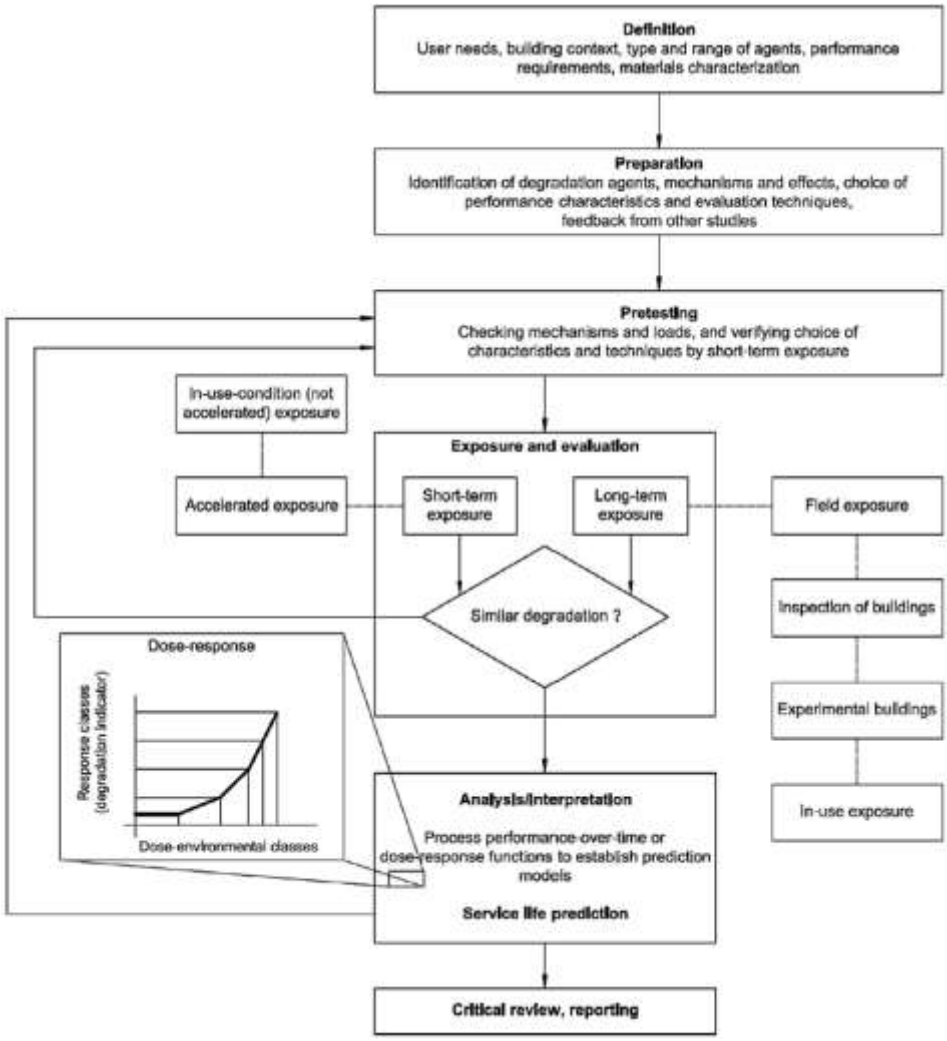

Fig. 3.7. Systematic methodology for service life prediction of building components (ISO 15686-2) [88]

Due to the various approaches and methods of service life prediction used across the world for the accelerated testing of building materials, there is a growing tendency to develop some standards that will allow comparison of results from different scientific centers. Some reviews of these trials and suggested methods are presented by cooperation between two technical committee CIB and RILEM and their examples can be found in technical reports ([67], [68]). If concerning roofing membranes refer to one of [167], [156], [35]. Some standards and procedures have been also developed to catch the durability aspect. An example of the European methodology according to ISO 15686-2 is presented in Fig. 3.7. In essence, it contains three main areas: preparation of ageing tests, exposure phase (ageing test) and final analysis with interpretation. The most important part is the comparison between naturally and artificially aged samples considering previously made assumptions ([73]). It gives the possibility to assess the correctness of performed procedure.

The author is aware of the fact that the presented literature review does not exhaust the full state of the art in the analyzed field. The ageing itself is a sophisticated phenomenon and the wide spectrum of different building materials makes it impossible to present the full review. Therefore, it has been decided to present here the publications concerning mainly polymer materials with special attention paid to technical fabrics that are in the center of interest in this research. For the ageing process, the service life prediction methods and their mathematical descriptions only a limited number of publications is presented. Obviously those are only examples among many others.

3.2 Ageing of polymer materials

3.2.1 Types of polymer ageing

The physical ageing is the most common form of ageing usually going on alongside the other types of ageing. It is unique for polymer materials and straight correlated with the state of the thermodynamic equilibrium. Most polymers have two distinct transition phases defined by the melting temperature T_m, when a material changes from its solid to liquid state, and the glass transition temperature T_g, which is a boundary between the glass and rubbery state ([1]). At temperature above T_g, the mobility of molecules (Brownian motion) is so high, that the increase/decrease of the thermodynamic quantities (volume V, enthalpy H and entropy $S')$ can follow the change of temperature. In contrary, under the temperature T_g the Brownian motion is reduced and the change of thermodynamic properties cannot keep pace with altering temperature any more (Fig. 3.8).

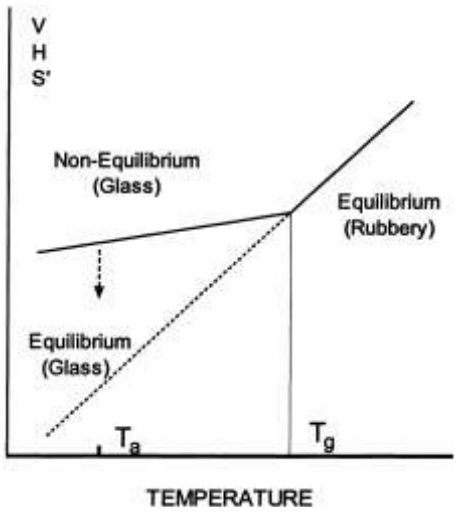

Fig. 3.8. Schematic illustration for the dependence of thermodynamic quantities (volume *V*, enthalpy *H* and entropy *S')* as a function of temperature ([165])

Physical ageing takes place when a polymer is in a non-equilibrium state (below its glass transition temperature T_g, in glassy phase), what results in a molecular process that relaxes towards the equilibrium state. The graph in Fig. 3.8 represents the physical aging occurring below T_g, as the change of the basic thermodynamic quantities. The higher is the ageing temperature T_a, the material would faster reach its equilibrium state and the smaller the final change in the particular property would be observed. As most of polymer applications is intended to service in surrounding characterized by the temperature below T_g, physical ageing always occurs.

The phenomenon of physical ageing is encountered in thermoplastics processes, when the melt polymer gets shaping procedure by injection, blow moulding, extrusion or film blowing. All these technics involve rapid cooling from above the melt temperature T_m to low (typically ambient) temperature, what results in initiation of physical ageing ([116], [240]). As the physical ageing comprises changes in thermodynamic quantities, it may affect time-dependent changes in the physical (density, dimensions, permeability, refractive index), mechanical (elastic modulus, yield stress, relaxation time), thermal (thermal expansion coefficient) or dielectric (dielectric constant) properties of a material ([165], [116], [70]).

The physical ageing is a thermo-reversible process for all amorphous polymers, meaning that heating of a polymer above its T_g and then rapid cooling can eliminate changes that have occurred during long-term ageing period at the service temperature (below T_g). It may explain in some way, why polymer materials (like roofing coatings) used for even 20 years in harsh environmental conditions with cyclic high and low temperatures stresses still retain their initial (production) tensile strength ([31], [94]).

The chemical ageing produces irreversible changes in material structure by chemical modification and the rupture of primary atomic bonds. It may be categorized by three mechanisms: depolymerization, destruction and degradation ([202]). The depolymerization process consists in the thermal decomposition of a polymer into monomers, whereas destruction results in decomposition into different bonds than monomer. The degradation is the most common phenomenon occurring in a polymer exploitation, therefore it is often identified with ageing. It involves molecular branching and crosslinking, fragmentation of molecular main chain, splitting off low molecular weight species and oxygenated groups ([130], [202]). The chemical ageing can be initiated by different factors, such as temperature, radiation, oxygen, water, microorganisms and mechanical stresses. Frequently, the chemical ageing results in the material densification, which in turn affects the physical ageing due to the change of T_g temperature ([1]). The protection against chemical ageing includes mainly the modification of a polymer mixture throughout the use of stabilizers, anti-oxidizing agents or UV absorbers.

The mechanical ageing of polymer composites involves irreversible changes of a macroscopic scale due to stresses action ([241], [30], [1]). Firstly, the reason of mechanical degradation lies in the non-isotropic structure of material including various local imperfections, in which the process of matrix cracking, delamination, interface degradation or fiber breaks may be initiated under acting loads. Secondly, if the load is too extensive, the material response is non elastic any more. It goes beyond the elastic limit resulting in the permanent (plastic) deformation state even after the removal of stress.

Very often the mechanical ageing starts after the physical or chemical degradation of material structure has taken place. For instance, the thermo-oxidative ageing leads to matrix cracks along surfaces exposed to the environment. Then, the cracks under mechanical stresses start to grow extendedly giving, in turn, more area for the thermo-oxidative process ([163]). Influencing each other in a particular loop system, both the thermal-oxidative and mechanical ageing fasten the overall ageing of a composite material.

For the evaluation of ageing process in polymer materials used outdoor the wide range of different laboratory tests can be used. The most widely carried out experiments can be divided in the following groups:

- strength properties characterized by tensile tests, especially elongation at break and the breaking strength ([173], [150], [59] [29], [71], [89], [133], [192])
- long-lasting properties described by creep or relaxation performance ([235], [52], [96], [70], [157], [258])
- chemical characterization that usually includes the plasticizer content and specific gravity ([150], [29], [94], [192]), as well water absorption ([59], [97], [173], [29],)
- cracks propagation and structure changes that are followed by the visual and microscope examination or spectroscopy methods ([29], [173], [71], [249], [130], [246], [196], [89])

3.2.2 Description of artificial polymer ageing

The analysis of the polymer ageing phenomenon is presented comprehensively in Hutchinson [116] and Brinson and Gates [52]. The ageing as the result of time-temperature process can be presented in the function form $f = f(T,t)$, which according to the time-temperature superposition principle (TTSP) ([127], [84]) is rewritten as the following relations:

$$\begin{aligned} f(T,t) &= f(T_0,t_z) \\ t_z &= \frac{t}{a_T(T)} \end{aligned}, \tag{3.4}$$

where: T is temperature, T_0 is a reference temperature, t is time, t_z is "reduced time" and $a_T(T)$ is the temperature shift factor. It states that the behavior of a material at high temperature and

under high strain level is similar to its behavior at low temperature and low strain level and can be calculated relative to this at the reference temperature by the simple multiplicative factor $a_T(T)$. Graphically, it corresponds to a shift of a curve on the log time scale. Materials showing this property have been called after Schwarlz and Staverman the thermo-rheologically simple ([213]). For linear viscoelasticity the most common function relating the shift factor and temperature has been proposed by Williams, Landel and Ferry ([243]):

$$\log a_T = \frac{-c_1(T - T_0)}{(c_2 + T + T_0)}, \tag{3.5}$$

where c_1, c_2 are constants. It is known as WLF (Williams-Landel-Ferry) and stays correct above T_g temperature. Below T_g the Arrhenius equation should be used ([1]):

$$a_T = \exp\frac{\Delta H}{R}\left(\frac{1}{T} - \frac{1}{T_0}\right), \tag{3.6}$$

where ΔH and R are the activation enthalpy and the gas constant, respectively. One major application of the TTSP approach is the accelerated testing. The long-term response can be obtained from several experiments carried out at different temperature levels and relatively short range time. Fig. 3.9a presents the series of the uniaxial tensile tests results after the isothermal ageing below T_g temperature. In the Fig. 3.9b the plots are collapsed to the reference temperature of 80°C (usually the lowest among analyzed ones) giving master curve. The shift factors used for shifting the particular plots are then plotted versus inverse ageing temperature resulting in the Arrhenius plot (Fig. 3.9c). If calculated activation energy E_{act} is assumed to stay constant below 80°C, the extrapolated time scale at 25°C (time of corresponding natural ageing) is displayed on the upper x-axis in Fig. 3.9b.

The phenomenon of the physical ageing in amorphous and semi-crystalline polymers has been extensively studied by Struik and his co-workers between 1962 and 1976 at the Centraal Laboratorium TNO Holland ([226]). This research has become the base for further investigations and still keeps to be the most referenced one in the terms of the physical ageing. According to Struik, the physical ageing is an elementary feature of the glassy state and affects all temperature dependent properties which change at T_g temperature. During ageing the material becomes stiffer and brittle, its damping as well the creep and stress-relaxation rates decrease.

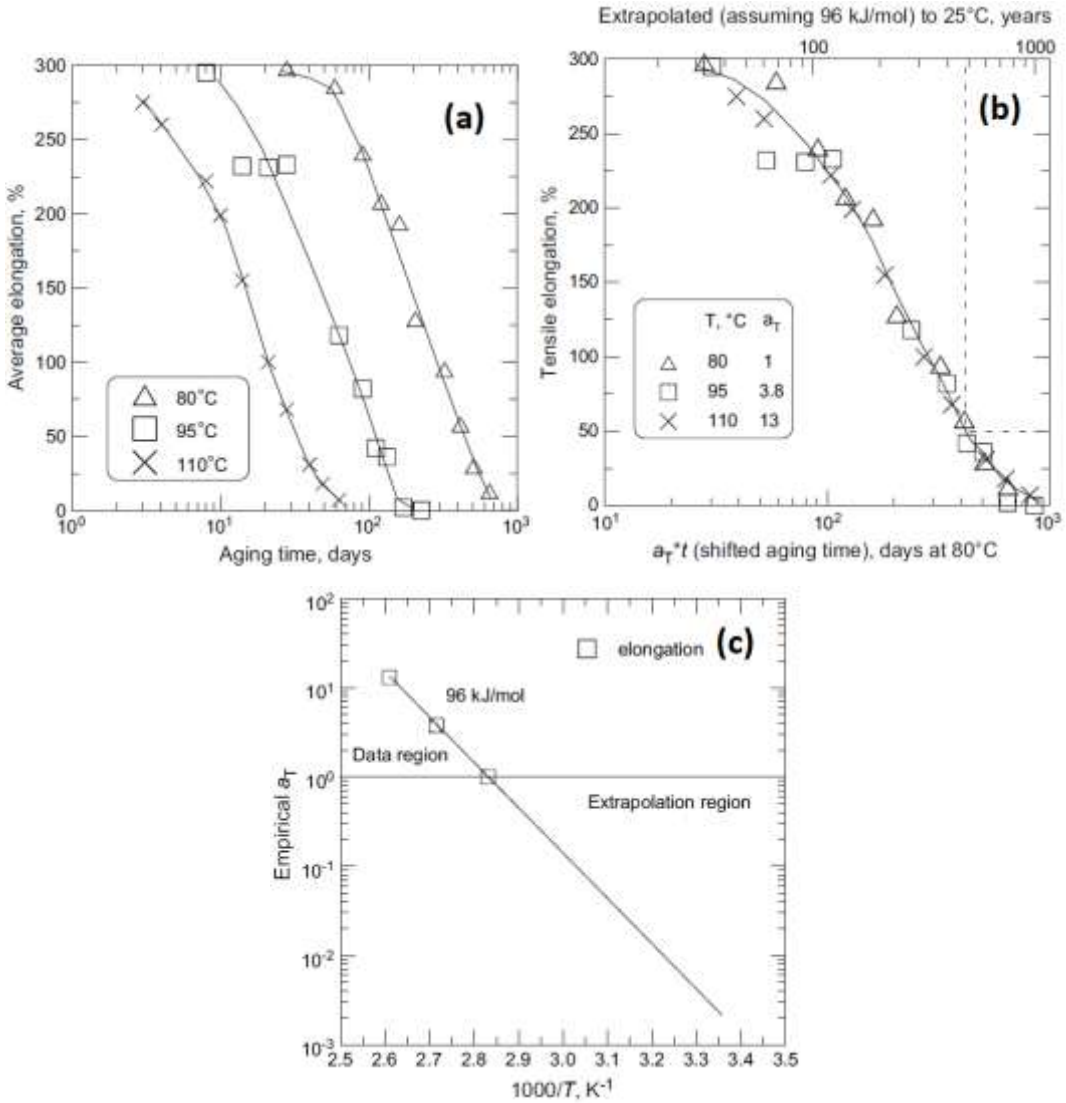

Fig. 3.9. TTSP with Arrhenius behavior: (a) ultimate elongation after isothermal ageing for 3 different temperatures; (b) plots collapsed to a master curve using shift factors a_T and temperature of 80°C as a reference temperature ($a_T = 1$ for 80°C); (c) Arrhenius plot of the shift factors versus inverse ageing temperature with extrapolation to temperature of 25°C ([91])

Furthermore, it has been shown that all polymers age in a similar way, while the process itself can be explained qualitatively by the free volume concept ([116]). It has been also noticed that polymers heated above T_g for a short time reach their thermodynamic equilibrium erasing any previous effects of ageing. This thermal reversibility allows to rejuvenate polymer materials quite easily. Because of the ongoing physical ageing it is also incorrect to use the time-temperature superposition, which generally overestimates the long creep behavior based on the short-term data ([84]). To assess the influence of the physical ageing on mechanical properties by the momentary creep compliance Struik has proposed to conduct a series of sequenced creep and recovery tests on a sample quenched from above its T_g to temperature below its T_g . The time the material exists

below its T_g is referred to as the ageing time t_e. This procedure and its results' example are schematically illustrated in Fig. 3.10a and Fig. 3.10b, respectively.

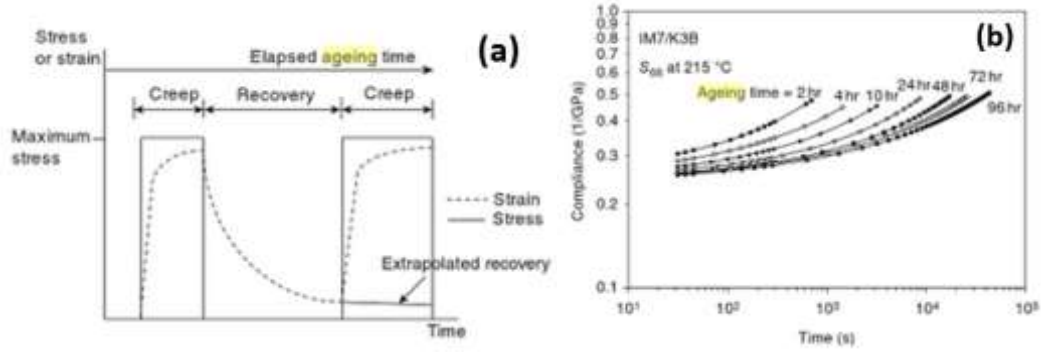

Fig. 3.10. Series of short creep and recovery tests run to measure the momentary creep compliance of the material ([1])

The momentary creep compliance can be simply modelled by the three parameter Kohlrausch model ([148], [52]):

$$S(t) = S_0 \, \mathrm{e}^{(t/\tau)^{\beta}}, \tag{3.7}$$

where S_0 is the initial compliance, β is the shape parameter, t is time and τ is the relaxation (retardation) time. It is possible to superpose the momentary creep curves measured at different ageing times through the horizontal (time) and vertical (compliance) shifts. It is commonly assumed that creep magnitude is unaffected by ageing ([116]), thus the horizontal shift is of the key importance. It resembles the methodology of the time-temperature superposition principle. However, many researches have studied the vertical shifting involved in ageing process and established corresponding mathematical descriptions. These can be found in Sullivan et al. ([227]) and Read et al. ([198], [197], [199]).

When the ageing time shift factor a_{t_e} is plotted as the function of ageing time t_e on a double log scale it follows a straight line with a slope of μ (Fig. 3.11):

$$\mu = -\frac{d \log a_{t_e}}{d \log t_e}, \tag{3.8}$$

where a_{t_e} is the ageing shift factor found through a test and is given as

$$a_{t_e} = \left(\frac{t_{e\,ref}}{t_{\mathrm{e}}} \right)^{\mu}, \tag{3.9}$$

where $t_{e\,ref}$ is the reference ageing time.

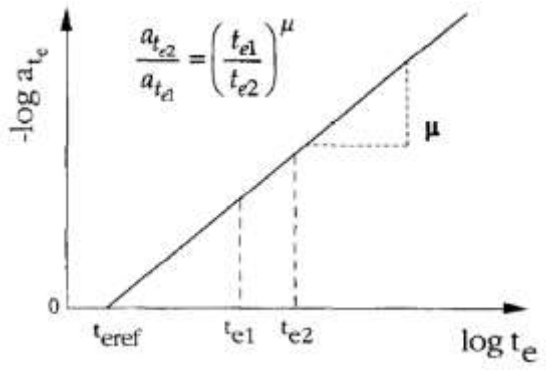

Fig. 3.11. Definition of shift rate μ ([52])

As the result of the creep curves horizontal shifting, the only parameter that changes as the function of ageing is the relaxation (retardation) time τ, which could be, then, written as

$$\tau(t_e) = \tau\left(t_{e\,ref}\right) / a_{t_e}. \tag{3.10}$$

Taking the initial aging time t_e^0 to be the reference aging time $t_{e\,ref} = t_e^0$, the shift factor a_{t_e} at any time point can be defined basing on the shift rate μ as follows:

$$a_{t_e^0}(t) = \left(\frac{t_e^0}{t_e^0 + t}\right)^{\mu} \tag{3.11}$$

The so-called "effective time" increment according to [176] or [226] is defined as

$$\mathrm{d}\lambda = a_{t_e^0}(t)\,\mathrm{d}t \tag{3.12}$$

and means that during the time interval between t and $t + \mathrm{d}t$ the same creep amount will occur as within the effective time interval $\mathrm{d}\lambda$, which corresponds to a short-term creep process where physical ageing occurs too slow to be observed. Consequently, the total test time can be reduced to the "effective time" (or "reduced time")

$$\lambda = \int_0^t a_{t_e}^0(\xi)\,\mathrm{d}\xi. \tag{3.13}$$

After integration of equation (3.13) using equation (3.10) the effective time can be expressed in two ways:

$$\begin{aligned} \lambda &= t_e^0 \ln\left(t / t_e^0 + 1\right) && \text{for } \mu = 1 \\ \lambda &= \frac{t_e^0}{1-\mu}\left[\left(1 + t / t_e^0\right)^{1-\mu} - 1\right] && \text{for } \mu \neq 1 \end{aligned}. \tag{3.14}$$

The concept of the "effective time" has been named after Struik as the effective time theory (ETT). Now, using the effective time in the place of real time in equation (3.7) produces the creep compliance in form

$$S(t) = S_0\, \mathrm{e}^{\left(\lambda / \tau\left(t_e^0\right)\right)^{\beta}}, \tag{3.15}$$

which allows to predict the long-term behavior based only on the material parameters determined from short-term tests. This way, using ETT Struik has modified the classic time-temperature superposition principle (TTSP) into the time-ageing time superposition principle (TASP).

In order to take into account the coupled effect of temperature and ageing time on a material behavior a combined approach has to be developed. It is known as the time-temperature-ageing time superposition principle. It is most easily achieved by conducting isothermal viscoelastic tests (e.g. creep or relaxation) at different temperature levels below T_g . The general time-temperature-ageing time shift factor can be expressed according to [227] as:

$$\log a = \log a_{t_e} + \log \bar{a}_T \tag{3.16}$$

where a_{t_e} is the ageing time shift factor as defined by equation (3.11) and $\bar{a}_T$ is the time-temperature shift factor, as described previously. Taking the ageing shift rate as a function of temperature ($\mu(T)$) and the time-temperature shift factor at a single ageing time, the value of $\bar{a}_T$ can be calculated at any ageing time using the expression ([52]):

$$\frac{\bar{a}_{T_1/T_2}^{t_{e2}}}{\bar{a}_{T_1/T_2}^{t_{e1}}} = \left(\frac{t_{e2}}{t_{e1}} \right)^{\mu(T_2)-\mu(T_1)}, \tag{3.17}$$

where T_1 and T_2 are two different temperatures and t_{e1} and t_{e2} are two different ageing times.

There have been developed various superposition principles aiming at accelerated testing, like the time-temperature-moisture superposition principle (TTMSP, [95], [171]) or the time-stress superposition principle (TSSP, [211], [210]). Several publications have appeared documenting different mathematical transformations and trials to develop the formulation including the ageing effects in polymer materials. They can be found e.g. in Chazal and Pitti ([64]), Guedes ([96]), Brinson and Gates ([52]), Ferhoum et al. ([83], Drozdov ([75]), Zhang et al. ([257]), Rahouadj and Cunat ([193]), Hassine et al. ([103]).

3.2.3 Ageing of PVC and PET materials

The polyvinyl chloride (PVC) is the third-most widely produced synthetic plastic polymer in the world, after polyethylene and polypropylene ([242]). On the fourth position we can find polyester in its most known form of polyethylene terephthalate (PET). PVC is used in two forms: rigid and flexible. The rigid one can be found e.g. in pipes constructions, door or window frames, bottles and payment cards. By adding of plasticizers it becomes softer, become more flexible and is then used e.g. in plumbing, for coating (cable insulation) and in other applications where it may replace rubber. Polyester is usually produced in the form of threads and yarns. It is extensively used in clothing industry and soft furnishings, whereas polyester fibers are applied e.g. in tire reinforcements, fabrics, safety belts, coated fabrics or insulating pipes, to mention only a few of them. Both PVC and PET belongs to thermoplastics from the family of polymer materials.

In the literature, many papers deal with naturally and artificially aged PVC and polyester mixtures ready to use as building materials. Laiarinandrasana et al. [157] have studied PVC water pipes, Linde et al. [165] have tested polyester/TGIC powder coatings, Lodi et al. [166] have analyzed polyester and polypropylene geotextiles, Real and Gardette ([200]), Rabinovitch et al. [192], Tawfik et al. [231] have focused on PVC mixtures designed for outdoor engineering applications.

The most interesting, however, are researches where the artificial ageing is compared to natural, in-service one. For instance, Gumargalieva et al. [99] have tested naturally and artificially aged samples and matched them with material used for 15-30 years in aircraft engines. The obtained results have proven that in dark, low temperature the dominant process of PVC ageing is desorption of plasticizer (measured by e.g. mass loss), while for the photo-ageing the main process is degradation of both polymer and plasticizer. Jakubowicz et al. ([129]) have investigated about 50 different PVC cables and sheathings from old houses and found only a small difference in the elongation at break and very good thermal stability of materials used up to 34 years. The overall technical quality of collected samples have been very good and consequently suggestion of reuse or mechanical recycling of PVC cables has been stated. The tested PVC model material aged in air at 80-90 °C has shown no change in the elongation at break, but the higher temperature of 100-110°C has caused decrease of 30% of this parameter. The authors have also confirmed that the mass loss of plasticizer is the dominant process in the ageing of plasticized PVC at low temperatures. As reported in different study by Jakubowicz [128], there has been no significant correlation between the results of the artificial and natural ageing of commercial PVC materials tested towards the impact strength and color change. The author has compared samples aged for 12 years in outdoor environment with the material aged in laboratory and subjected to the weathering cycles composed of variations in humidity, temperature and UV light duration. In the following paper of the same scientists group (Yarahmadi et al. [251]), they have focused on PVC flooring material collected from 30-40 year old buildings. Apart from confirming previously drawn conclusions, the have highlighted the problem of the chemical interaction between concrete and PVC glued to it. The high alkalinity of moist concrete can lead to the decomposition of the plasticizer of PVC flooring, but what is even worst, to the creation of butanol and octanol products that can cause environmental problems designated as" sick building syndrome". Another research concerning the wastes of electrically aged cable insulation conducted by Brebu et al. ([48]) has also shown the excellent characteristic of PVC material required for reprocessing. Andjelkovic and Rajakovic [14] have implemented coupled electrical and thermal ageing procedure for cable life tests. They have concluded that the degradation caused by the single factor separately (electric current and temperature) cannot be correlated. They have also observed that temperature has greater influence on the breakdown voltage and dielectric loss angle than the voltage.

Several publications have appeared recent years documenting the ageing and weathering of roofing materials. Berdahl et al. ([33]) have overviewed degradation of plastics induced by ultraviolet radiation; the effects of moisture on decay of wood, corrosion of metals, staining of clay; and reduction of solar reflectance due to soiling. Razak et al. ([196]) have pointed out that harsher tropical climate (hot and humid) causes greater degradation of material surface. They have subjected 10 different types of fabric to an outdoor exposure test and demonstrated that cracking and peeling of the coating are more apparent on the PVC-coated than on the PTFE-coated fabrics. Besides, it has been also proven that additive of $Ti0_2$ films results in better self-cleaning of the PVC-coated fabrics. Xing and Taylor ([246]) have tested 13 types of thermoplastic polyolefin (TPO) membrane towards UV and thermal breakdown. They have observed that TPO membranes designed to work at high temperatures (e.g. 138°C) have also excellent UV stability. They have obtained great correlation between laboratory, field and thermal ageing tests. Their work contains, in addition, the precise presentation of powerful apparatus for laboratory and natural accelerated weathering. Another interesting study has been accomplished by Sleiman et al. [221]. They have focused on the soiling problem and its impact on the reflectance properties of the cool roofs. The cool roofs are meant to decrease the energy necessary for air conditioning of the buildings by simply reflecting the solar heat radiation and cooling the structure beneath them. It is widely studied subject, especially due to sustainability and energy saving aspects. These scientists have managed to prepare and verify a new laboratory protocol, which requires just 3 days to simulate 3 years of outdoor weathering.

The methods of the ageing process simulation, both naturally and artificially accelerated, will never take into account the wide spectrum of various factors affecting the performance of materials under natural, outdoor exposure. Nothing is more useful and informative than the actual field experience ([58]). It provides direct facts on the ageing phenomenon and can serve as a basis for the validation of any simulation program. The in-situ research consists of simple visual inspection and/or collection of samples for further laboratory testing. An example of the field study is the analysis of 10-year performance of PVC roofing materials that has been accomplished by American military laboratories in years 1982-1993 ([29], [204], [87]). The unreinforced and reinforced types of roofing membranes installed by different techniques have been tested. The basic mechanical properties of textiles have been identified and their evolution in time has been approximated by linear functions, giving satisfying results.

The next example is a group of American, Canadian and Switzerland scientists that have tested 44 different roof membranes collected from old houses in America and Europe in 2001-2002 ([239], [94], [31]). They have performed the series of experiments (e.g. tensile properties, low temperature flexibility, hail resistance, dimensional stability, plasticizer content, seam strength) and compared the results to requirements of national standards ASTM, DIN, SIA ([21], [74], [219]). The laboratory testing confirmed that, although the products tested lost some of their

initial physical properties due to ageing process, they generally behaved very well in comparison to the normative minimum values for testing new PVC roofing membranes. It should be highlighted that most of the samples were installed before establishing the first single-ply roofing standards in particular countries. The DIN and SIA standards were introduced in 1976 and 1977 respectively, while the American standard ASTM in 1985. Moreover, all the tested on site PVC roofing systems maintained well (without leakage) and were capable of being welded despite their age. All in all, it was indicated, that if being properly treated, the roofing textiles would probably perform satisfactorily for the next decade.

Cash et al. ([59]) have presented the comparative analysis of 12 different types of roofing membranes exposed to 2 and 4 year outdoor weathering and proposed a rating system to assess their durability. A review and development of other field studies of PVC roof system is presented by Koontz [150]. He has also suggested that materials manufacturers should provide customers with the information of membrane failure histories and the performance criteria to assess the time for a particular roofing product to be replaced before dangerous breakdown would occur.

The great worldwide development of PVC and PET has started after the World War II. They are willingly used in civil engineering, especially for covering and roofing applications. However, these synthetic materials are relatively new in engineering industry and therefore require more attention and comprehensive studies, especially concerning their ageing and recycling processes.

3.3 Summary

This chapter has concerned the ageing phenomenon in building materials, with special focus addressed to the ageing of polymers, especially PVC and PET materials. Types of ageing have also been described followed by the presentation of mathematical approaches used to evaluate the artificial ageing. From many different approaches of laboratory accelerated ageing the isothermal conditioning has been selected to be executed in this study. For ageing estimation, the most common Arrhenius methodology has been chosen.

4 Material models for ageing analysis

4.1 Introduction

For the precise coated membranes behavior analysis we need description of the fabric geometry (kinematics) and the material constitutive relations. Numerical software usually demands analytical representation of them both. In this work the author focuses on the stress-strain relations that can be easily coupled with the dense net model that takes into account two threads families of the fabric structure (the warp and fill; for more details study the Section 2.2). Therefore, material properties for this model should be separately defined for the warp and fill direction. The author proposes to analyze architectural fabrics behavior over passing time in its all working phases, starting from elastic range, through viscoelastic and ending up with viscoplastic domain.

Due to the complicated woven/knitted structure of technical fabrics, it may be difficult to establish correctly the tensile properties, especially for the fill direction of a material. Thus, the author proposes to start the analysis with the load-unload tensile cyclic tests, which should throw light on the elastic behavior of architectural fabrics. The non-linear piecewise elastic model is used thereafter to bring together the values of immediate longitudinal stiffness and corresponding elongations, which are necessary for pre-designing purposes and are of the key importance during tensioning fabrics on the construction assembly ([8], [7], [9]).

Basing on research and engineering observation, the long-lasting behavior of technical fabrics fastened on a real construction is defined as viscoelastic. For its identification, the rheological tests of creep or relaxation type are required. When modelling, Argyris' ([15], [16]) and more advanced Schapery's non-linear approaches can be used ([142]). The constitutive models initially destined for metals have been also applied for studies of architectural fabrics in viscoelastic domain. For instance, the creep potential model with three orthotropic parameters has been investigated upon the polyethylene terephthalate fabric coated with PVC ([140]). However, to fulfill the objective of the presented study, the Burgers model appears to be sufficient. It is one of the commonly applied formulation. Here, it is brought in for monitoring the long-term creep behavior.

After all, designers must remember about exceptional loading conditions that induce in fabrics the permanent inelastic elongations. Extremely high stresses or velocities may arise in roofing membranes as a result of truly gusty wind, structure breakdowns or also during improper installation process. At that point, the analysis of fabrics calls for viscoplastic models. These models permit the examination of dynamic loads cases and make it possible to study behavior of the material above the yield limit, which is also useful in the modeling of damage processes. Therefore, the main goal of the presented study is to assess and analytically describe the influence

of the natural and artificial ageing process on technical fabrics in the viscoplastic range. Among many constitutive formulations the Bodner-Partom model has been selected. It has been proven before that this mathematical model approximates fabrics behavior very well in both the warp and fill direction ([144]). Besides, its parameters identification requires only the uniaxial tensile tests that can be easily and quickly conducted. Proposed in this study evaluation of the aging phenomenon demands many repetitive experiments. It is then particularly important to use a mathematical tool that involves short time tests and simple modeling procedures. For these reasons, the Bodner-Partom model seems to be the right choice.

This chapter contains the detailed mathematical formulation and the description of parameters identification procedures for each selected material model.

4.2 Piecewise linear model

The concept of the piecewise linear model material is based on the observation , that even a very sophisticated shape of an experimental stress-strain curve can be approximated by the set of linear functions followed by ranges of their applicability according to the following equations:

$$\begin{aligned} f_1(x) &= a_1 x + b_1,\ x \in \langle 0; x_1 \rangle \\ f_2(x) &= a_2 x + b_2,\ x \in \langle x_1; x_2 \rangle \\ f_3(x) &= a_3 x + b_3,\ x \in \langle x_2; x_3 \rangle \\ &\ldots \\ f_i(x) &= a_i x + b_i,\ x \in \langle x_{i-1}; x_i \rangle \end{aligned} \tag{4.1}$$

The piecewise linear model allows to conduct first (and very quick) evaluation of the material behavior in the elastic and non-elastic ranges. The example of the model application for the uniaxial tensile test of architectural fabric is presented in Fig. 2.1. In some cases the particular longitudinal stiffness of a material is equal to its Young's modulus. For technical fabrics their stress-strain response under the tensile test is complex and one should be very careful in estimating the true value of elastic modulus. This problem will be wider analyzed in a further part of the study (Section 6.2.1).

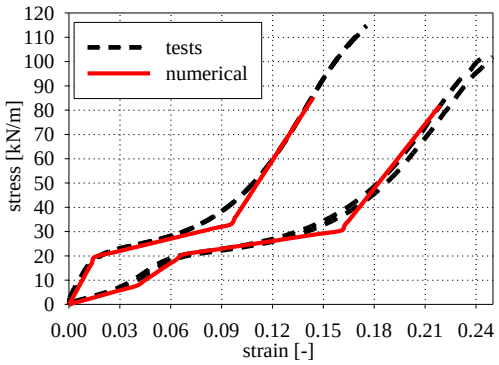

Fig. 4.1. Example of experimental results with numerical simulation using non-linear piecewise model for uniaxial tensile test of technical fabric [9]

4.3 Viscoelastic Burgers model

The Burgers model is a four parameter model representing the linear viscoelasticity properties of a material using derivative relations. It is a series combination of the Maxwell and Kelvin-Voigt models ([183]): the instantaneous deformation ε_1 comes from the Maxwell spring, viscous deformation ε_2 from Maxwell dash-pot and viscoelastic deformation ε_3 from Kelvin-Voigt unit (Fig. 4.2).

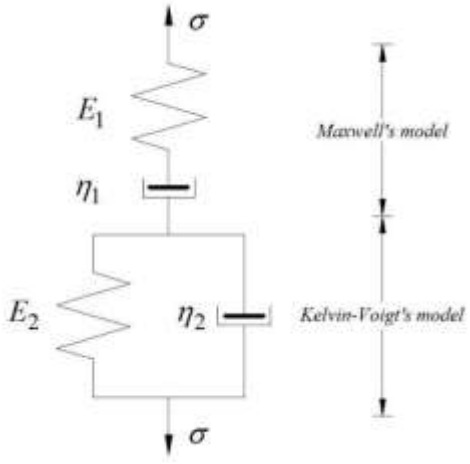

Fig. 4.2. Representation of the Burgers model

As a consequence the total deformation at time t is the sum of particular parts:

$$\varepsilon = \varepsilon_1 + \varepsilon_2 + \varepsilon_3 , \tag{4.2}$$

where

$$\varepsilon_1 = \frac{\sigma}{E_1}; \quad \dot{\varepsilon}_2 = \frac{\sigma}{\eta_1}; \quad \dot{\varepsilon}_3 + \frac{E_2}{\eta_2}\varepsilon_2 = \frac{\sigma}{\eta_2} \ . \tag{4.3}$$

The elimination of the elementary strains from equations (4.2) and (4.3) gives the constitutive formulation of the Burgers model in the form of the second order differential equation [127]:

$$\sigma + \left(\frac{\eta_1}{E_1} + \frac{\eta_1}{E_2} + \frac{\eta_2}{E_2} \right) \dot{\sigma} + \frac{\eta_1 \eta_2}{E_1 E_2} \ddot{\sigma} = \eta_1 \dot{\varepsilon} + \frac{\eta_1 \eta_2}{E_2} \ddot{\varepsilon} \ . \tag{4.4}$$

For the state of constant stress level $\sigma = \sigma_0 = \text{constant}$ (a creep test) the equation (4.4) can be solved using the Laplace transformation, upon the assumption that for the time $t = 0$:

$$\varepsilon = \varepsilon_1 = \frac{\sigma_0}{E_1}, \ \varepsilon_2 = \varepsilon_3 = 0 \tag{4.5}$$

and

$$\dot{\varepsilon} = \frac{\sigma_0}{\eta_1} + \frac{\sigma_0}{\eta_2} \ . \tag{4.6}$$

The final form of the Burgers model for the uniaxial case of creep test gets the following formula:

$$\varepsilon(t) = \frac{\sigma_0}{E_1} + \frac{\sigma_0}{\eta_1} t + \frac{\sigma_0}{E_2}\left(1 - e^{\frac{-E_2}{\eta_2} t}\right). \tag{4.7}$$

The first two parts of the equation (4.7) represent elastic strain and viscous flow, respectively, while the last one states for the delayed elastic deformation of the Kalvin-Voigt model [84].

The equation (4.7) can be also rewritten for the state of relaxation. However, it is rarely used as the quality of that solution is very close to the much simpler Maxwell model [127].

Among the other viscoelastic linear models, only the Burgers model describes precisely the creep behavior with the permanent strain. The Burgers equation is mainly used for the viscoelastic analysis of fluids. The Burgers model is general enough to include the one-dimensional Oldroyd, Maxwell, and Navier–Stokes models as subsets ([220]). Apart from the fluid analysis, the Burgers formulation is willingly applied with satisfactory results into the analysis of metals ([127]), polycarbonate panels ([256]) or natural fiber/polymer composites ([247], [63]).

4.3.1 Identification of the Burgers model parameters

The Burgers description of a material response to the constant stress is presented in (4.7). It is assumed that for the constant stress level $\sigma_0 = \text{constant}$ the immediate strain ε_0 is reached at time t_0. Consequently, the instantaneous elastic modulus E_1 can be obtained as

$$E_1 = \frac{\sigma_0}{\varepsilon_0}. \tag{4.8}$$

For the strain versus time curve of the typical creep test (Fig. 4.3) two distinct phases can be selected: the nonlinear (in the time range $t_0 - t_1$) and the proportional (in the time range $t_1 - t_2$). From the latter one the viscous coefficient η_1 can be easily written as

$$\eta_1 = \sigma_0 \frac{t_2 - t_1}{\varepsilon_2 - \varepsilon_1}. \tag{4.9}$$

Due to the proportional part of the equation (4.7) it is possible to find the value of auxiliary strain

$$\varepsilon_k = \varepsilon_1 - \frac{\sigma_0}{\eta_1} t \tag{4.10}$$

The difference between the immediate strain ε_0 and the auxiliary strain ε_k is due to the nonlinear part, what results in

$$E_2 = \frac{\sigma_0}{\varepsilon_k - \varepsilon_0}. \tag{4.11}$$

The viscous coefficient η_2 can be found by the approximation of the function (4.7) in time range $t_0 - t_1$ using the least square method and introducing the all already identified parameters.

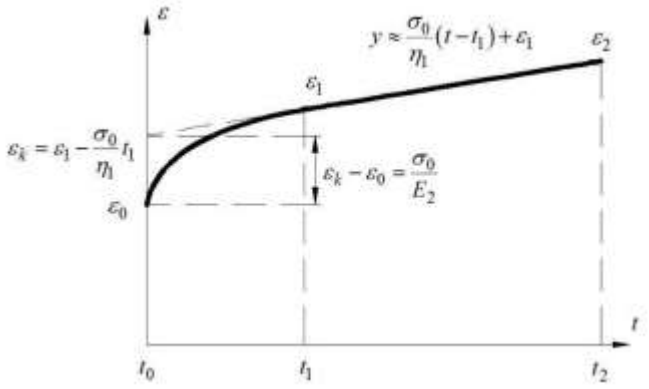

Fig. 4.3. Methodology of Burgers model parameters identification [147]

4.4 Viscoplastic Bodner-Partom model

The Bodner-Partom constitutive equations were originally proposed by Bodner and Partom in 1975 for prediction of the nonlinear viscoplastic strain-hardening response of a titanium alloy in the range of small strains and for isotropic materials ([41]). In the following several years the Bodner-Partom model has been refined to take into account the kinematic and thermal recovery ([175]), as well as damage effects ([38]). During the last 40 years the basic formulations have been extended through advanced computing implementations ([208], [13], [85]), various modifications ([253], [151], [217], [60]) and wider applications especially for non-metallic materials such as polymers ([191], [253]), living tissues ([205], [170]) and architectural fabrics ([144], [253]). The Bodner-Partom model is willingly employed for material description, because it requires only a few coefficients, which can be obtained from uniaxial tensile tests through a quite simple identification procedure.

The Bodner-Partom model (in uniaxial approach) is known as the inelastic strain rate $\dot{\varepsilon}_p$ relation in two variants. In case of uniaxial monotonic tension without thermal and recovery effects they can be written as:

$$\dot{\varepsilon}_p = \frac{2}{\sqrt{3}} D_0 \exp\left[-\frac{1}{2}\left(\frac{R+D}{\sigma} \right)^{2n} \frac{n+1}{n} \right] \mathrm{sgn}(\sigma) \tag{4.12}$$

or

$$\dot{\varepsilon}_p = \frac{2}{\sqrt{3}} D_0 \exp\left[-\frac{1}{2}\left(\frac{R+D}{\sigma} \right)^{2n} \right] \mathrm{sgn}(\sigma), \tag{4.13}$$

where D_0, n are model parameters. The isotropic (R) and kinematic (D) hardening functions are described by the set of evolution equations and are generally presented in a saturation-type format with prescribed initial conditions:

$$\dot{R} = m_1 (R_1 - R) W_p \; ; \qquad R(0) = R_0 \; ; \tag{4.14}$$

$$
\begin{aligned}
&D = \sqrt{2/3}X\,\mathrm{sgn}(\sigma)\ ;\\
&\dot{X} = m_2\left(\sqrt{3/2}D_1\,\mathrm{sgn}(\sigma) - X\right)W_p\ ; \quad X(0) = 0\ ;\\
&\dot{W}_p = \sigma\dot{\varepsilon}_p\ .
\end{aligned}
\tag{4.15}
$$

The kinematic hardening rate function $\dot{X}$ refers to the stress level and depends also on the kinematic hardening X and the plastic work W_p. The parameters m_1 and m_2 are saturation rate coefficients of the isotropic and kinematic hardening, respectively. The integration of formulas (4.14) and (4.15) gives the hardening functions in the following forms:

$$
\begin{aligned}
&R = R_1\left[1-\exp\left(-m_1W_p\right)\right] + R_0\exp\left(-m_1W_p\right)\ ;\\
&X = \sqrt{3/2}D_1\,\mathrm{sgn}(\sigma)\left[1-\exp\left(-m_2W_p\right)\right]\ ;\\
&D = D_1\left[1-\exp\left(-m_2W_p\right)\right]\ ;\\
&W_p = \sigma\varepsilon_p\ .
\end{aligned}
\tag{4.16}
$$

The relation between stress σ, inelastic strain rate $\dot{\varepsilon}_p$, temperature T and hardening variables R, D can be demonstrated as the functional f_1, which is the combination of the Prandtl-Reuss law and some parts of the kinetic equations and is given in the general formula as:

$$
\frac{\sigma}{R+D} = f_1\left(\dot{\varepsilon}_p, T\right) \tag{4.17}
$$

For the Bodner-Partom formulation (equations (4.12), (4.13), respectively) the functional (4.17) can be expressed as follows:

$$
f_1 = \left[\frac{2n}{n+1}\ln\left(\frac{2D_0}{\sqrt{3}\dot{\varepsilon}_p}\right)\right]^{-\frac{1}{2n}} \tag{4.18}
$$

or

$$
f_1 = \left[2\ln\left(\frac{2D_0}{\sqrt{3}\dot{\varepsilon}_p}\right)\right]^{-\frac{1}{2n}} \tag{4.19}
$$

All the parameters of the Bodner-Partom model and their units adapted for technical fabrics are compiled in Table 4.1. For the more detailed explanations of the Bodner-Partom constitutive model, its wider mathematical description and different loading examples refer to [38], [13], [60], [205], [39] or [40].

Table 4.1. Bodner-Partom model parameters with units for technical fabrics

Parameter	**Units**	**Description**
E	kN/m	Young's modulus
v	-	Poisson's coefficient
m_1	$[kN/m]^{-1}$	Coefficient for isotropic hardening
m_2	$[kN/m]^{-1}$	Coefficient for kinematic hardening
A_1	s^{-1}	Recovery rate coefficient for isotropic hardening
A_2	s^{-1}	Recovery rate coefficient for kinematic hardening
D_0	s^{-1}	Limiting (maximum) strain rate
R_0	kN/m	Initial value for isotropic hardening
R_1	kN/m	Limiting (maximum) value for isotropic hardening
R_2	kN/m	Fully recovered (minimum) value for isotropic hardening
D_1	kN/m	Limiting (maximum) value for kinematic hardening
n	–	Strain rate sensitivity parameter
r_1	–	Recovery exponent for isotropic hardening
r_2	–	Recovery exponent for kinematic hardening

4.4.1 Identification of the Bodner-Partom model parameters

The Bodner-Partom model's parameters identification has been carried out according to the procedure earlier proposed for metals by Chan et al. ([60]). For technical fabrics the identification procedure of that model has been presented in Kłosowski et al. ([144]).

In essence, the identification procedure of the Bodner-Partom model parameters consists of the following steps:

- Uniaxial tensile tests with at least three different but constant strain rates form the basis of the identification giving the stress-strain function $\sigma(\varepsilon)$ obtained for each strain rate separately.
- The inelastic strain ε_p can been calculated from the total strain using the classic Hook's law describing the elastic strain $\varepsilon_e = \sigma / E$. The inelastic strain rate $\dot{\varepsilon}_p$ is assumed as equivalent to the total strain rate $\dot{\varepsilon} = \dot{\varepsilon}_p$ in the plastic domain (as $\dot{\varepsilon}_e \ll \dot{\varepsilon}_p$).
- The stress-inelastic strain relation $\sigma(\varepsilon_p)$ is plotted and subsequently approximated by an arbitrary chosen analytical function. For technical fabrics the following function is proposed:

$$\sigma(\varepsilon_p) = a\left(1-\exp\left(-b\varepsilon_p\right)\right) + c\left(1-\exp\left(-d\varepsilon_p\right)\right) + f\,, \tag{4.20}$$

where the parameters a, b, c, d, f have been determined using the least square method with the Marquardt-Levenberg algorithm (Fig. 4.4).

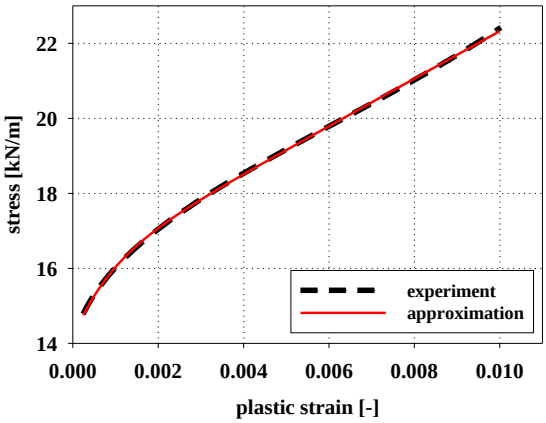

Fig. 4.4. Typical stress-plastic strain plot with approximation

- The work hardening rate $\bar{\gamma}$ can be calculated from the formula:

$$\bar{\gamma} = \frac{d\sigma}{dW_p} = \frac{d\sigma}{d\varepsilon_p} \cdot \frac{1}{\sigma}, \tag{4.21}$$

where the first segment of the formula (4.21) is a derivative of the function given in equation (4.20). According to equations (4.14), (4.15) and (4.17) it can be rewritten as:

$$\bar{\gamma} = f_1\left[m_1\left(R_1 - R\right) + m_2\left(D_1 - D\right)\right] \tag{4.22}$$

- The work hardening rate $\bar{\gamma}$ is now drawn as the function of stress $\bar{\gamma}(\sigma)$. It allows to find parameters m_2 and m_1 as the slopes of tangents to the curve for the beginning part of the plot corresponding to the small plastic strains ($\varepsilon_p = 0.2\%$), and in the range of the upper plastic strains ($\varepsilon_p = 2\%$), respectively (Fig. 4.5).

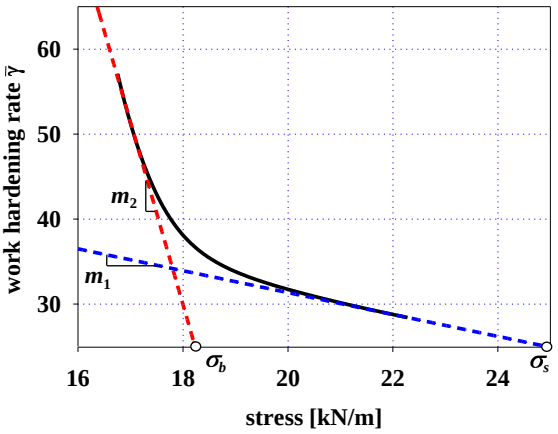

Fig. 4.5. Identification of parameters m_1, m_2, σ_b, σ_s

- The constant D_0 corresponds to the highest possible strain rate that can arise in the material. It is usually arbitrary selected on the base of the literature study. For example, in [40] and [114] the parameter D_0 is set at 10^4 1 s^{-1} for the strain rate of 10 s^{-1}, while for the higher strain rates (10^1-10^3 s^{-1}) $D_0 = 10^6$ s^{-1} is proposed. For the analysis of explosions it reaches even $D_0 = 10^8$ s^{-1}.
- As an example, the first variant (equation (4.12)) of the Bodner-Partom constitutive equation is used. Combining equation (4.17) with equation (4.18) upon the assumption that at the beginning, at very low inelastic strains ($\varepsilon_p = 0.2\%$), the isotropic hardening is almost identical to its starting value $R \approx R_0$ and the kinematic hardening has not appeared yet, (therefore $D \approx 0$), the initial yield limit σ_{02} for the Bodner-Partom model can be obtained in the form

$$\sigma_{02} = \left[\frac{2n}{n+1} \ln\left(\frac{2D_0}{\sqrt{3}\dot{\varepsilon}_p} \right) \right]^{-\frac{1}{2n}} R_0 \tag{4.23}$$

The values of σ_{02} are then determined for three different, but constant strain rates separately. After that, the relation (4.23) allows estimation of the parameters n and R_0 (Fig. 4.6).

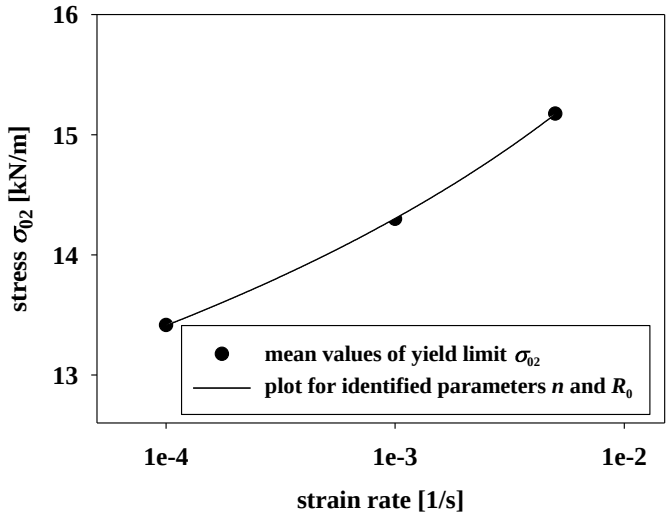

Fig. 4.6. Identification of the parameters n, R_0

- Supposing the equation (4.22) for $\bar{\gamma} = 0$, the parameters D_1 and R_1 can be calculated from the equations:

$$\begin{aligned} D_1 &= \frac{m_2\sigma_b - m_1\sigma_s}{f_1\left(\dot{\varepsilon}_{p02}\right)\left(m_2 - m_1\right)} - R_0 \\ R_1 &= \frac{m_2\sigma_s - m_2\sigma_b}{f_1\left(\dot{\varepsilon}_{p02}\right)\left(m_2 - m_1\right)} + R_0 \end{aligned}, \tag{4.24}$$

where σ_b and σ_s are the points at which tangents with m_2 and m_1 slopes, respectively, intercept the stress axis at the $\bar{\gamma}\left(\sigma\right)$ plot (Fig. 4.5).

4.5 Summary

In this chapter, the constitutive laws carefully chosen for behavior analysis of technical fabrics have been presented. A detailed description of the piecewise linear model, the viscoelastic Burgers model and the viscoplastic Bodner-Partom model has been given. The necessary equations, transformations and identification procedures have been also included.

5 Experimental study

5.1 Introduction

The laboratory tests performed for the requirements of this study have been realized in Institute PRISME at the University of Orleans and at Gdańsk University of Technology in Faculty of Civil and Environmental Engineering, Department of Structural Mechanics.

5.2 Laboratory equipment

To realize a wide spectrum of mechanical tests, a special laboratory equipment is necessary. In the present study four high-classed strength machines have been used. The strength machine Zwick Z020 with the video extensometer is designed for performing the whole range of various uniaxial tests (Fig. 5.1). The machine for biaxial tests is a combination of four Zwick Z020 apparatus set by pairs in two perpendicular directions (Fig. 5.2). Like previously, it uses the same video-extensometer measuring system. The strength machine Zwick Z400 with mechanical extensometer is accompanied by thermal chamber, which is able to obtain temperatures ranging from -70°C to +250 °C with precision of 0.1 °C. (Fig. 5.3). The last equipment set is a 10-stands machine for the long-lasting rheological creep experiments with the maximum load of 3 kN per stand (Fig. 5.4). It is equipped with induction and laser measurements devices. It should be noted that the author of the presented study has been one of the main designers of this machine. He has personally coordinated whole necessary constructing and manufacturing processes of this device.

All presented strength machines are fully computers controlled (except the machine for creep tests, where load is put by hand through steel plates) with constant electronic registration of user-selected properties, which for realization of this study has been: time, force, grips separation and video-extensometer gauge length change (if possible).

Fig. 5.1. Zwick Z020 with video-extensometer

Fig. 5.2. Zwick strength machines for biaxial tests with video-extensometer

Fig. 5.3. Zwick Z400 with thermal chamber

Fig. 5.4. Experimental 10-stands machine for creep tests

5.3 Samples and tests

Two different technical fabrics in the present study has been tested: VALMEX and AF9032. Both of them are the PVC coated polyester reinforced fabrics. Table 5.1 summarizes the basic information of these architectural fabrics ([107], [189]).

Table 5.1. Basic information of the VALMEX and AF9032 technical fabrics

Trade name of fabric	Valmex FR 1000 Hallentype III Universal	Shelter-Rite AF9032
Year of production	1988/89	2010
Trademark Holder /Supplier	Mehler Company	Seaman Corporation
Base fabric weight	(no data)	339 g/m^2
Finish fabric weight	1200 g/m^2	1085 g/m^2
Thickness	0.95 mm	1.04 mm
Fibres	polyester	polyester
Coating	PVC	PVC
Tensile strength (warp/fill)	110/110 kN/m	115,6/115,6 kN/m

VALMEX FR 1000 Hallen type III Universal

The VALMEX fabric has been produced by German company Mehler Texnologies in early nineties of the previous century. The type FR 1000 Hallen type III Universal analyzed in this study is no more manufactured. Some examples of VALMEX fabric applications realized up to now are presented in Section 1.3 in Fig. 1.3-Fig. 1.7.

Two different kinds of the same VALMEX FR 1000 Hallen type III Universal fabric have been examined in this study. The first one is the fabric used for 20 years as the canopy of the Forest Opera (called throughout the whole thesis - the USED material). For more details the reader should refer to Section 1.3.1. One should conclude that during exploitation for almost 20 years the first VALMEX material type underwent at least 20 cycles of stretching and unstretching, and additionally was exposed to environment influences all the time. It has confidently underwent ageing, in both weathering and mechanical aspects. The second kind of VALMEX fabric is the material from the same production part as the USED one, but it was kept as a spare material to repair the roof if necessary (called throughout the whole thesis - the NOT USED material). It was stored at constant temperature and without light access in a basement of a building, hidden from unfavorable weather conditions. It can be assumed that it has endured only natural, non-

mechanical ageing process (passing time and presence of oxygen have been the only acting factors). The difference in conditioning between both material types is clearly seen when they are visually inspected (Fig. 5.5-Fig. 5.6). On the USED samples, on the outer surface (faced to the sun), the presence of algae and fungi, as well as pollution ash is detected. The change in color between outer and inner surface of the USED samples is visible. If compared to the NOT USED material, the difference in color is obvious.

In order to find differences in mechanical properties between the USED and NOT USED samples separately for the warp and fill direction of a fabric a set of four tests is proposed in this investigation. For a start, the uniaxial tensile tests have been performed to obtain basic tensile properties of the tested materials. To inspect the fabrics performance more precisely in elastic range the author has also carried out the cyclic load-unload tensile tests. The achieved results can be a basis for failure analysis, which is beyond the scope of this study. Then, the biaxial experiments have been executed to show how time impacted interactions between the warp and fill threads. Finally, as the architectural fabrics are most commonly characterized by its viscoelastic properties, the creep test have been realized ([255]).

Fig. 5.5. View on the roof structure of the Forest Opera form the outer and inner position

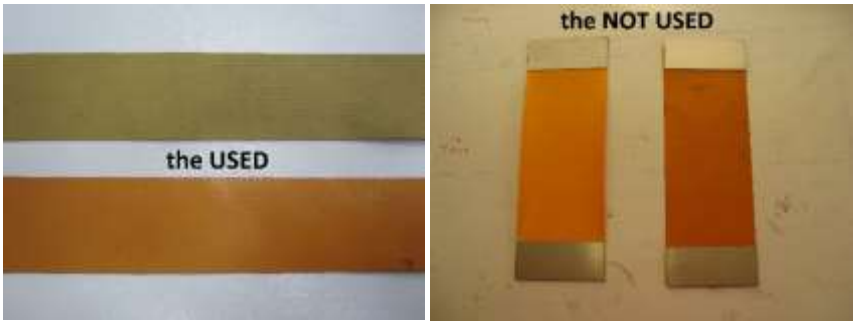

Fig. 5.6. The VALMEX fabric samples. The USED with visible presence of algae and ash pollution on the outer site

AF9032

The architectural fabric AF9032 is produced by American Shelter-Rite subcompany of Seaman Corporation. It is commonly used on the North America continent as presented in example applications in Fig. 5.7-Fig. 5.9. AF9032 fabric has been planned to cover the new roof structure of the Forest Opera in Sopot (Poland) ([5]). It has been of the greatest significance, then, to assess the prospective performance of this material. Therefore, the AF9032 fabric has been subjected to accelerated, artificial ageing at elevated temperature and undergone uniaxial tensile tests afterwards.

Fig. 5.7.Verizon Wireless Amphitheatre, Atlanta, USA [107]

Fig. 5.8. Honolulu International Airport [107]

Fig. 5.9. Rice & Arlington Sports Dome, Minessota, USA [107]

5.4 Experiments

5.4.1 Influence of external environment

5.4.1.1 Uniaxial tensile tests

Uniaxial monotonic tensile tests have been performed to give basis for fabrics properties description by simple piecewise linear model and viscoplastic Bodner-Partom model. To achieve these goals the tensile tests with three different, but constant strain rates of 0.005, 0.001, 0.0001 1/s have been conducted. Dimensions of the specimens have been chosen according to the ISO 1421 national standard ([122]). The width of a specimen has been 50±0.5 mm, while the grip separation has been set to 200±0.5 mm. The strength machine Zwick Z020 with a video-extensometer has been used for the testing. For purpose of this work the following components have been recorded during each test: time, force and video-extensometer gauge length. For each strain rate, for the USED and NOT USED type of VALMEX fabric at least 5 tests have been carried out. The testing procedure has been conducted separately for the warp and fill direction.

The representative stress-strain curves obtained for different strain rates for the coated fabric VALMEX are depicted in Fig. 5.10. It shows that the fabric exhibits rate-dependent behavior for the NOT USED and USED samples. The results of the remaining tests are collected in Annex 1A. Comparing both fabric types, it can be noticed that for the warp direction the change in strain rate causes lower variations of the material response. It is probably the result of tensioning the USED fabric during service, causing decrease in flexibility and increase in stiffness of the material. For the fill direction the strain rate has influenced both fabrics types response with similar scale. The dependence on experiment rate indicates that viscous constitutive models can be implemented for the performance description of this textile.

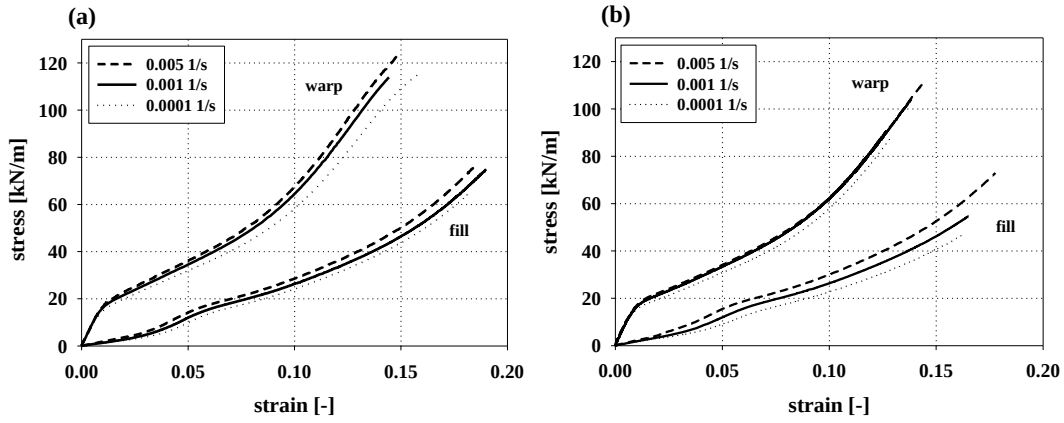

Fig. 5.10. Typical stress-strain curves for the NOT USED (a) and USED (b) samples of the technical fabric VALMEX for different strain rates - uniaxial tensile tests

During the analysis of the stress-strain trajectories, it is possible to distinguish three or four particular ranges for the warp and fill direction of the fabric, respectively. The experimental curve

for the fill direction is more complex in its initial stage. Below the stress level of about 20 kN/m for the warp direction there is only one distinct linear phase, while for the fill direction two stages of different slopes can be observed. The difference is probably caused by various weaving technics in both fabric's directions. The threads in the warp direction are straight and the threads of the fill are interspersed through them. Besides, the yarns in the warp direction are usually pre-stressed during manufacturing coating process, which technic infrequently occurs for the fill direction.

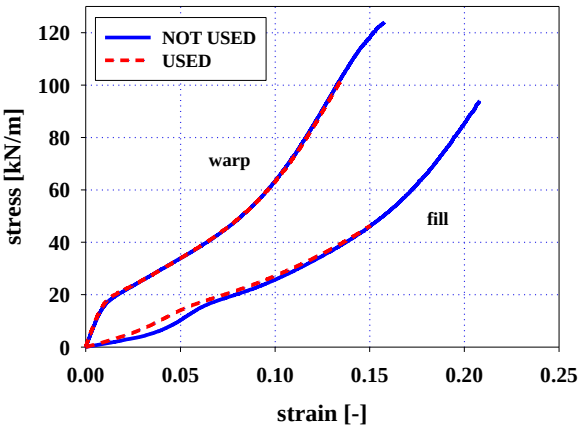

Fig. 5.11. Example of the uniaxial tensile tests for the USED and NOT USED VALMEX fabric for a strain rate of 0.001 1/s

Fig. 5.11 shows the difference between the USED and NOT USED type of membrane. For the warp direction the experimental tests have been repeatable and have always given the same response. On the contrary, for the fill direction the greatest differences at the beginning of the stress-strain curve is observed. It is an interesting phenomenon that will be studied in further part of this research. The illustrative result for one strain rate is given, as for the other strain rates the outcomes are very similar and show the same tendencies. All experimental tests for two types of VALMEX fabric and for the warp and fill direction separately are presented in Annex 1A.

5.4.1.2 Biaxial tensile tests

The author has conducted the biaxial tensile tests to follow the response of the VALMEX fabric by the piecewise linear model likewise in the case of the uniaxial tensile tests.

The tests with crosshead speed of 100 mm/minute (the same in each direction) have been conducted on the special cruciform samples. The specimen width has been 100 mm, whereas the grip separation has been 300 mm in each direction. The biaxial strength machine has been used for these tests. Like previously, the following components have been recorded during each test: time, force and video-extensometer gauge length. For each type of VALMEX fabric 3 tests have been carried out.

In Fig. 5.12 the results of stress versus strain plots are shown for the warp and fill direction of the VALMEX fabric. As for the uniaxial tests, the same trend is noticed here: results of the warp direction are similar paralleling the USED and NOT USED samples, whereas for the fill direction the greatest difference arises in the beginning part of the stress-strain curve. In the case of the biaxial tests the discrepancies for the fill direction are more pronounced. Additionally, it can be observed that for the biaxial tests the results of ultimate tensile strength are distinctly lower than for the uniaxial tests for both material directions. Only one typical test of the USED and one of the NOT USED sample are demonstrated, as the rest of outcomes are analogous. All experimental tests for two types of VALMEX fabric are given in Annex 2.

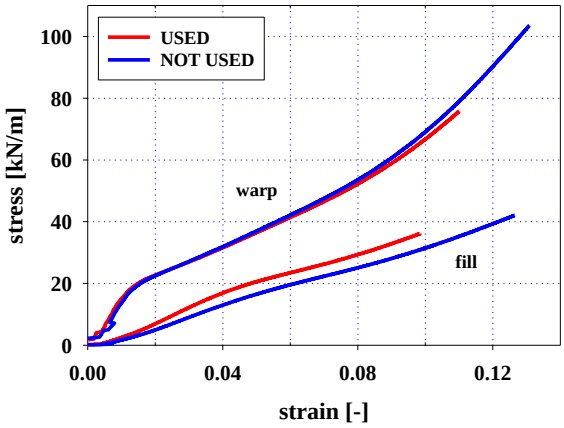

Fig. 5.12. Results of biaxial tests for the warp and fill direction of the USED and NOT USED VALMEX fabric

5.4.1.3 Load-unload tensile cyclic tests

The load-unload tensile cyclic tests of the USED and NOT USED VALMEX samples have been conducted with the constant strain rate of 0.001 1/s in both the loading and unloading phase. In each subsequent cycle the peak strain level has been increased by 1.5% of the total strain increment. The relaxation periods of 10 s only have been realized each time the phase has changed. Also here the width of a specimen has been 50±0.5 mm, while the grip separation has been set to 200±0.5 mm. The strength machine Zwick Z020 with video-extensometer has been used for the testing. The recorded values of force, elongation and time has been used to calculate the overall material response in the form of stress-strain curves. For both types of VALMEX fabric and for each direction 4 specimens have been tested.

The example results of the VALMEX fabric are presented in Fig. 5.13. Once again, the response for the warp direction is more repeatable and the discrepancies between the USED and NOT USED samples quite low in comparison to differences observed for the fill direction. The results of a single typical test is given here due to its complex form and to the fact, that the rest of the test results are very alike and express the same tendencies. All load-unload tensile cyclic tests

for two types of VALMEX fabric and for the warp and fill direction separately are included in Annex 3A.

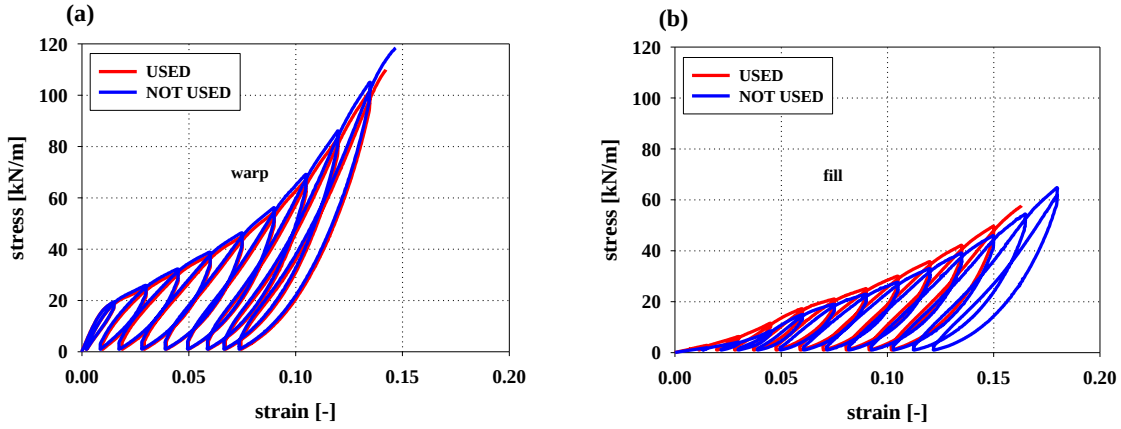

Fig. 5.13. Results of load-unload tensile cyclic tests for the warp (a) and fill (b) direction of the USED and NOT USED VALMEX fabric

5.4.1.4 Creep tests

In the present research the viscoelasticity of architectural fabrics has been investigated by short and long term creep tests. The short term creep tests have been performend on the strength machnie Z020 and have lasted 48 hours and have included stress level of 40kN/m for the warp direction and three stress levels of 10, 20 and 40kN/m for the fill direction. The long-term experiments have had duration of about 1 month for the fill direction and 2 weeks for the warp direction. The identicial stress level of 30 kN/m for both directions has been introduced. All the tests have been conducted for the USED or NOT USED VALMEX samples. The width of a specimen has been 50±0.5 mm, while the grip separation has been 150±0.5 mm. In case of the short term tests only one sample has been tested for each stress level for each direction, while in case of the long term tests two samples have been used for each direction. The strength machine used for this study has been the 10-stands apparatus for long-lasting creep tests.

In Fig. 5.14 (short-term experiments) and Fig. 5.15 (long-term experiments) the plots of strain versus time are presented for each level of creep stress for both material directions.

It is clearly seen that for the warp direction there is no difference between the USED and NOT USED fabric. On the contrary, for each stress level in the case of the fill direction the discrepancies are great reaching about 3-4% of the total strain. The responses of the NOT USED material always give greater values of strain level. It can be explained by the fact, that the USED material have been tensioned during service getting the permanent elongations, so its initial strain due to the creep test would be always lower than for the NOT USED fabric. However, the absence of differences in the case of the warp direction does not match to this clarification. One have to remember, that the yarns in the warp direction are usually pre-tensioned during manufacturing process, what can be the possible explanation. As a consequence, the stress put to the material in

the warp direction during creep test have not influenced at all the already prestressed yarns. It may suggest, that during manufacturing, the yarns in the warp direction must have been tensioned to higher level.

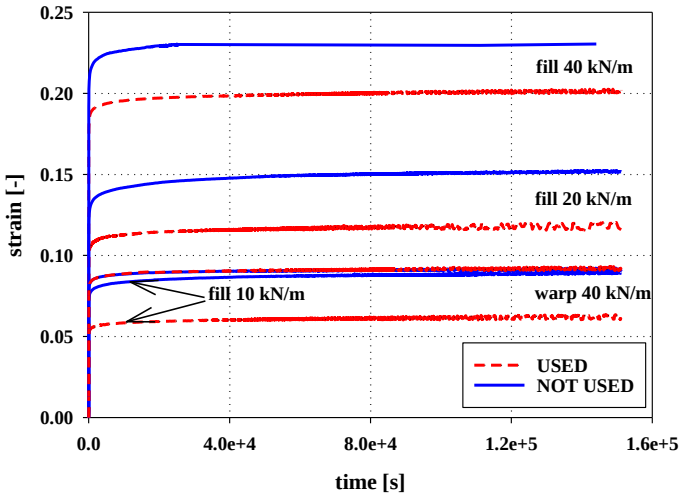

Fig. 5.14. Results of short-term creep tests for the warp and fill direction of the USED and NOT USED VALMEX fabric

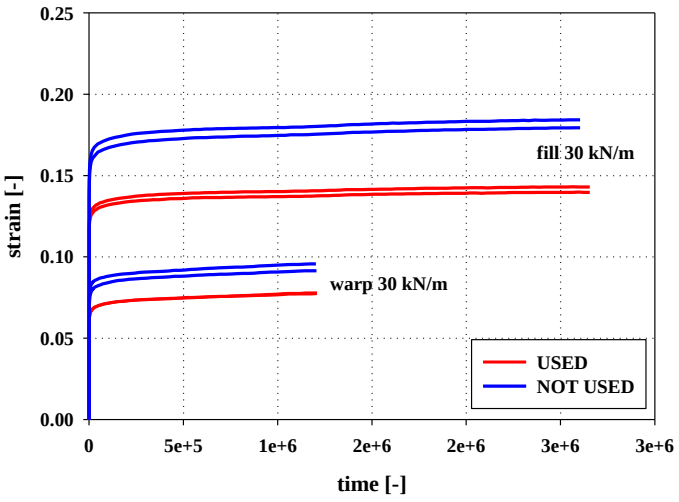

Fig. 5.15. Results of long-term creep tests for the warp and fill direction of the USED and NOT USED VALMEX fabric

5.4.2 Artificial thermal ageing

In the present work it has been decided to induce an accelerated ageing by the thermal treatment that is one of the most commonly used method. The factor of the highest importance in this case is obviously the level of ageing temperature. The temperature of accelerated ageing for polymers should be established at the level below the glass transition temperature T_g to ensure that the physical ageing takes place. Additionally, the ageing temperature cannot initiate any

chemical processes that would never occur in the normal outdoor service performance of a composite material.

The analyzed here architectural fabric AF9032 is composed of polyester reinforcement (in the form of fabric mat) and PVC coating. Producer has not provided any information about chemical mixture for any of used component materials. Therefore, a comprehensive study of literature in this subject has been realized. The glass transition of the PVC is generally established at 80-87°C ([48], [169]), while for the polyester it is set between 100-180°C ([177]). It must be remarked here, that the glass transition temperature can changed due to exposure period. It is commonly observed and studied phenomenon ([1], [70]). The melting temperature of PVC ranges between temperature of 160°C and 260°C ([242]), while polyester material can resist even 250 - 290°C ([203], [164]). The producer guarantees that roofing membrane AF9032 can be used in the temperatures ranging from -40°C up to +70°C. However, the temperature on the surface of roofing material can sometimes reach higher values, especially during sunny summer periods. Besides, the color (especially dark colors) of material plays here the crucial role, as it absorbs radiation causing temperature increase in the material to the level of 70°C for white color and even 98°C for black color [192]. It is important remark, as the material during exposure mostly change its basic color becoming darker. It is affected by chemical process and also surface changes owing to growth of fungi, algae etc. and pollution ash settlement. A huge scientific research has been realized up to now in the subject of thermal ageing of PVC and polyester composite materials. A part of it is summarized in Table 5.2 with information of the material and temperature used for the artificial laboratory ageing.

Taking into account all of above facts, it has been decided to carry out simulation of ageing at two main temperatures: 80°C and 90°C. The thermal chamber with constant air flow, which enables to obtain the temperatures ranging from -70°C to +250 °C has been used for inducing artificial ageing process. The strip samples of 300x50 mm have been cut in both material directions and then have been subjected to the thermal ageing with relative humidity of 50%. The first part has been maintained for the period of 5 weeks at 90°C while the second one for 12 weeks at 80°C. Every week (for 90°C case) or every two weeks (for 80°C case) the part of specimens has been withdrawn and kept at room temperature for the following week before testing. To track only the temperature influence on the material behavior the additional reference tests of the specimens maintained only for 1 hour at elevated temperature of 80°C and 90°C (and then consequently 1 week at room temperature) has also been carried out.

For each part of the AF9032 fabric maintained at elevated temperature the uniaxial tensile test with three different strain rates have been carried out. For each strain rate 2 samples for the warp and 2 samples for the fill direction have been conducted. Totally, it has made up six tests for one material direction.

Table 5.2. PVC and polyester materials with their ageing temperature based on literature study

Material	Ageing temperature [°C]	Reference
PVC flooring and sheathings	80	[251]
plasticized PVC	63; 80; 110; 120	[124], [27], [28]
thin films of PVC-based compounds	65; 80; 95; 110	[200]
PVC pipes	84; 85	[157]
0.7 mm sheets simulating cables or sheathings	80; 90; 100; 110	[129]
rigid PVC	60	[192]
jute-roving-reinforced polyester composites	100	[3]
polyester/glass fiber reinforced composites	60; 63; 70	[177], [236]
polyester non-woven membrane	80	[180]
PVC blended with various polyesters	90	[231]

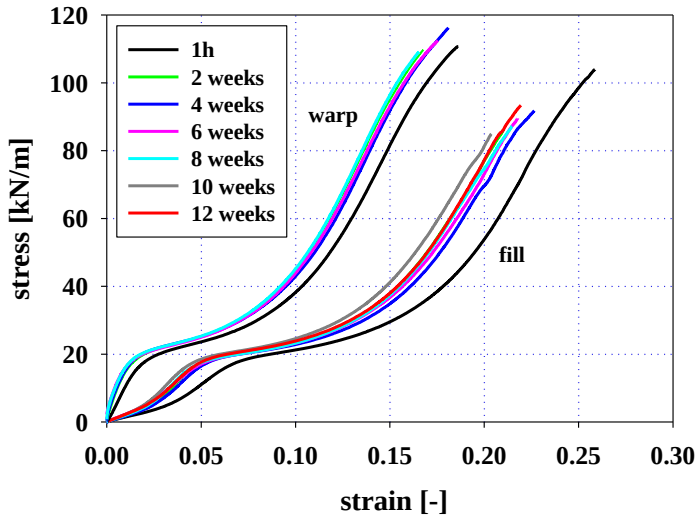

Fig. 5.16. Influence of time with thermal ageing at 80°C on the stress-strain response for the warp and fill direction of the AF9032 fabric for the strain rate of 0.001 1/s

The results of all experiments are given in Annex 5A, here some examples of the stress-strain curves for the temperature of 80°C and a strain rate of 0.001 1/s are presented (Fig. 5.16). There is an outstanding difference between ageing for 1 hour (1h) only and the rest of proposed periods. For the case of the warp direction the ageing time seems not to affect the material response very much. For the fill direction the discrepancies are more distinct, implying that increase in ageing time results in increase in the stiffness and decrease in the ultimate tensile strength.

5.5 Summary

The main aim of this chapter has been to demonstrate the experimental study performed to gather data for the further parameters identification and analysis purpose. Therefore, it contains

the detailed overview of technical fabrics types under investigation, as well as all laboratory setup and test procedures, which have been performed during realization of this research.

All experimental work has been performed with the highest possible to achieve precision during the realization and during elaborating the results. The author has carried out all of the presented experiments personally and also all elaboration of results has been done by him. Some of the presented experimental devices have been as well developed by him.

6 Parameters determination and analysis

6.1 Introduction

Every identification study should be accompanied by the calculation of some basic statistical values. They usually give the overall quantity and quality view on the performed experiments and identification procedures. The principal mathematical value used throughout the presented study is the arithmetic mean value defined as follows ([232])

$$MEAN = \bar{x} = \frac{1}{n}\sum_{i=1}^{n} x_i \,, \tag{6.1}$$

where x_i is an *i*-th value from the size *n* set, representing values from the particular experiment or identification. Then, the standard deviation (defined as the measure of the variability or dispersion of the obtained results from the average value) is calculated

$$SD = \sqrt{\frac{1}{n-1}\sum_{i=1}^{n}\left(x_i - \bar{x}\right)^2} \,. \tag{6.2}$$

For required in this study an approximation purpose, the curve fitter tool built in the commercial program SigmaPlot has been used. The linear and non-linear regression methods with the Marquardt-Levenberg minimizing algorithm ([162], [168]) have been used for finding the best fit between a proposed equation and the data. This algorithm searches for the values of parameters that minimize the sum of squares differences between the observed values and the predicted values of the dependent variable

$$SS = \sum_{i=1}^{n} w_i \left(y_i - \hat{y}_i\right)^2 \,, \tag{6.3}$$

where SS is the minimized sum, y_i, $\hat{y}_i$ are the observed and the predicted value of the dependent variable, respectively, and w_i is the weight parameter. To assess the quality of performed regression the coefficient of determination R^2 and correlation $R = \sqrt{R^2}$ have been calculated ([62], [143])

$$R^2 = \frac{S_t - S_r}{S_t}, \quad S_r = \sum_{i=1}^{n}\left(y_i - f_i\right)^2, \quad S_t = \sum_{i=1}^{n}\left(y_i - \bar{y}\right)^2 \,, \tag{6.4}$$

where f_i is an *i*-th value of a function obtained in approximation. The values of the correlation coefficient come from the range $R \in \langle 0;1 \rangle$, where the value *R*=1 means full fitting and is the most desirable result.

6.2 Influence of outdoor environment

6.2.1 Strength parameters for uniaxial and biaxial tensile tests

At first, the estimation of the tensile properties of the material has been done. For the warp direction two (E_{Wi} , where *i*= 1,2) and for the fill direction three (E_{Fj} , where *j*= 0, 1, 2) inclination coefficients (longitudinal stiffnesses) for characteristic linear sections have been determined (Fig. 6.1). The intersections points ($\varepsilon_{0/1}$; $\varepsilon_{1/2}$; ε_f) have been calculated resulting in the applicability ranges of the particular longitudinal stiffness values. The values of the longitudinal stiffness and the intersection points have been obtained as the mean values of all the tests from all three strain rates of the uniaxial tests, separately for the warp and fill direction. As the biaxial tests have been performed with the same crosshead rate in both material directions, the results of piecewise model parameters have been calculated as the mean value from all the tests, regarding the warp and fill direction. The author limited the study of fabrics behavior to the strain level of 0.05 in the warp ($\varepsilon_f = 0.05$), and to the strain level of 0.1 ($\varepsilon_f = 0.1$) in the fill direction. This restriction is applied due to the practical and designing reasons. These elongations correspond to the stress levels and geometrical requirements usually practiced in civil engineering structures ([51]).

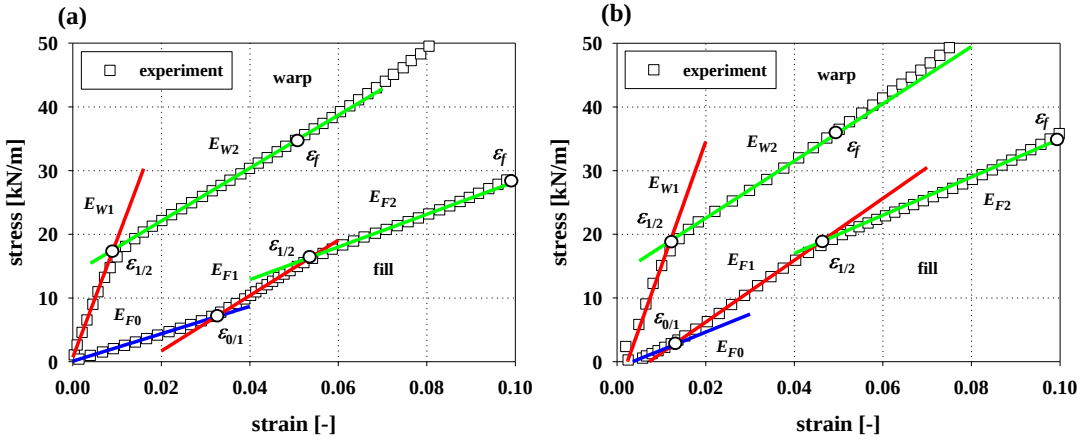

Fig. 6.1. Typical stress-strain curves of coated fabrics with characteristic linear sections for uniaxial (a) and biaxial (b) results)

The obtained results are collected in Table 6.1 and Table 6.2 for the uniaxial and biaxial tests, respectively. The relative difference has been calculated according to the formula $\delta = \left[(\text{NOT USED} - \text{USED}) / \text{NOT USED}\right] \times 100\%$. The main change between the USED and the NOT USED VALMEX samples can be noticed in the fill direction for the slope E_{F0}, which is related to the covering material – PVC. For the USED fabric the modulus E_{F0} is about 32 % (uniaxial) and 21% (biaxial) higher than for the NOT USED material. It comes from the fact, that the PVC has apparently become more rigid due to the environmental ageing. This phenomenon

is wider studied in the Section 6.2.2. Next, the inclinations E_{W1}, E_{F1} have been analyzed. They are related to the polyester yarns of fabric reinforcement and can be assumed as the moduli of the material in elastic range for the warp and fill direction, respectively. The values of E_{W1}, E_{F1} stiffness for both types of VALMEX fabric generally does not change, except for the case of biaxial testing for the results in the warp direction (difference of about 11%). This outcome indicates that the polyester yarns have kept their initial elastic properties for 20 years. It suggests that polyester yarns have been sufficiently protected by PVC coating from unfavorable external conditions or that the polyester yarns are not sensitive for external environment influence at all.

Table 6.1. Results of uniaxial tensile tests – strength parameters

Direction		WARP			FILL		
Fabric type		NOT USED	USED	δ	NOT USED	USED	δ
Parameter	Unit	Strength parameters & non-linear piecewise model parameters					
E_{F0}	[kN/m]	-	-	-	143 ± 24	189 ± 7	-32
$\varepsilon_{0/1}$	[-]				0.0356 ± 0.0005	0.0345 ± 0.0002	3
$E_{F1}; E_{W1}$	[kN/m]	1828 ± 32	1803 ± 66	1	377 ± 28	391 ± 11	-4
$\varepsilon_{1/2}$	[-]	0.0091 ± 0.0003	0.0088 ± 0.0005	4	0.0576 ± 0.0004	0.056 ± 0.002	2
$E_{F2}; E_{W2}$	[kN/m]	419 ± 8	396 ± 7	5	238 ± 10	252 ± 4	-6
UTS	[kN/m]	117 ± 3	100 ± 9	14	63 ± 9	61 ± 3	3
ε_{ult}	[-]	0.150 ± 0.001	0.136 ± 0.006	9	0.181 ± 0.016	0.173 ± 0.004	5
σ_{02}	[kN/m]	16.7 ± 1.0	17.1 ± 1.1	-2	14.6 ± 1.2	16.7 ± 0.8	-15

Table 6.2. Results of biaxial tensile tests – strength parameters

Direction		WARP			FILL		
Fabric type		NOT USED	USED	δ	NOT USED	USED	δ
Parameter	Unit	Strength parameters & non-linear piecewise model parameters					
E_{F0}	[kN/m]	-	-	-	401 ± 4	486 ± 4	-21
$\varepsilon_{0/1}$	[-]				0.048 ± 0.002	0.045 ± 0.002	6
$E_{F1}; E_{W1}$	[kN/m]	2204 ± 19	1954 ± 14	11	280 ± 6	282 ± 2	-1
$\varepsilon_{1/2}$	[-]	0.012 ± 0.0001	0.012 ± 0.0005	0	0.094 ± 0.008	0.080 ± 0.003	14
$E_{F2}; E_{W2}$	[kN/m]	478 ± 8	449 ± 8	6	387 ± 2	365 ± 3	6
UTS	[kN/m]	97 ± 6	75 ± 1	23	40 ± 2	36 ± 1	10
ε_{ult}	[-]	0.127 ± 0.004	0.109 ± 0.001	14	0.121 ± 0.005	0.100 ± 0.001	18
σ_{02}	[kN/m]	18.2 ± 0.7	16.8 ± 0.6	8	17.8 ± 0.7	20.0 ± 0.8	-12

The ultimate tensile strength (*UTS*) declines for the USED material of about 10-23 %, with exception for the uniaxial test in the fill direction. The values of the elongation at break (ε_{ult}) decrease for all cases, achieving for the biaxial tests even 18% of reduction in the fill direction. These observations confirm that the ultimate strength parameters (*UTS*, ε_{ult}) have been influenced by working and environmental conditions, as well passing time. In the fill direction for the uniaxial tests the drops of parameters values are not high. The threads in this direction have been crimped during a weaving and coating process, what resulted in their higher elongation limits when they are simply tensioned. However, during the biaxial test, when interrelation between the

warp and fill yarns appears, the material in the fill direction loses its high ultimate strength. It indicates, that for comprehensive analysis of the technical fabrics behavior, the biaxial tensile tests are obligatory. The outcomes of the yield limit σ_{02} (found for the 0.02% of the total elongation) show that it grows for the USED fabric, especially in the fill direction (15% of rise for uniaxial tests). It stays in accordance with the reasoning described before. The USED material have been tensioned during service therefore the yield limit σ_{02} has increased. The yarns in the fill direction, initially crimped, have been firstly straightened and then tensioned under working conditions and therefore the greatest growth of the yield limit σ_{02} is observed in this direction. The other obtained parameters do not change their value.

Summing up the uniaxial and biaxial tensile tests, it can be concluded that the environmental conditions and the service tension have influenced primarily stiffness properties of the PVC coating. Properties of the polyester yarns have been unaffected by ageing, only the ultimate strength properties have decreased. All in all, the technical fabric VALMEX has maintained its initial elastic tensile properties over 20 years of working and could probably perform further as the roof structure without breakdown for next years. However, in this particular case, the roof had to be replaced due to bad condition of the sewed links of the fabric.

6.2.2 Analysis of cyclic load-unload tests

The cyclic tests have been performed to compare the USED and NOT USED material performance under changing loading conditions and to examine behavior in the elastic region of the deformation, primarily in the fill direction. In the procedure proposed here, each unloading and then successive reloading cycle has been separately approximated by a linear function $f(x) = a \cdot x + b$. Inclinations a representing longitudinal moduli) of the achieved straights are denoted, then, as E_{DOWN} and E_{UPP} for the unloading and reloading phase, respectively. The results from both loading stages are very similar to each other, so the value of the longitudinal modulus for every cycle has been calculated as the mean value of the E_{DOWN} and E_{UPP}. The short relaxation periods between each loading phase have been omitted in the identification process. This methodology is presented for several cycles in Fig. 6.2 for the warp and fill direction.

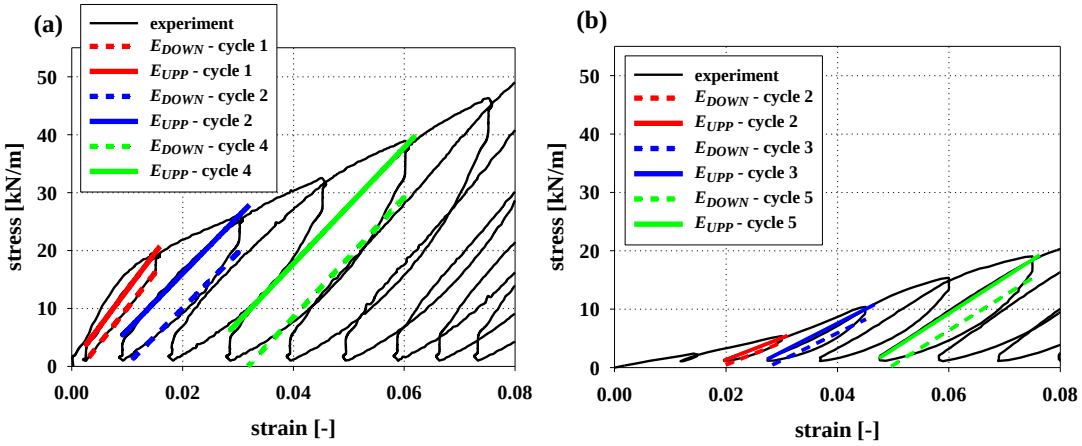

Fig. 6.2. Methodology of elastic modulus identification in each load-unload cycle for the warp (a) and fill (b) direction

The procedure has been executed for the USED and NOT USED VALMEX samples, for the warp and fill direction and its results are gathered in Table 6.3. More detailed tables can be found in Annex 3B.

Fig. 6.3 shows the mean value of the elasticity modulus for each cycle for the warp and fill direction separately. The author has assumed the loading loop consists of the unloading and then reloading stage. Due to that fact, the cycle number "0" refers to the very first loading phase that does not have any preceding unloading part (Fig. 6.2). Comparing the NOT USED and USED material the difference are not very pronounced. There greatest discrepancy is detected for the "0" cycle, which for the warp direction corresponds to the immediate elastic modulus and for the fill direction for the stiffness of the coating made of PVC. This observation will be studied comprehensive in the further section of this chapter. Another reflection during studying Fig. 6.3 concerns number of cycles that each type of VALMEX has experienced and the evolution of the related elasticity moduli. In the case of the warp direction the NOT USED samples are a bit more robust, while for the fill direction the results are opposite. One should remember that the USED material underwent about 20 long-time cycles of stretching and unstretching during installation repeated every year of its usage. Additionally, the warp direction is the main working direction, characterized by higher strength properties and lower elongations ranges. These properties come from the pretension during manufacturing process resulting in the straight threads in the warp direction.

Therefore, the author concludes that the material in the warp direction has gained its ultimate elongation limit and the elasticity modulus started to decrease gradually (damage occurred – red squares below blue circles in Fig. 6.3). For that reason the USED fabric has endured one cycle less that the NOT USED one. At the same time, material in the fill direction has been tensioned with equal number of cycles, however to the lower stress level than for the warp direction. It resulted in hardening of the material (red squares above blue circles in Fig. 6.3), but still far from

its elongation limit. Therefore, it can be concluded that the damage has not occurred yet. Thus, both VALMEX types for the fill direction have experienced the same amount of cycles. The last investigated phenomenon, is the overall behavior of the material. For the warp direction, for both materials types, the elasticity modulus first decreases rapidly and then begins to grow from the fourth cycle (Table 6.3). In the meantime, the material in the fill direction exhibits increasing trend from the very beginning, additionally with several distinct phases of almost linear growth.

The load-unload cyclic tests are commonly performed for estimation of the damage influence on the elastic properties of a material. It is one of the indirect methods for damage measurement ([161]). However, the damage analysis is out of the scope of the presented study and will be investigated in the further research.

Table 6.3. Moduli identified for the cyclic unload-reload tensile tests for the warp and fill direction of the USED and NOT USED VALMEX fabric

		WARP				FILL			
		NOT USED		USED		NOT USED		USED	
Cycle number	Phase	Value [kN/m]	E_{MEAN} [kN/m]	Value [kN/m]	E_{MEAN} [kN/m]	Value [kN/m]	E_{MEAN} [kN/m]	Value [kN/m]	E_{MEAN} [kN/m]
0	E_{UPP}	1856	**1856**	1793	**1793**	143	**143**	192	**192**
1	E_{DOWN}	1227	**1263**	1214	**1258**	317	**309**	348	**344**
	E_{UPP}	1299		1302		301		340	
2	E_{DOWN}	977	**984**	968	**976**	354	**342**	349	**357**
	E_{UPP}	990		985		331		365	
3	E_{DOWN}	981	**973**	991	**975**	462	**466**	473	**469**
	E_{UPP}	965		958		470		464	
4	E_{DOWN}	1045	**1027**	1043	**1021**	576	**593**	585	**585**
	E_{UPP}	1009		1000		609		586	
5	E_{DOWN}	1137	**1113**	1123	**1096**	617	**623**	621	**626**
	E_{UPP}	1090		1069		630		631	
6	E_{DOWN}	1251	**1222**	1218	**1192**	646	**651**	660	**662**
	E_{UPP}	1194		1165		657		663	
7	E_{DOWN}	1375	**1346**	1348	**1315**	689	**694**	714	**711**
	E_{UPP}	1316		1283		699		709	
8	E_{DOWN}	1506	**1476**	1485	**1449**	740	**740**	774	**767**
	E_{UPP}	1446		1413		740		760	
9	E_{DOWN}	1625	**1596**	1586	**1576**	794	**792**	851	**834**
	E_{UPP}	1566		1565		791		816	
10	E_{DOWN}	1693	**1648**			862	**858**	925	**903**
	E_{UPP}	1603				855		881	
11	E_{DOWN}					941	**932**	985	**958**
	E_{UPP}					923		930	
12	E_{DOWN}					1088	**1046**	1084	**1049**
	E_{UPP}					1004		1014	

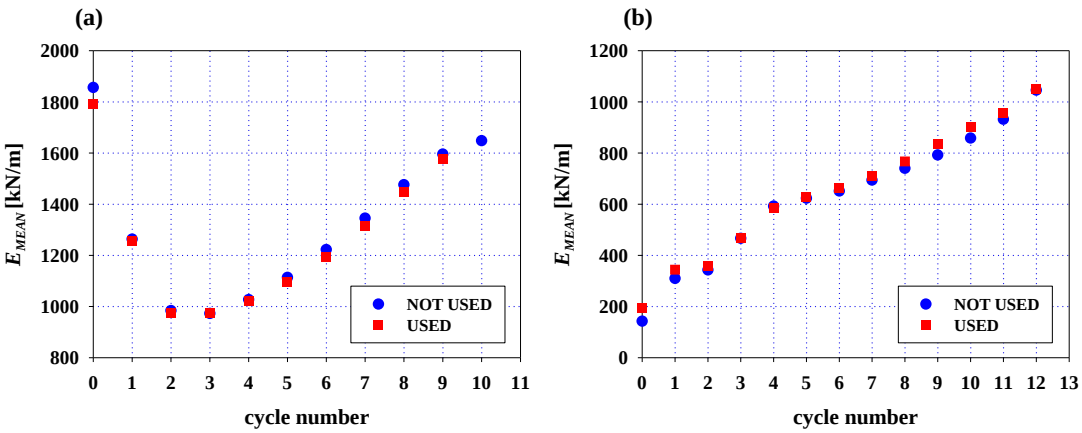

Fig. 6.3. Comparison between the mean values of the longitudinal stiffness E_{MEAN} for the warp (a) and fill (b) direction of the NOT USED and USED VALMEX fabric

The performed analysis has proven that fabric behavior during the initial stage of loading for the fill direction is more complex than for the warp direction.

Taking into account results of the uniaxial tensile tests and cyclic load-unload tensile tests it is possible to perform more detailed analysis of the material properties in the fill direction. The interest is now focused on fabric behavior in the range of the first two longitudinal stiffness values: E_{F0} and E_{F1}. Therefore, the first three unload-load cycles and values of their longitudinal stiffness E_{MEAN} are presented in details in Fig. 6.4. The results of the uniaxial tensile tests with identified values of E_{F0}, E_{F1} and E_{F2} are also drawn in the same graph. It can be observed now, that for both ranges (E_{F0} and E_{F1}) the approximation of cycles gives results very close to the second modulus E_{F1} found from the uniaxial tests. This statement stays true for the USED and also for the NOT USED type of VALMEX fabric. The most reasonable explanation of this phenomenon lies in the composite structure of technical fabrics. During the initial part of the tensile test, the fill threads undergo straightening, as they are primarily crimped due to weaving in the fabric manufacturing process. As a consequence, for the fill direction (limited to about 2-2,5% of total strain) the stiffness modulus E_{F0} (having relatively low value) is mainly related to the mechanical properties of the coating (PVC) and the slippage of the not tensioned fill threads. For that reason it cannot represent the elasticity modulus for the whole fabric in the fill direction. The E_{F1} domain stands for the state, where threads are fully straightened and carry subjected force. Concluding, in the fill direction of the VALMEX material the second modulus E_{F1} should represent the elasticity modulus in a linear range.

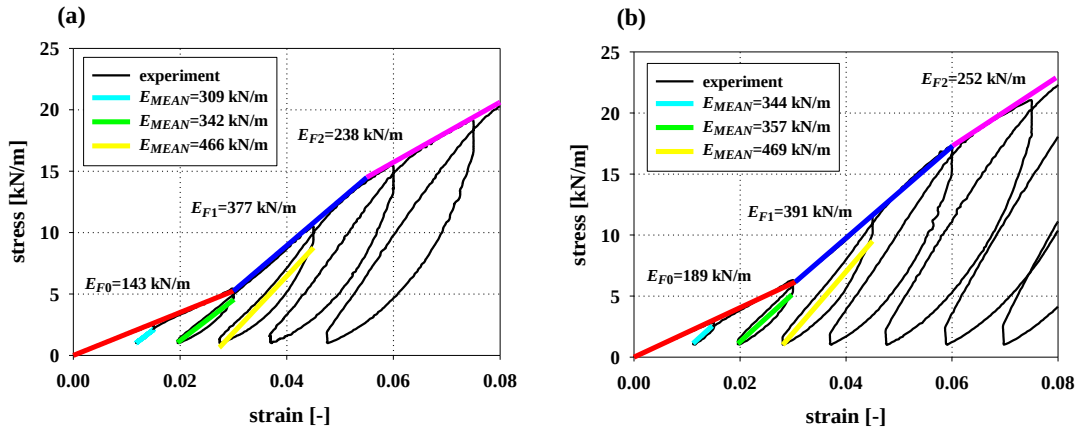

Fig. 6.4. Cyclic test for the fill direction of the technical fabric VALMEX: (a) the NOT USED; (b) the USED

Considering the above observations, it is proposed that the first section of the strain-stress curve for the fill direction can be neglected, for instance in the viscoplastic analysis of this type of material. Consequently, two representations of stress-strain curves below the yield limit are offered: the one-modulus and two moduli concept (Fig. 6.5).

In the first one, the stress-strain curve is shifted accordingly to the stiffness modulus E_{F1} (true value of the Young's modulus) to obtain zero stress for null strains. This approach seems to be mainly useful in the finite element calculations of textile hanging roofs, when stress limits are meaningful. Furthermore, the one-modulus concept would find wider application in the laboratory analysis of the textile materials, where pre-tensioning of the fabric is usually omitted and attention is focused on the durability parameters, e.g. ultimate tensile strength.

In the second proposed concept, both longitudinal stiffness coefficients are taken in the calculations. Therefore, the stress-strain graph is not shifted. This approach can also be presented in a simplified form with neglecting the first value of stiffness modulus and taking the section initially used for shifting the experimental curves as the adopting phase, in which the fill threads undergo undulation (blue line in Fig. 6.5). After being fully stretched (at strain value of about 2-2.5%, with negligible stresses) the fill yarns start to carry the subjected force. This approach presents the real behavior of the fabric under an initial stress state, which is of the key importance during installation on a construction site and plays a great role in the shape analysis of the roofs made of textiles. Besides, the values of E_{F0} modulus and corresponding elongation level can be used for calculation of the fabric compensation, which is important for the cut patterns design during preparation of the technical fabric sheets to fit to a particular structure geometry, especially after installation process of the fabric.

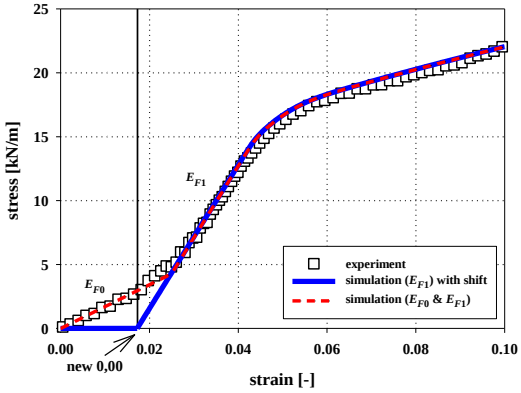

Fig. 6.5. Application comparison of the simulations for the fill direction of technical fabrics

6.2.3 Burgers model parameters - Creep tests

The identification of the Burgers model parameters has been conducted according the algorithm described in Section 4.3. The procedure will be presented here for the sample of the USED VALMEX for the warp direction (sample No. PELZ14). Final identification results of the all tested samples are collected in Annex 4A.

Firstly, the time t_0, at which the pure creep starts (after reaching the stress level $\sigma_0 = 31.7$ kN/m = constant) has been found. The total load has been applied during approximately 5 s, therefore the loading time has been omitted in further calculations ($t_0 = 0$ s). Next, the experimental stress-strain curve has been divided into two parts: the nonlinear (in the time range $t_0 - t_1$) and the linear (in the time range $t_1 - t_2$). The boundary value between these ranges has been set at $t_1 = 2\text{e+}5$ s and the immediate elongation ε_0 has been evaluated from the experimental curve. These initial steps are shown in Fig. 6.6.

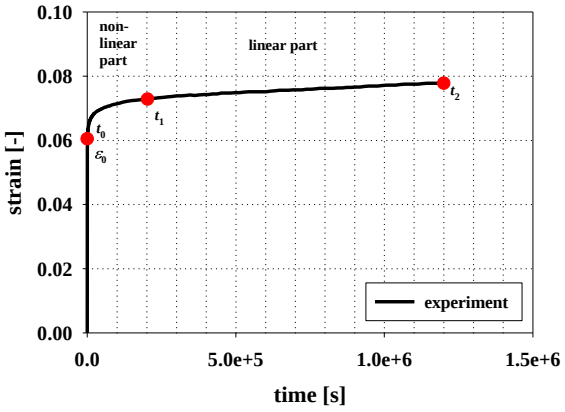

Fig. 6.6. Preparation for identification of the Burgers model – the USED VALMEX fabric for the warp direction (sample PELZ14)

Then, the parameters E_1, E_2, ε_k, η_1 has been determined according to (4.8) - (4.11). Subsequently, these values have been used for the evaluation of the parameter η_2 value from the

nonlinear part of the curve using the least square method. The typical regression with E_1, E_2, ε_k, η_1 as constants failed. Therefore already obtained parameters E_1, E_2, ε_k, η_1 have been treated together with η_2 as unknowns in the regression process. Their values have been used as the initial values. The result values of E_1, E_2, ε_k, η_1 have slightly changed but the value of η_2 has been successfully calculated. Example of these calculations is presented in Table 6.4.
The identification results of all experiments for the NOT USED and USED VALMEX fabric regarding different values of the immediate strain ε_0 and boundary time t_1 are presented in the form of tables in Annex 4B, for the warp and fill direction individually.

Analysis of the obtained results has exposed that the correctness of the identification depends strongly on the value of the immediate strain ε_0 taken for calculations. Therefore the sensitivity analysis with respect to immediate strain ε_0 and the boundary time t_1 has been performed. The Fig. 6.7-Fig. 6.8 present results of the identification and verification process for the USED VALMEX fabric for the warp direction (sample No. PELZ14) for three different levels of ε_0: $\varepsilon_0 = 0.055\ [-]$, $\varepsilon_0 = 0.060\ [-]$ and $\varepsilon_0 = 0.065\ [-]$. The verification has been accomplished by calculating the overall response of the material by using the final values of the obtained parameters.

Table 6.4. Burgers model parameters for the USED VALMEX (the warp direction, $t_1 = 4e{+}5$)

VALMEX - WARP USED						
Initial values	t_0	[s]	0			
	t_1	[s]	4.00E+05			
	t_2	[s]	1.20E+06			
	ε_0	[-]	0.055		0.065	
	ε_1	[-]	0.0742			
	ε_2	[-]	0.0776			
	σ_0	[kN/m]	32			
Calculated values	η_1	[-]	7.47E+09			
	ε_k	[-]	0.0725			
	E_1	[kN/m]	580		450	
	E_2	[kN/m]	1810		4230	
			MEAN	***SD***	***MEAN***	***SD***
Identification results	E_1	[kN/m]	510	10	490	10
	E_2	[kN/m]	3160	80	4220	90
	η_1	[-]	7.47E+09	3.04E+08	7.47E+09	3.04E+08
	η_2	[-]	1.39E+08	9.27E+05	1.40E+08	3.21E+06

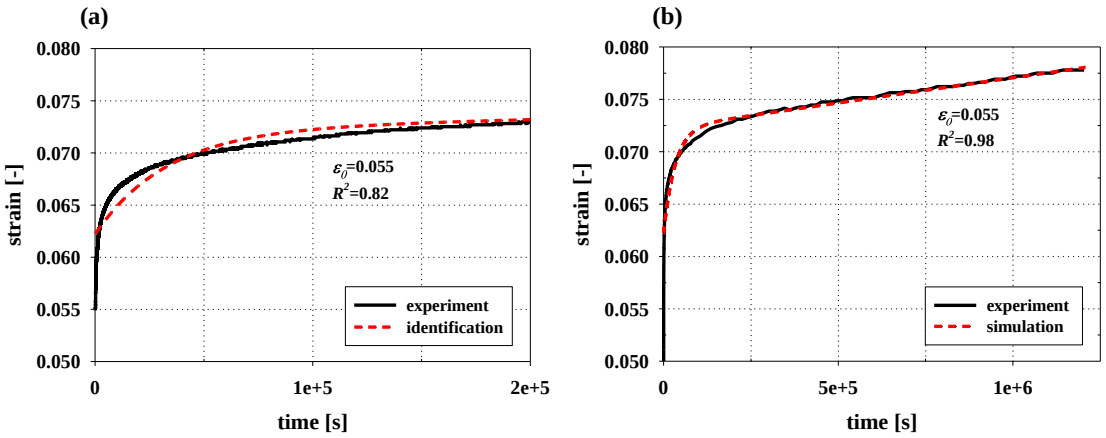

Fig. 6.7. Burgers model parameters for $t_1 = 2\text{e+}5$ s and $\varepsilon_0 = 0.055$ $[-]$: (a) identification of parameters; (b) verification by numerical simulation

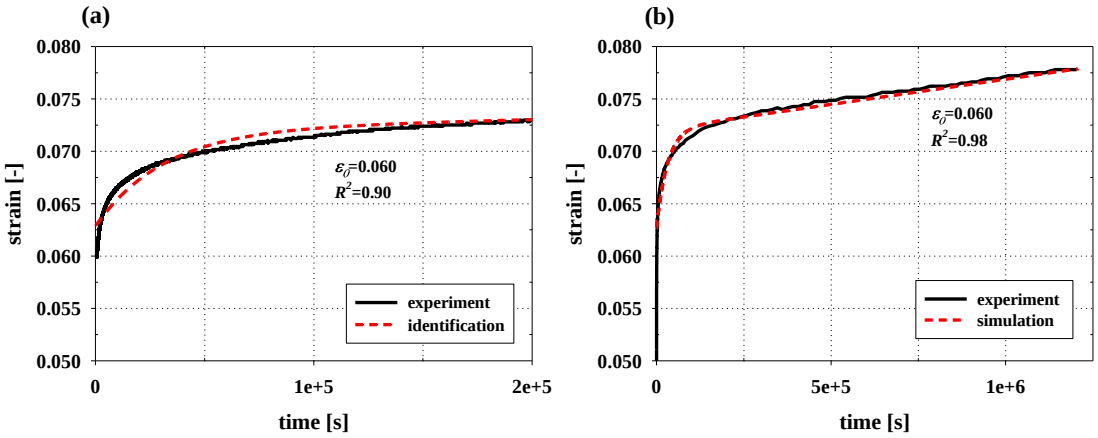

Fig. 6.8. Burgers model parameters for $t_1 = 2\text{e+}5$ s and $\varepsilon_0 = 0.060$ $[-]$: (a) identification of parameters; (b) verification by numerical simulation

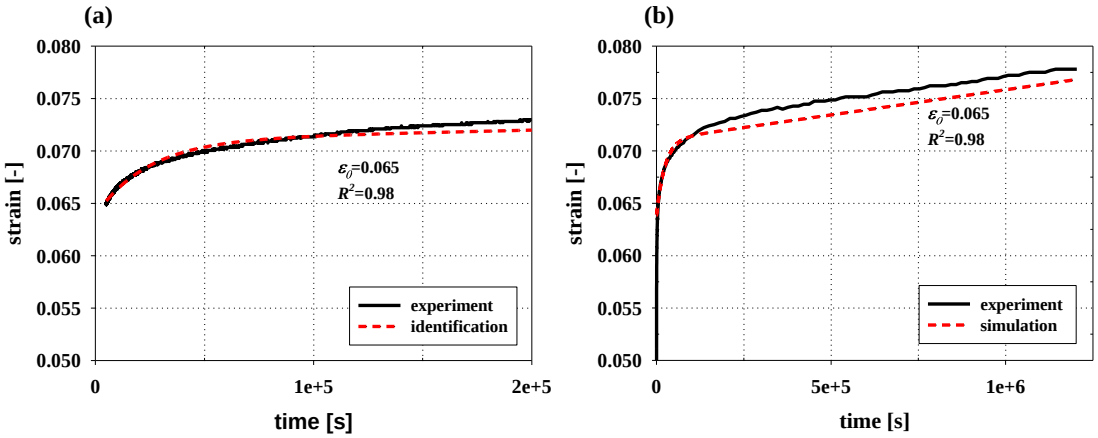

Fig. 6.9. Burgers model parameters for $t_1 = 2\text{e+}5$ s and $\varepsilon_0 = 0.065$ $[-]$: (a) identification of parameters; (b) verification by numerical simulation

It can be noticed that for all presented cases the determination coefficient R^2 of both identification and verification has very high value. However, the greater the immediate strain ε_0

is, the better correlation of identification in the range $t = 0 \div 2\text{e+}5\ \text{s}$ is observed (Fig. 6.7(a)-Fig. 6.8(a)). On the other hand, the higher the correlation coefficient of identification is, the worse the fitting of the simulation for the whole creep test is, especially in the linear range. To confirm the observed behavior, the author has decided to perform the same identification process for the same samples, but with different boundary time $t_1 = 4\text{e+}5\ \text{s}$. The results are depicted in Fig. 6.10-Fig. 6.12 and reveal the same tendencies, as observed before. It proves that the value of the immediate strain ε_0 is of the greatest influence on the identification's results.

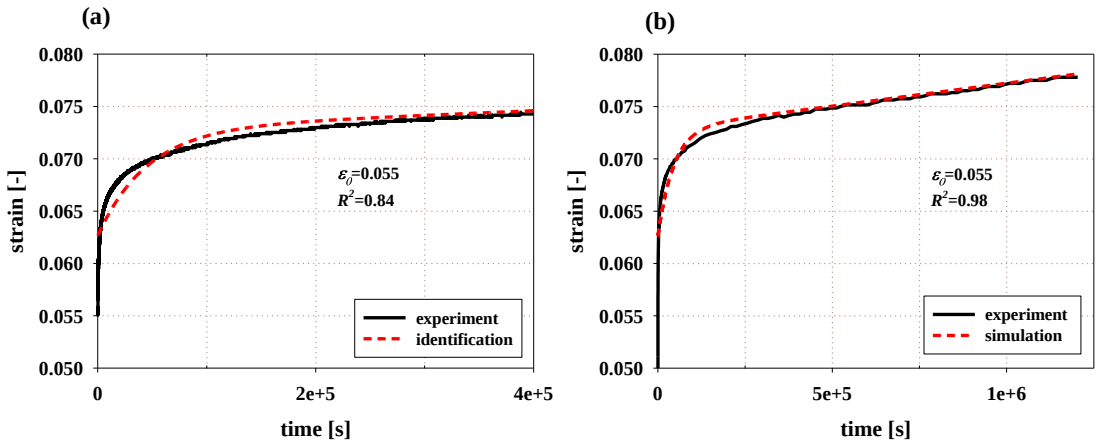

Fig. 6.10. Burgers model parameters for $t_1 = 4\text{e+}5\ \text{s}$ and $\varepsilon_0 = 0.055\ [-]$: (a) identification of parameters; (b) verification by numerical simulation

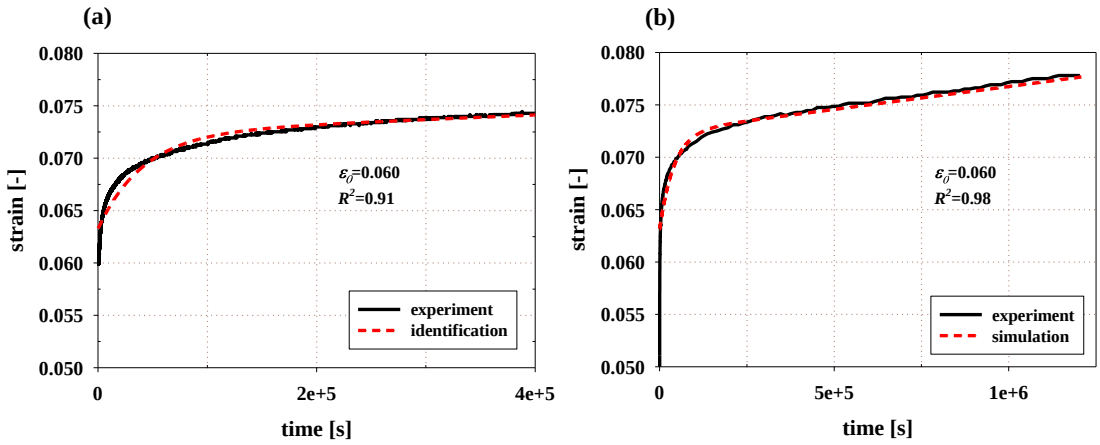

Fig. 6.11. Burgers model parameters for $t_1 = 4\text{e+}5\ \text{s}$ and $\varepsilon_0 = 0.060\ [-]$: (a) identification of parameters; (b) verification by numerical simulation

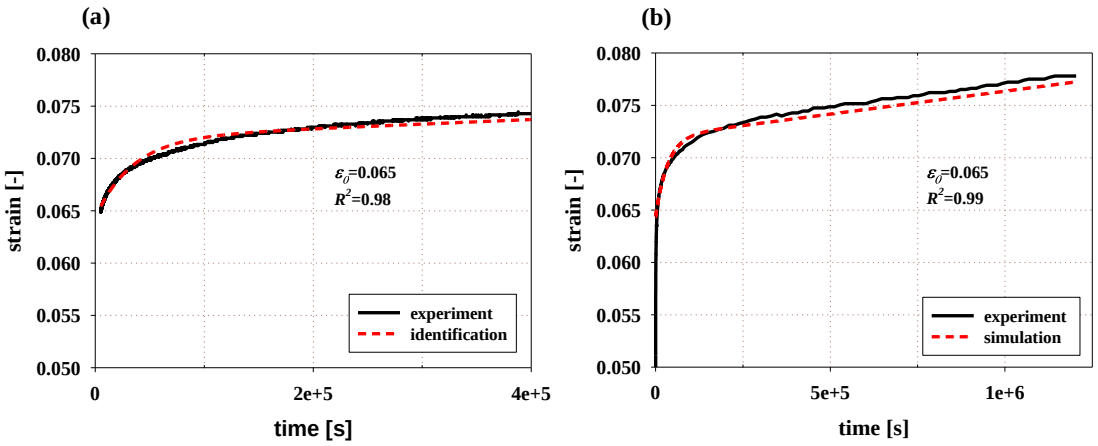

Fig. 6.12. Burgers model parameters for $t_1 = 4\text{e+}5$ s and $\varepsilon_0 = 0.065$ [–]: (a) identification of parameters; (b) verification by numerical simulation

Despite the fact, that all presented identification results have produced satisfactory convergence with experimental findings (R^2>0.95), the Burgers model is not good enough to model precisely the plastic behavior of VALMEX fabric in the whole range. Application of the model of higher order would probably improve the simulation results.

Nonetheless, the obtained results can be used for practical purposes. Well modelled behavior in the first stage of creep will be welcomed by engineers preparing the cut patterns of the fabric sheets. It has been suggested before in Section 6.2.2, that using the appropriate stiffness modulus, the behavior of the coated membranes in the beginning phase of loading in the stress-strain linear range can be predicted. Now, using the Burgers model (with higher value of ε_0), it is possible to describe this particular behavior also in the first period of inelastic deformation.

The Burgers model with parameters detected for the lower value of ε_0 can reflect better the long-lasting behavior under long-term constant loading. It would be of primary importance for prediction of material performance built in a real construction and used for many years.

The above identification has concerned the long-lasting creep tests. In this study also the short creep tests of 48 hours have been conducted. These tests have not been used for the identification purpose, as their time span is within the shorter time $t_1 = 2\text{e+}5$ s used for identification previously described in this chapter. Consequently, the identification form short tests would not be complete and the obtained results would not be comparable with long-term creep tests.

Taking above observations into account, the author has decided to compare the NOT USED and USED VALMEX fabric bearing in mind the parameters that have given the best fitting of the simulation curve in analyzed ranges separately: in the non-linear and linear part of the creep relation, and for two different boundary times $t_1 = 2\text{e+}5$ s and $t_1 = 4\text{e+}5$ s.

The difference between the Burgers model parameters for the NOT USED and USED samples are collected in Table 6.5. The relative difference has been calculated according to the formula $\delta = \left[(\text{NOT USED} - \text{USED}) / \text{NOT USED}\right] \times 100\%$.

Table 6.5. Relative errors between Burgers model parameters for the NOT USED and USED VALMEX fabric for the warp and fill direction

WARP					
t_1	[s]	2.00E+05		4.00E+05	
ε_0 (NOT USED/ USED)	[-]	0.055/0.0485	0.065/0.0585	0.055/0.0485	0.065/0.0585
Parameters		**Relative difference δ [%]**			
E_1	[kN/m]	11	10	11	10
E_2	[kN/m]	-5	-4	-4	-3
η_1	[-]	-11	-11	-10	-10
η_2	[-]	-0.4	-0.2	-0.6	-0.2
FILL					
t_1	[s]	2.00E+05		4.00E+05	
ε_0 (NOT USED/ USED)	[-]	0.1325/0.115	0.1425/0.125	0.1325/0.115	0.1425/0.125
Parameters		**Relative difference δ [%]**			
E_1	[kN/m]	-12	-12	-12	-12
E_2	[kN/m]	-12	-14	-16	-12
η_1	[-]	-20	-20	-19	-19
η_2	[-]	-0.8	-0.9	-0.8	-0.8

The low and high values of the immediate strain ε_0 (first and second column in the warp and fill section) have produced almost the same variation of the identification results for the NOT USED and USED fabric. It is seen for each material direction, that the difference between the NOT USED and USED samples does not depend on the level of the immediate strain ε_0, that has been not the same for both types of the material. Analysis of each parameter separately has given the following observations:

- the change of the value E_1 is the same for the warp and fill direction;
- the changes of the values E_2 and η_1 are two times greater for the fill direction than for the warp one;
- the value of η_2 stays unchanged for each identification and direction of the material and its value is very low.

Summing up, the ageing process is more distinct when analyzing the fill direction of the fabric material. The environmental ageing has influenced mainly the parameters E_1, E_2, η_1, that are related to the linear (long-lasting) part of the creep test. The coefficient η_2 identified from the non-linear (initial) part of the creep curve can be neglected in ageing analysis of the VALMEX

fabric. It proves that ageing has not affected the initial stage of creep, regarding the development of strains below t_1. Consequently, when using the polyester reinforced PVC coated membranes several times (like in the structure of the Forest Opera for 20 years), each time the material would adjust in the same way to the desired geometry, but with respect to the immediate elongation ε_0. Finally, for the long-term prediction of VALMEX performance the parameters E_1, E_2, η_1 are of the greatest importance.

The author is aware of the fact, that the loading level used in experiments for some cases presented in this study has been too high for typical creep tests, but good convergence of performed simulations has proven, that Burgers model can nevertheless be used for modelling behavior of architectural fabrics under even high loads. The identification results of the Burgers model parameters obtained in presented research form a basis for further numerical calculations of polyester reinforced PVC coated membranes structures in viscoelastic domain. The computer simulations including coverings made of architectural fabrics will be a part of further scientific work that are beyond the scope of this study.

6.2.4 Bodner-Partom model parameters

6.2.4.1 Identification and verification

The identification of the Bodner-Partom model parameters has been realized according to the procedure described in Section 4.4.1. The usage conditions of the coated fabrics permits consideration that a structure remains in a quasi-static state (low values of strain rates), so the limit of the strain rate has been arbitrarily set to $D_0 = 1$. The value of this parameter has been also chosen according to Kłosowski et al. ([144]) and Zagubień ([252]), who have conducted experiments on the very similar polyester reinforced PVC-coated technical fabric PANAMA several years ago, getting very consistent results. The main drawback of that identification is that parameters for the fill direction have been assumed the same as for the warp direction.

In the present work it is aimed at determining the Bodner-Partom law parameters for the VALMEX fabric for the warp and fill direction separately. To achieve this goal the author has proposed to shift experimental curves to obtain zero stress for zero strain value using appropriate elastic modulus ([254]). Presented approach is based on the precise analysis of the material response under cyclic load-unload tests (for details see Section 6.2.2). To remind shortly previous conclusions, the strain range corresponding to E_{F0} modulus for the fill direction is correlated to the initial stretching of the threads. It does not influence (or has very small influence on) the stress state and can be neglected, particularly when the architectural fabrics are pre-stressed during construction assembly. Therefore, in the approximation process of the experimental stress-strain curves, the first part of the data plot in the fill direction has been omitted (E_{F0}) and the value of

E_{F1} has been used to shift the stress-strain curve for purpose of further calculations. For the warp direction, the value of modulus E_{W0} has been used for shifting the experimental curve. The stress-strain curves obtained from experiments and ready for the Bodner-Partom model parameters identification in selected ranges (0.05 and 0.1 of the total strain for the warp and fill direction respectively) are drawn with blue lines in Fig. 6.13

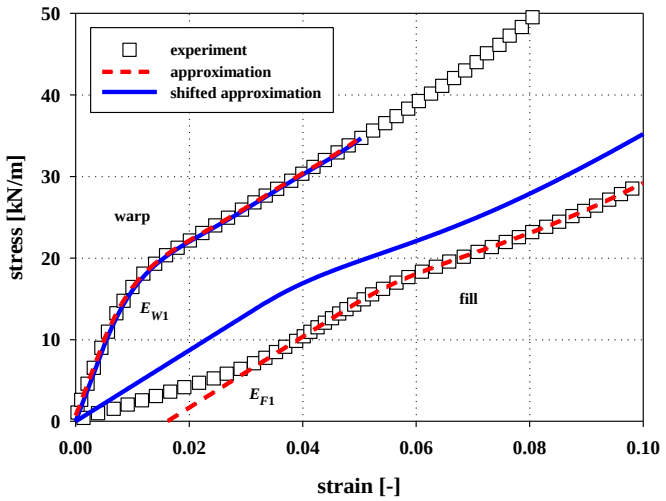

Fig. 6.13. Approximation of experimental data for the warp and fill direction of technical fabrics

Table 6.6 collects the results obtained by the identification process. Comparing the USED and the NOT USED material it is clearly seen that the main differences in both directions appear for the parameters m_1, m_2 (related to the isotropic and kinematic hardening coefficients, respectively) and for the parameter D_1, which stands for the limiting (maximum) value for kinematic hardening. Other observations are, that all parameters for the fill direction (except for the limiting value of the isotropic hardening R_1) change significantly.

Table 6.6. Results of the Bodner-Partom model parameters identification – comparison of the USED and NOT USED VALMEX fabric

Direction		WARP			FILL		
Fabric type		NOT USED	USED	δ	NOT USED	USED	δ
Parameter	Unit	Bodner-Partom model parameters					
m_1	$[kN/m]^{-1}$	0.82577 ± 0.06	0.5947 ± 0.02981	28	1.68997 ± 0.23	1.24323 ± 0.22956	26
m_2		34 ± 1	44 ± 6	-31	27 ± 7	18 ± 2	34
D_0	[kN/m]	1	1	-	1	1	-
D_1		3.0 ± 0.2	2.4 ± 0.6	21	2.8 ± 0.8	1.3 ± 0.3	54
n	[-]	1.89 R^2 1.00	1.79 R^2 0.99	5	1.42 R^2 0.97	2.36 R^2 0.97	-67
R_0	[kN/m]	30	32	-5	31	27	12
R_1		90 ± 7	102 ± 5	-13	72 ± 8	74 ± 5	-2

Keeping in mind, that differences between the experimental curves for the USED and NOT USED fabric for the fill direction have shown the same tendency, it may confirm in some way the correctness of performed identification.

The identification results of the Bodner-Partom model parameters have been verified by the numerical simulations of the laboratory tests using the determined material parameters and the software described in [245]. For the modeling of the fill direction response, obtained results have been applied in two ways. In the first one, only the longitudinal stiffness modulus E_{F1} has been taken into account, while in the second one the values of two moduli E_{F0} and E_{F1} have been implemented in the computer simulations. Fig. 6.14a and Fig. 6.14b present the experimental results compared to the one- and two-moduli simulations for the strain rate of 0.001 1/s for the NOT USED and USED samples, respectively. The stress-strain simulations for the warp direction are presented in Fig. 6.15. The results obtained for another strain rates are very similar and are presented in Annex 1B.

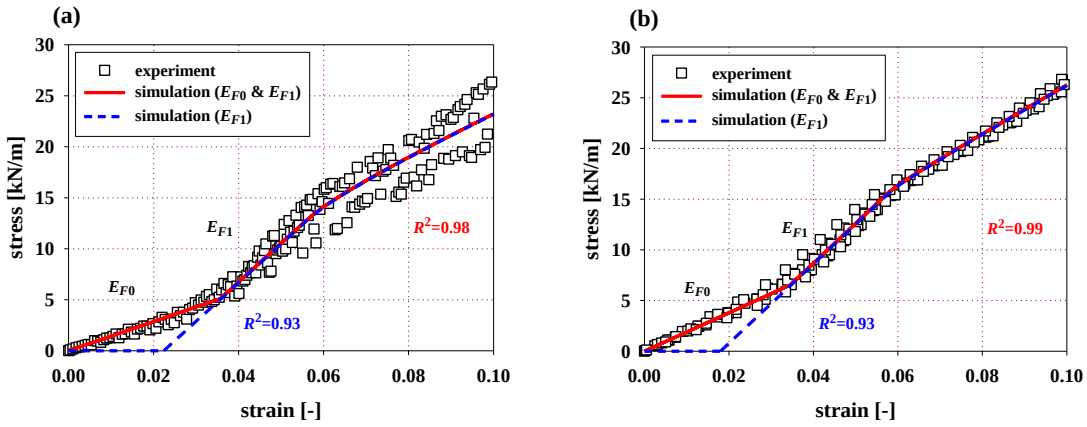

Fig. 6.14. Simulation results for the fill direction of the VALMEX fabric for the strain rate of 0.001 1/s: (a) the NOT USED; (b) the USED

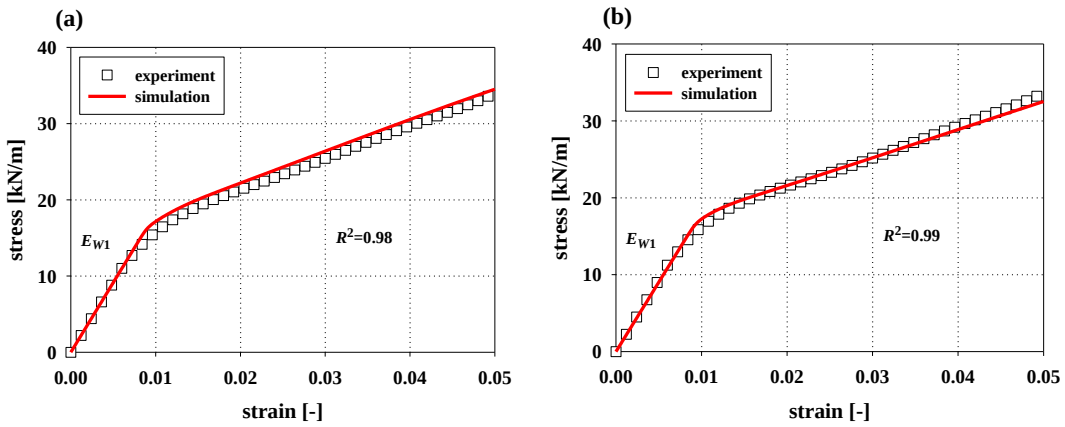

Fig. 6.15. Simulation results for the warp direction of the VALMEX fabric for the strain rate of 0.001 1/s: (a) the NOT USED; (b) the USED

The numerical simulations have confirmed the correctness of the performed parameters identification. Previously, similar analysis has been proposed by Kłosowski et al. ([144]) for the analysis of the PANAMA fabric. However, they have not found the parameters for the fill direction. In that paper authors managed to identify parameters only for the warp direction and assumed that they are the same in the fill direction as both threads families are produced from the same material and have the same density and micro-structure. For the PANAMA material that approach is satisfactory, as numerical simulations for both directions have given good agreement with the experimental data. In the present study it has been proposed to take for the identification procedure the appropriate part of the stress-strain curve. This method has allowed the author to conduct effective analysis also for the fill direction. The identification process can be therefore realized separately for the warp and fill direction of the fabric and takes into account different physical properties of the threads in both directions. Concluding, the Bodner-Partom model can be now implemented for describing technical fabrics behavior for the warp and fill direction giving sound convergences with the experimental outcomes.

6.2.4.2 Sensitivity analysis of the Bodner-Partom model parameters

To know which parameters of the model are of the greatest importance for its overall response, the sensitivity analysis of the model should be performed. The sensitivity analysis assess how the uncertainties in the model inputs affect the outputs of a mathematical model or system. It should be also accompanied by uncertainty analysis, which put greater attention on the uncertainty quantification and propagation of uncertainty. For civil engineering calculations it is also significant to perform the numerical simulation of the whole construction with implemented constitutive models. Analysis of finally obtained deflections and stresses in the structure is then used for assessing the correctness of performed theoretical assumptions. This analysis is beyond the scope of the present study and will be a main part of the future work.

One of the simplest and widely applied method of sensitivity analysis is that one of changing one-factor-at-a-time (called OFAT), known also as one-at-time (OAT), and then see what influence this produces on the model output ([207]). One of its advantage is the fact, that altering only one variable at a time, the rest of variables are kept at their baseline. As a result we exactly know which parameters is responsible for particular change in model response. Moreover, it increases comparability of the results and reduces a computation effort. On the other hand, it does not take into account interaction between changing several variables simultaneously that can give a different result than a sum of them varying separately, especially in non-linear approaches. The superposition of results is not valid here ([102]).

In this investigation the author has decided to use the OFAT methodology. A set of parameters identified for the fill direction of the NOT USED VALMEX has been established as a baseline for sensitivity calculations. These parameters can be found in Table 6.6. Each parameter has been

then varied with steps of 10%, in ranges ±50% of its initial value. For each obtained set of the Bodner-Partom model's parameters the simulation with the constant strain rate of 0.001 1/s has been executed. Its results in the form of the strain-stress curves are presented in Fig. 6.16a-Fig. 6.21a.

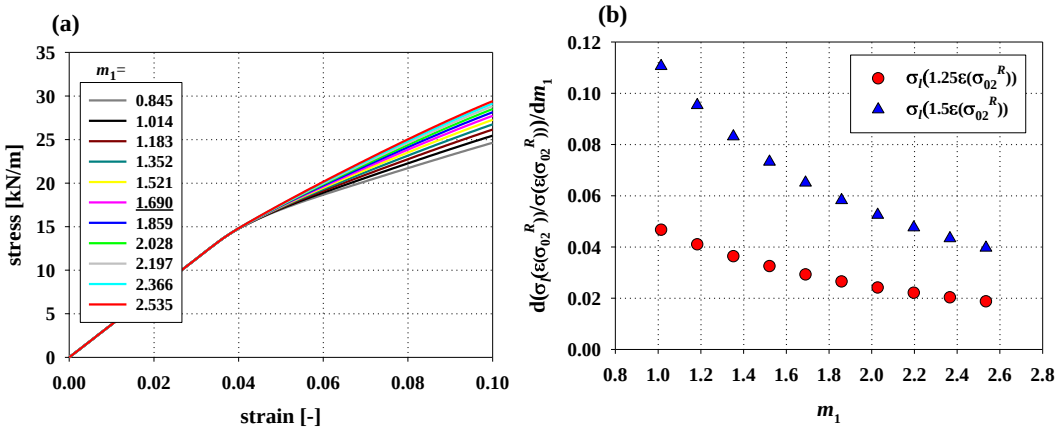

Fig. 6.16. Influence of the parameter m_1: the simulation curve (a); evolution of derivative (b)

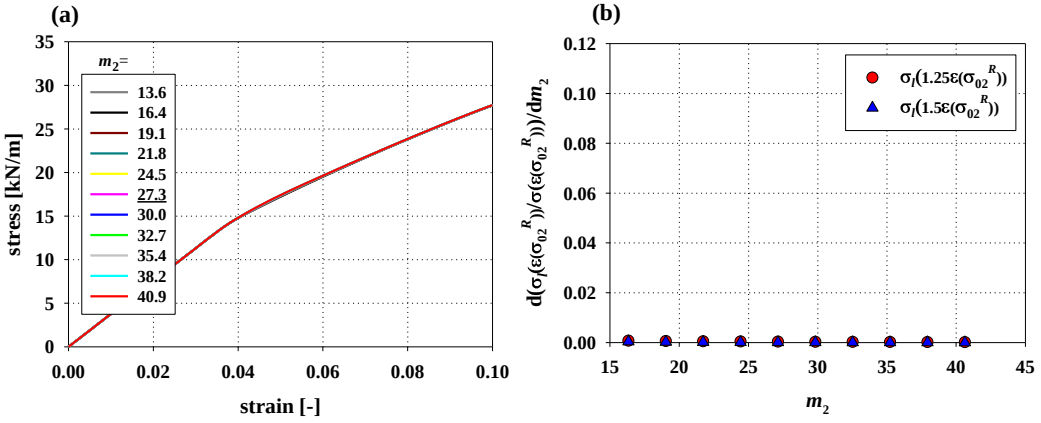

Fig. 6.17. Influence of the parameter m_2: the simulation curve (a); evolution of derivative (b)

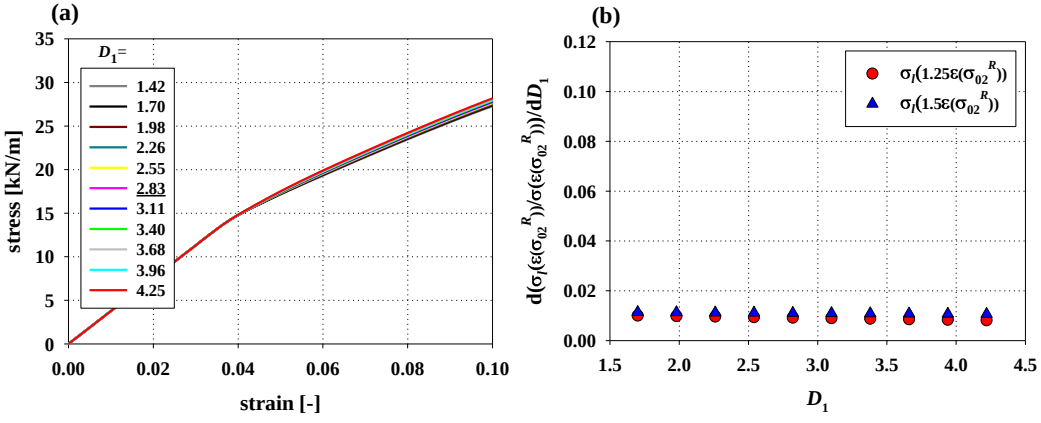

Fig. 6.18. Influence of the parameter D_1: the simulation curve (a); evolution of derivative (b)

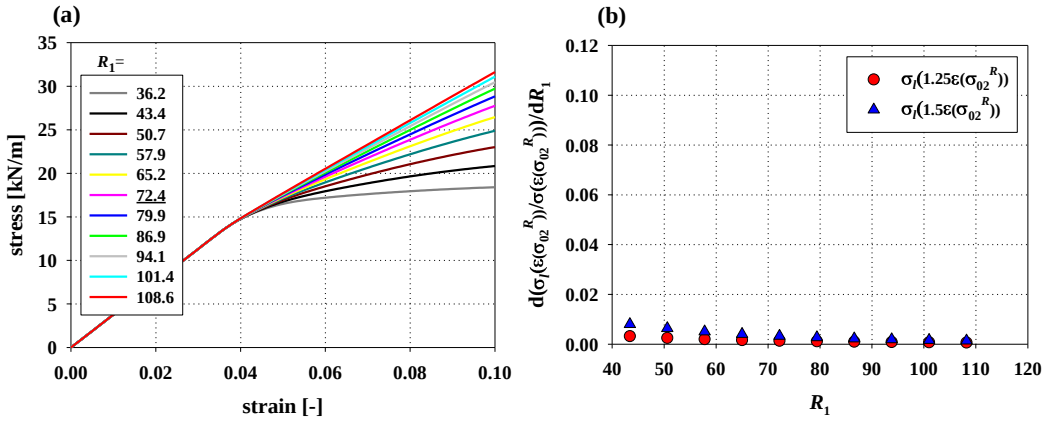

Fig. 6.19. Influence of the parameter R_1: the simulation curve (a); evolution of derivative (b)

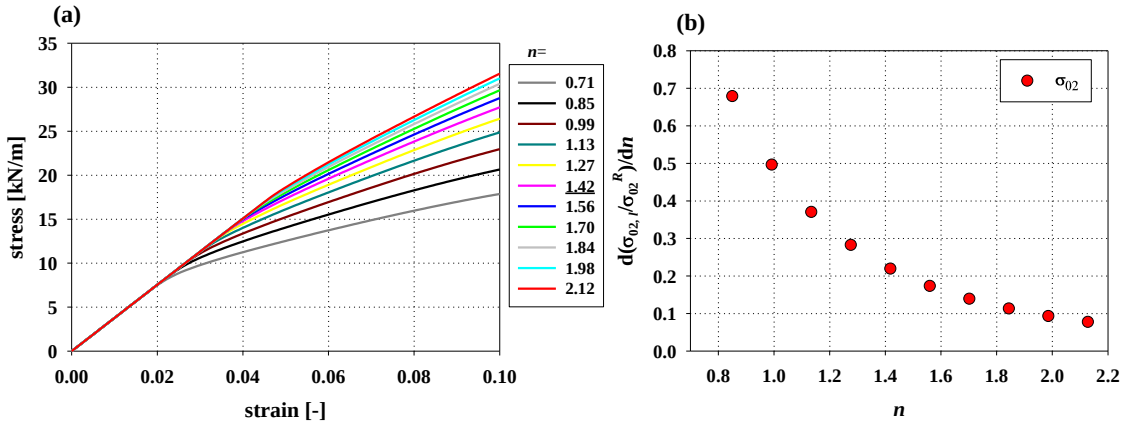

Fig. 6.20. Influence of the parameter n: the simulation curve (a); evolution of derivative (b)

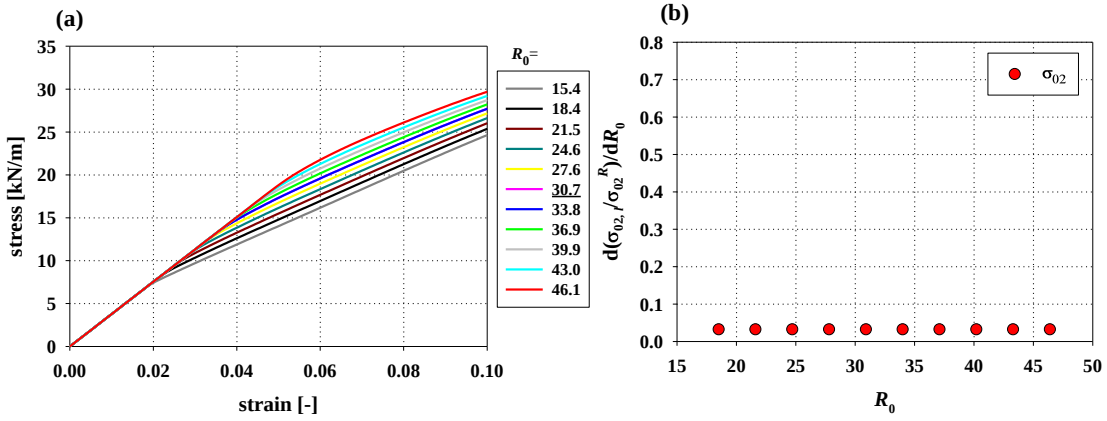

Fig. 6.21. Influence of the parameter R_0: the simulation curve (a); evolution of derivative (b)

The initial (original) value of the particular parameter is underlined in the graph legend. To monitor changes in the output is has been proposed to measure the stress value. Firstly, the yield limit $\sigma_{02}{}^{R}$ yield limit related to the original set of parameters has been established and then two values of stress ($\sigma_l^{1.25} = \sigma_l\left(1.25\varepsilon\left(\sigma_{02}{}^{R}\right)\right)$ and $\sigma_l^{1.5} = \sigma_l\left(1.5\varepsilon\left(\sigma_{02}{}^{R}\right)\right)$, where l states for the

variation step) have been withdrawn for every step of the variation. Next, the obtained stresses have been normalized by the reference stress value ($\sigma\left(Y\varepsilon\left(\sigma_{02}{}^{R}\right)\right)$, where $Y=1.25,\ 1.5$). From such prepared values, the derivatives of the one-at-a-time analyzed parameter have been numerically calculated. The results of derivatives are presented in Fig. 6.16b-Fig. 6.19b. This procedure has been accomplished for parameters, for which the yield limit has a constant value ($m_1,\ m_2,\ D_1,\ R_1$). The parameter D_0 has not been analyzed, as during identification process it has been arbitrary set to $D_0=1\,1/\mathrm{s}$. The parameters $n,\ R_0$ are responsible for the change of σ_{02}, so it has been decided to monitor this change as an output for the sensitivity analysis (Fig. 6.20b and Fig. 6.21b).

The scale of all the graphs is the same for simplicity of comparison. From the obtained results, it can be seen that for the Bodner-Partom model parameters identified for the fill direction of the NOT USED VALMEX the most sensitive are the parameters m_1 and n. Additionally, the derivative of n variable changes significantly, so drawing conclusions from results concerning parameter n should be done with highest care.

6.3 Influence of artificial thermal ageing - parameters for AF9032 fabric

The parameters identification of AF9032 fabrics for the piecewise and the Bodner-Partom model has been realized upon experiments presented in Chapter 5 and according to procedures described in Section 4.2 and 4.4, respectively. Evolution of obtained parameters versus ageing time will serve as base for the evaluation of ageing influence on technical fabric behavior.

6.3.1 Strength parameters (piecewise linear model)

Due to the fact that the proposed testing protocol has led to many results, it has been decided to include them all in tables in Annex 5B. Here, the demonstration of the outcomes in the form of graphs is given. To better understand the evolution of particular parameters values, each of them has been separately plotted versus the ageing time with distinction for the warp and fill direction. All of the results are presented in the normalized form of X/X^0, where X refers to the actual value of the particular variable and X^0 represents the initial/reference (1 hour aged sample) value of this variable. The time of the simulated ageing is presented in hours. The scale of the graphs has been also unified wherever it has been possible or has been set up in the way that makes the comparisons and observations easier.

As shown in Fig. 6.22, the stiffness E_{F0} related to PVC coating increases linearly in time for both temperatures and the rise for temperature of 90°C is much greater than for 80°C. It is a clear evidence, that PVC subjected to relatively dry, high temperature treatment undergoes inner

changes resulting in the growth of its rigidity. It is probably caused by the physical ageing (for details study Section 3.2.1), which usually includes the recombination of material's structure. The same behavior has been observed previously regarding the influence of the natural ageing on the VALMEX fabric (Section 6.2.1).

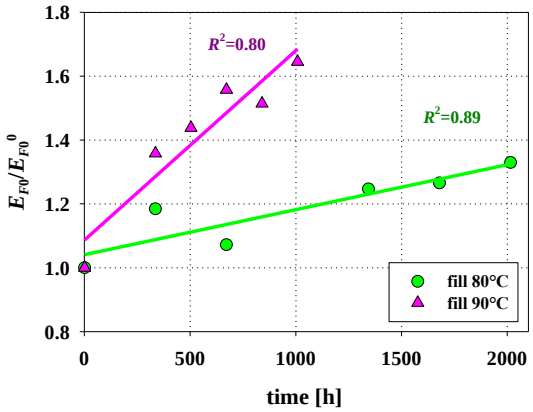

Fig. 6.22. Evolution of the longitudinal stiffness E_{F0} for the fill direction of the technical fabric AF9032 aged at temperature of 80°C and 90°C

The value of the stiffness modulus (E_{W1}, E_{F1}) acts in a different way (Fig. 6.23). For both fabric directions and the aging temperature of 80°C the increase of E_{W1} and E_{F1} in the ageing time is obvious. For the warp direction the linear growth is observed (reaching about 145 % of initial value after 8 weeks), but for the fill direction there is immediate leap to the level of 125 % of the initial value and then stable behavior. For both directions and the ageing temperature of 90°C there is no change of E_{F1} over passing time. The fact that the ageing temperature of 80°C has greater impact over time on the stiffness may suggest that this level of temperature stays below the glass transition temperature T_g of the polyester component and that the physical ageing has taken place causing the change of the stiffness. The temperature of 90°C is probably above the T_g and also far away from the temperature level that can induce any chemical reaction, which would result in changes of the mechanical properties. It suggests that the polyester threads already reached their thermo-dynamical equilibrium. Considering Fig. 6.24, it can be observed that the last analyzed longitudinal stiffness E_2 has not change at all at both temperature levels and for the warp and fill direction of the fabric.

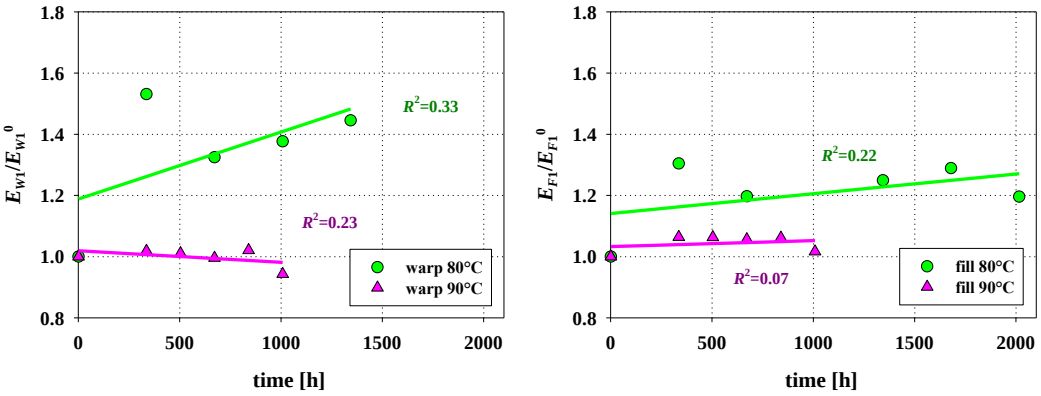

Fig. 6.23. Evolution of longitudinal stiffness (E_{W1}, E_{F1}) for the warp and fill direction of the technical fabric AF9032 aged at temperature of 80°C and 90°C.

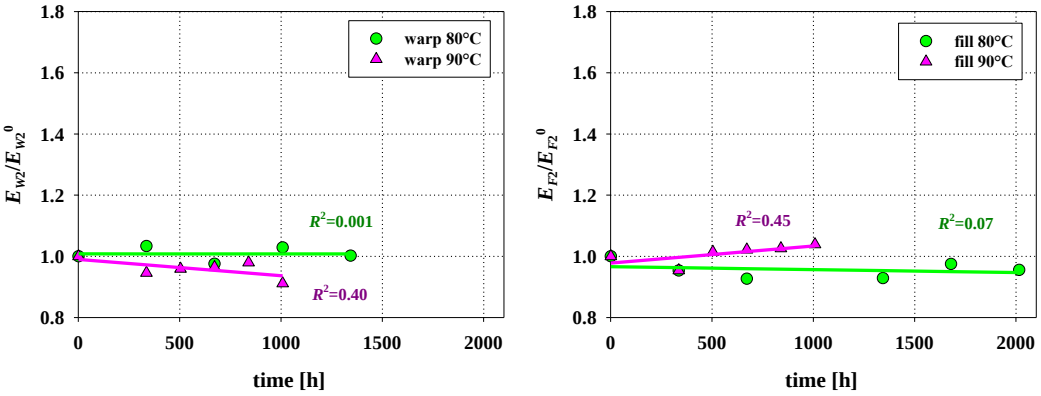

Fig. 6.24. Evolution of longitudinal stiffness (E_{W2}, E_{F2}) for the warp and fill direction of the technical fabric AF9032 aged at temperature of 80°C and 90°C.

The time evolution of the technical yield limit σ_{02} is depicted in Fig. 6.25. It firstly demonstrates that σ_{02} for the material in the fill direction is more prone to the thermal treatment as it shows growing tendency in time for both temperatures. Secondly, the higher ageing temperature has caused almost the same rate of growth for the warp and fill direction.

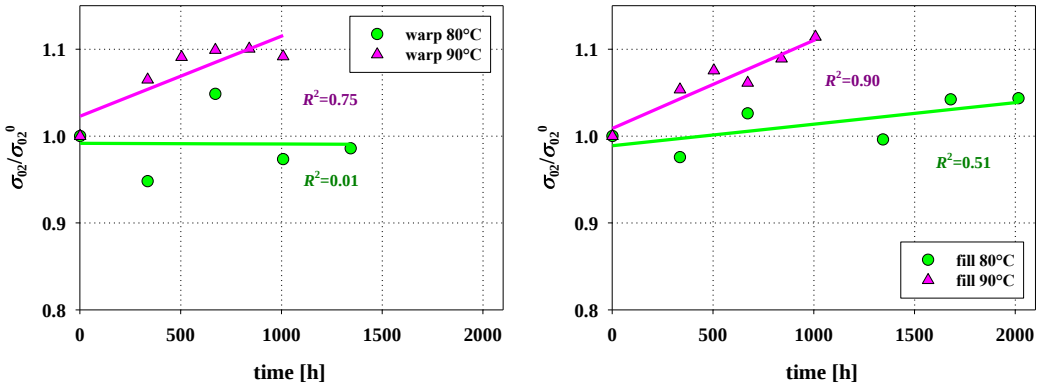

Fig. 6.25. Evolution of technical yield limit σ_{02} for the warp and fill direction of the technical fabric AF9032 aged at temperature of 80°C and 90°C.

The ultimate tensile properties (UTS, ε_{ult}) for the fill direction drop over time for the fill direction and for both temperatures. For resulting plot, see Fig. 6.26 and Fig. 6.27 for the UTS and ε_{ult}, respectively. From these figures it can be also seen that UTS for the warp direction expresses no variation over time, while the value of ε_{ult} depends strongly of the temperature level, decreasing for 80°C and growing for 90°C. To explain this behavior more experimental data is necessary and it will be analyzed more comprehensive in the future work.

Summing up the obtained results of the strength parameters, it can be concluded that the thermal ageing has influenced mostly the behavior of PVC coating, which has become more rigid and brittle over time. The technical fabric AF9032 has also shown to be more prone to the accelerated ageing at elevated temperatures for the fill direction. It stay in accordance with observations made before for the natural ageing of the VALMEX fabric. It can be noticed, that most differences has occurred for the fill direction of the material as well.

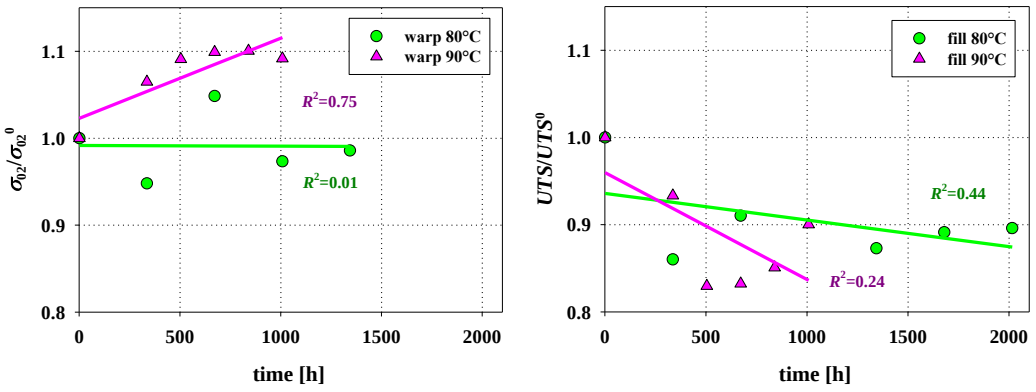

Fig. 6.26. Evolution of ultimate tensile strength UTS of technical fabric AF9032 aged at temperature of 80°C and 90°C for the warp and fill direction

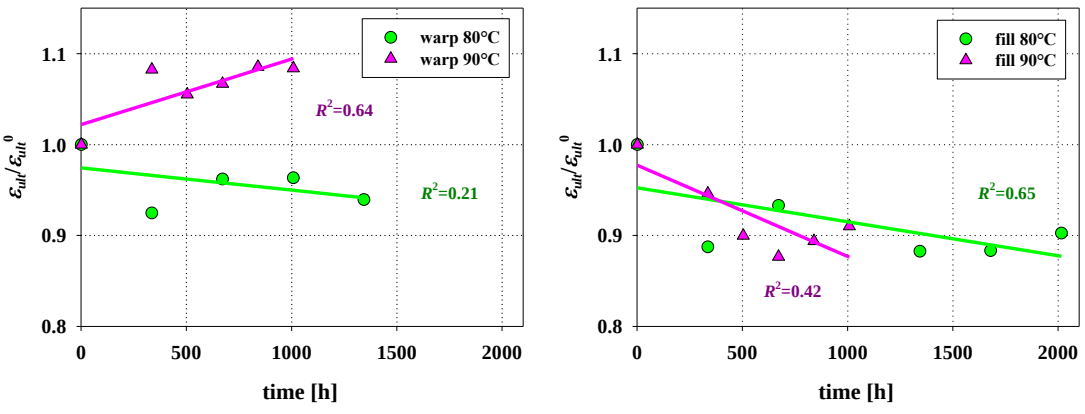

Fig. 6.27. Evolution of elongation at break ε_{ult} (ultimate elongation) of technical fabric AF9032 aged at temperature of 80°C and 90°C for the warp and fill direction

Another interesting observation is that almost all strength parameters for AF9032 fabric (apart from UTS and ε_{ult} for the fill direction and temperature of 90°C) change over time with linear dependency for both temperatures.

6.3.2 Bodner-Partom model parameters

The identification results of the Bodner-Partom model parameters are compiled in Tables in Annex 5B. Like before, for the clarity of results presentation, each parameter has been normalized by the initial/reference value determined for sample aged only for 1 hour and then plotted versus ageing time, for the warp and fill direction separately.

Firstly, analysis of the parameters related to the isotropic hardening is presented. The initial R_0 and maximum R_1 values for the isotropic hardening seem to be independent of the temperature level and always develop in the same manner for the fill direction. They demonstrate a linear decline of almost parallel character for both temperature levels. This is illustrated in Fig. 6.28 - Fig. 6.30.

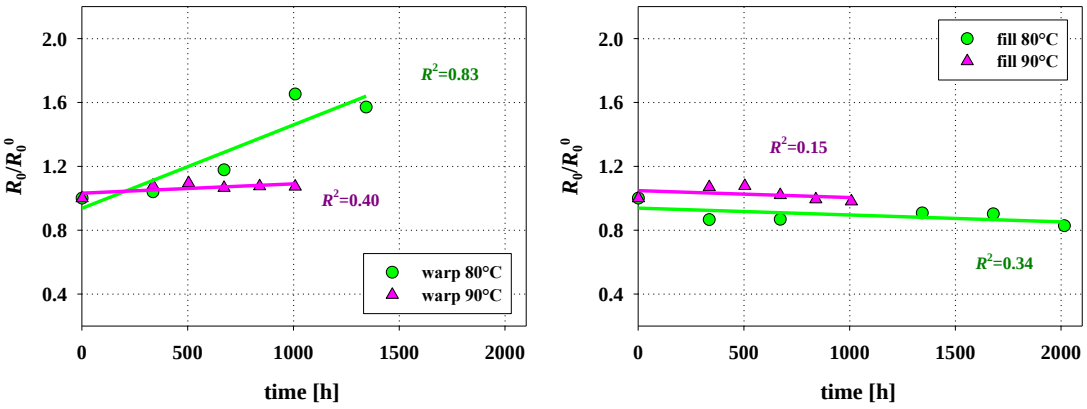

Fig. 6.28. Evolution of the Bodner-Partom model parameters for the warp and fill direction of the technical fabric AF9032 aged at temperature of 80°C and 90°C. R_0 - initial value for isotropic hardening

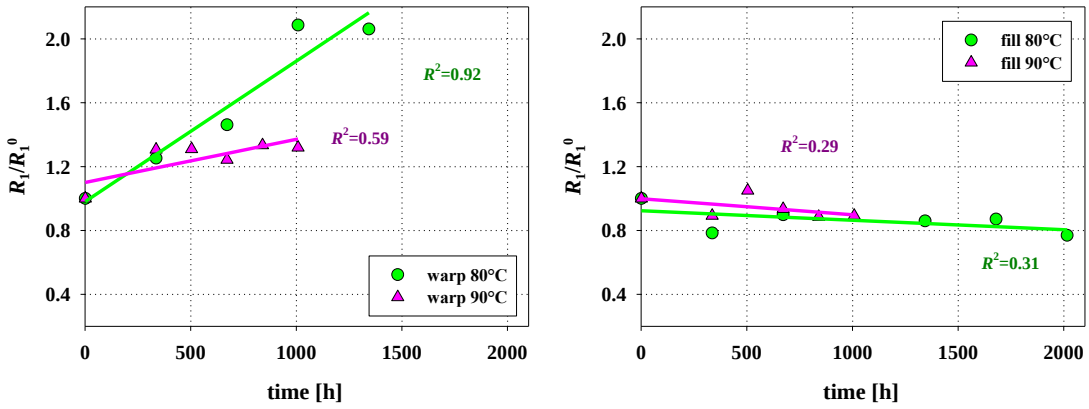

Fig. 6.29. Evolution of the Bodner-Partom model parameters for the warp and fill direction of the technical fabric AF9032 aged at temperature of 80°C and 90°C. R_1 - maximum value for isotropic hardening

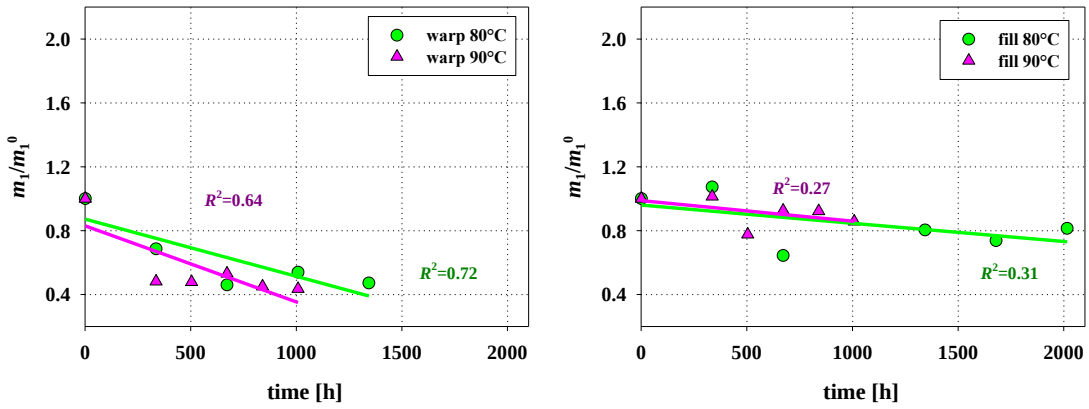

Fig. 6.30. Evolution of the Bodner-Partom model parameters for the warp and fill direction of the technical fabric AF9032 aged at temperature of 80°C and 90°C. m_1 - coefficient for isotropic hardening

For the warp direction the same parameters act in a different way. The lower temperature has caused great linear rise for both R_0 and R_1 values. For the temperature of 90° the linear growth is also noticed but of a far lower magnificance. General observation states that the initial value R_0 always goes up for the warp direction and falls down for the fill direction due to the thermal ageing. The same tendency stays true for the maxiumum R_1 value. The parameter m_1 controlling the rate of the isotropic hardening always falls down rapidly by the same inclination for each temperature and for both fabrics direction

Now, lets' take a closer look at the parameters controlling the kinematic hardening. Maximum value for kinematic hardening D_1 climbs rapidly at temperature of 80°C for the warp direction, while for the fill direction it jumps to the level of 110 % of its reference value at the beginning and then stays at this level. For the temperature of 90°C the trends are a bit different. For the warp

direction value of D_1 does not change at all over passing time, whereas for the fill direction it jumps higher to the level of 130% of its initial value and remains at this level. The parameter m_2, which governs the rate of the kinematic hardening, demonstrates slight variations around its initial value for the warp direction. For the fill direction is falls down linearly and for the higher temperature the slope is more significant. Comparison of the coefficients m_1 and m_2 indicates that they both decrease for the fill direction, independently of the temperature level. For the warp direction only parameter m_1 drops down significantly, whereas the factor m_2 stays unchanged.

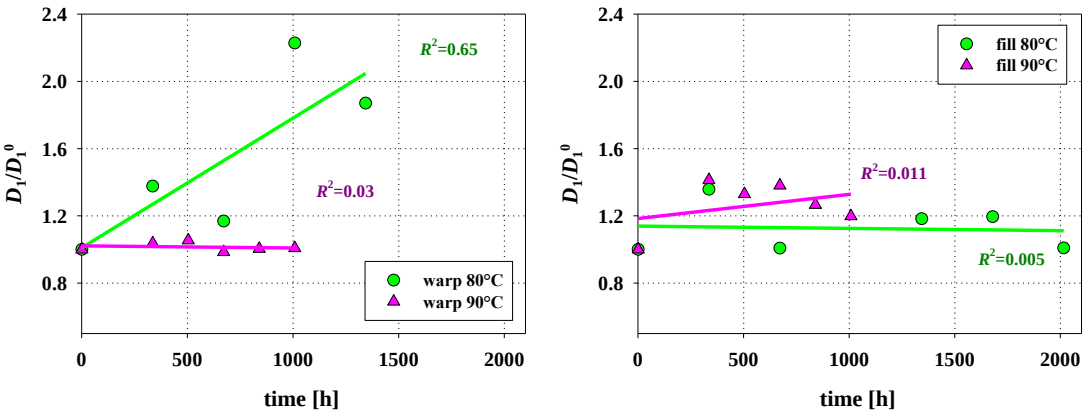

Fig. 6.31. Evolution of the Bodner-Partom model parameters for the warp and fill direction of the technical fabric AF9032 aged at temperature of 80°C and 90°C. D_1 - maximum value for kinematic hardening

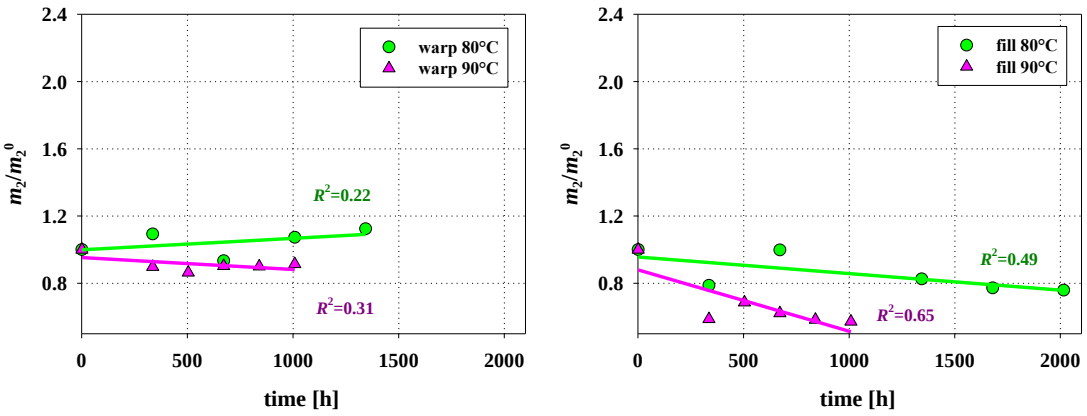

Fig. 6.32. Evolution of the Bodner-Partom model parameters for the warp and fill direction of the technical fabric AF9032 aged at temperature of 80°C and 90°C. m_2 - coefficient for kinematic hardening

The last parameter to analyze is the strain rate sensitivity parameter n. From Fig. 6.33 it can be seen that for the warp direction, the temperature of 90°C does not influence value of n. However, the lower temperature causes great decrease of the parameter values. For the fill direction the tendency is the same for both temperatures - it results in a growth, a little more

pronounced for the temperature of 90°C. All observed behaviors can be always described by linear functions with good convergence.

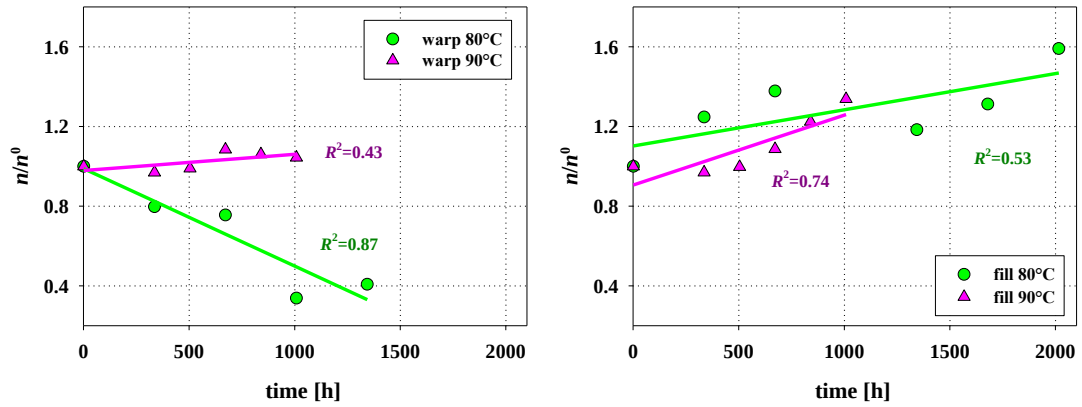

Fig. 6.33. Evolution of the Bodner-Partom model parameters for the warp and fill direction of the technical fabric AF9032 aged at temperature of 80°C and 90°C. n - strain rate sensitivity parameter.

On the basis of the results, it can be concluded that the development of the Bodner-Partom model parameters show the same decreasing (or increasing) tendencies for both temperatures for the fill direction. Regarding the warp direction, some discrepancies are observed, for example for parameters D_1 and n. It may suggest that in the fill direction the response is more repeatable. analyzed when subjected to the thermal treatment. The same conclusions have been drawn from the analysis of the strength and the tensile properties of the AF9032 fabric (for details study Section 6.3.1). Another overall important remark is that all of the parameters evolution over time can be easily approximated by linear functions with very good correlation. This finding is of direct practical relevance. It can be used for modelling behavior of the fabric material in numerical calculations for the elastoviscoplastic range. When using the Hook's law and the Bodner-Partom constitutive equations for material description, the particular model parameters can be implemented in the form of the linear dependence of temperature and time. If the future performance of the fabric is necessary to be evaluated, the true service life time can be calculated using for example the Arrhenius' relation.

6.3.3 Arrhenius extrapolation

The results of the thermal ageing can be extrapolated for much longer time periods using the Arrhenius methodology described in Section 3.1. It has been assumed that the energy activation of chemical reactions for technical fabrics stays below $E_{act} = 120\ \mathrm{Jmol}^{-1}$ ([1]). It has allowed to use the "10 degree rule" for recalculation of the ageing time of samples maintained at elevated temperature to "real time". In short, the accelerating reaction rate constant is given as follows:

$$f = 2^{\Delta T/10} \tag{6.5}$$

where $\Delta T = T - T_{\text{ref}}$ denotes the difference between the ageing temperature T and the service temperature T_{ref} of a material. The service temperature has been adopted as the temperature in the surrounding of the Forest Opera in Sopot. It has been taken from the meteorological station positioned on the roof of the new Forest Opera structure and calculated as the mean value from all days and nights measurements in the year 2013. The service temperature has then been obtained as $T_{\text{ref}} = 8°\text{C}$. The temperature levels for accelerate ageing have been previously chosen as $T = 80°\text{C}$ and $T = 90°\text{C}$ (for details study the Section 5.4.2). The reaction rate constant f has been calculated and then ageing time expressed in weeks has been extrapolated to years according to the Arrhenius simplified equation (6.5). The results of the extrapolation ageing time of up to 12 weeks are presented in Table 6.7.

Table 6.7. Extrapolation of ageing time according to Arrhenius equation for two ageing temperatures

real time [weeks]		1	2	3	4	5	6	7	8	9	10	11	12
Arrhenius time [years]	**80°C**	2.8	5.7	8.5	11.3	14.1	17.0	19.8	22.6	25.4	28.3	31.1	33.9
	90°C	5.7	11.3	17.0	22.6	28.3	33.9	39.6	45.2	50.9	56.6	62.2	67.9

In the same table, the recalculated ageing time for experiments performed in this study is marked by gray color (for details study the Section 5.4.2). It can be seen, that according to the Arrhenius methodology, increasing the ageing time by 10°C theoretically doubles the rate of ageing, e.g. ageing of a sample for 6 weeks at 80°C is equal to ageing of it at 90°C for only 3 weeks. Consequently, the author has decided to redraw the obtained in previous sections results with respect to the ageing time recalculated into "real" time according to the Arrhenius law. If parameters evolution curves of both temperatures will fall into the same path, it will confirm that the values of obtained parameters actually follow the Arrhenius equation. Fig. 6.34 represents the tensile strength parameters (E_{F0}, E_{W1}, E_{F1}, E_{W2}, E_{F2}, σ_{02}, ε_{ult}, UTS) for the warp and fill direction of the AF9032 fabric with appropriate recalculation of the results. It can be seen that the ultimate tensile strength (UTS), the elongation at break (ε_{ult}) and the longitudinal stiffness for the fill direction E_{F2} curves collapse to one line almost perfectly. Rest of the parameters for the fill direction express parallel trends. In the case of the warp direction neither clear tendency nor parallel character of curves can be observed.

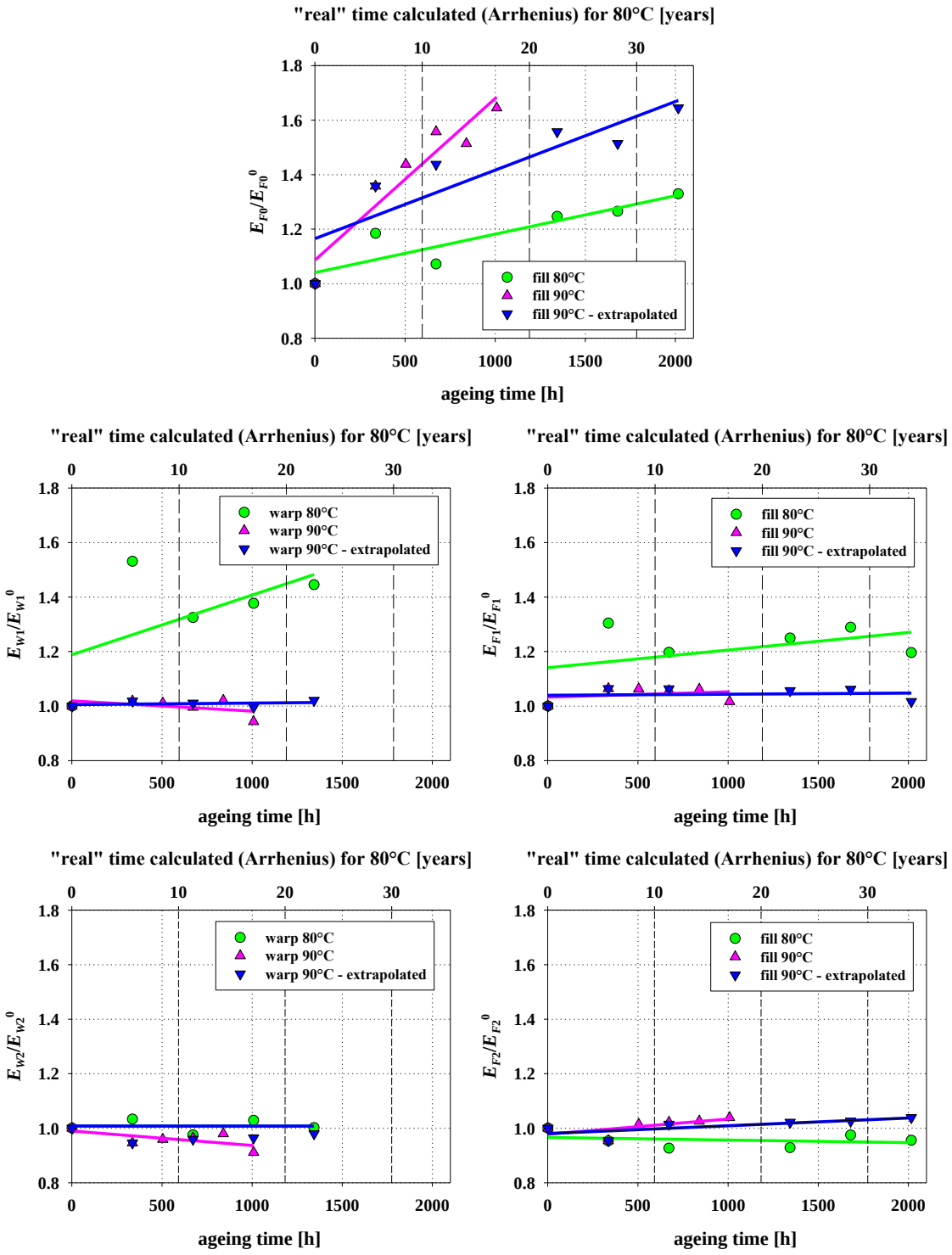

Fig. 6.34A The tensile strength parameters (E_0, E_1, E_2, σ_{02}, ε_{ult}, UTS) for the warp and fill direction of the AF9032 fabric for ageing time recalculated according to Arrhenius simplified equation for reference temperature of 8°C and ageing temperature of 80°C.

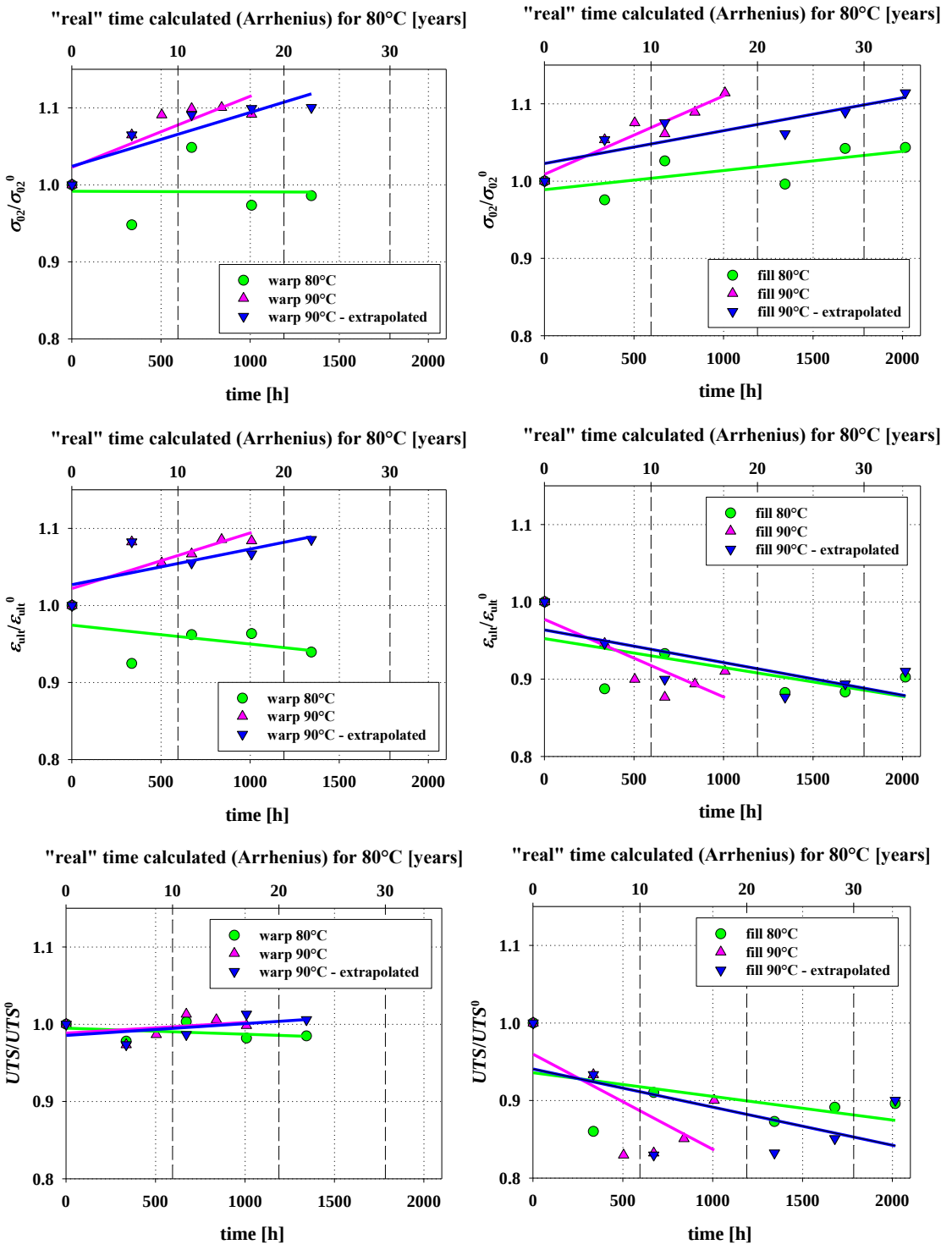

Fig. 6.34B. The tensile strength parameters (E_0, E_1, E_2, σ_{02}, ε_{ult}, UTS) for the warp and fill direction of the AF9032 fabric for ageing time recalculated according to Arrhenius simplified equation for reference temperature of 8°C and ageing temperature of 80°C.

The similar performance is detected for the parameters of the Bodner-Partom model that are shown in Fig. 6.35. All of the parameters in the fill direction coincide well and the parameters R_0, R_1, m_1 collapse into one line. For the warp direction there is no convergence between curves for 80°C and extrapolated 90°C at all. The results of 80°C have for most cases different tangents

and opposite tendencies than the ones of extrapolated 90°C. It is suggested that technical fabrics for the fill direction subjected to thermal ageing follow the Arrhenius relation. However, in order to draw profound conclusions the more comprehensive investigation is advisable. Firstly, the test program should include the third different temperature level of the artificial ageing. Then, it will be possible to use the time-temperature superposition principle (TTSP) to get master curve and calculate the activation energy and rate coefficient according to Arrhenius full equation. This investigation will be a part of future research. Presented here calculations are some initial trials to deal with the ageing problem. Nevertheless, they show that the polyester reinforced PVC coated architectural membranes are influenced by the thermal ageing and that this influence can be evaluated by the Bodner-Partom model parameters. Evolution of these parameters, in turn, seems to obey the Arrhenius methodology, but still requires further research to be confirmed.

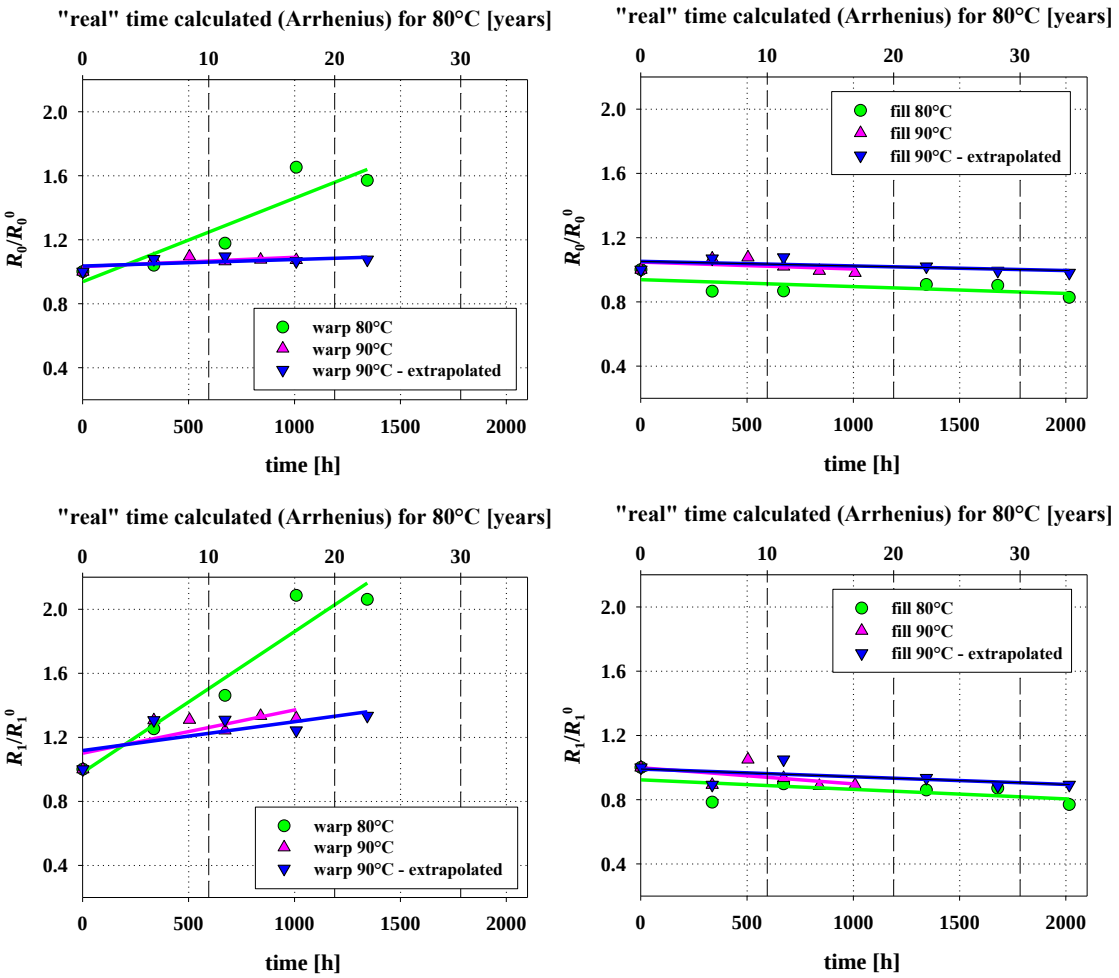

Fig. 6.35A. The Bodner-Partom model parameters (R_0, R_1, m_1, D_1, m_2, n) for the warp and fill direction of the AF9032 fabric for ageing time recalculated according to Arrhenius simplified equation for reference temperature of 8°C and aging temperature of 80°C.

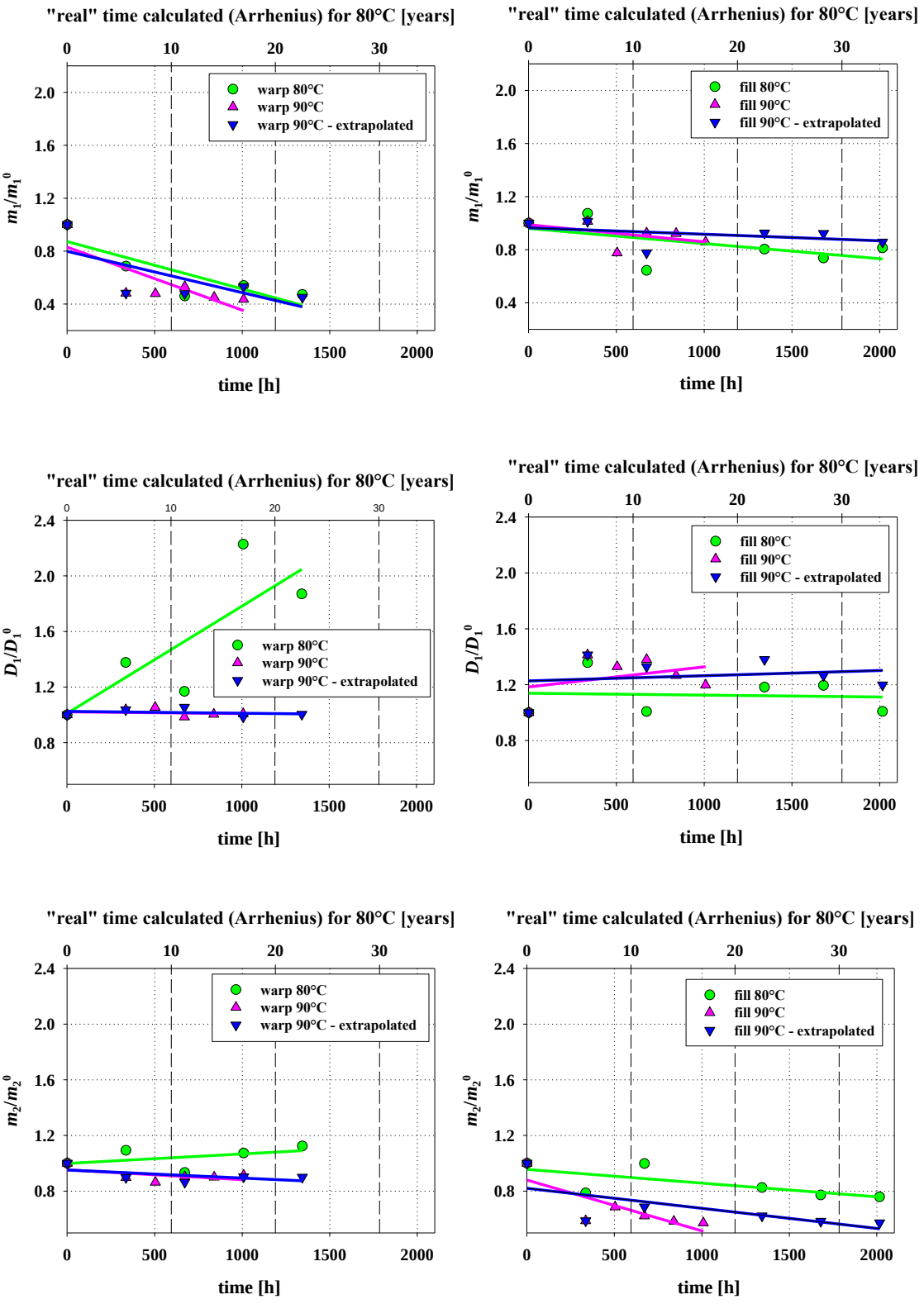

Fig. 6.35B. The Bodner-Partom model parameters (R_0, R_1, m_1, D_1, m_2, n) for the warp and fill direction of the AF9032 fabric for ageing time recalculated according to Arrhenius simplified equation for reference temperature of 8°C and aging temperature of 80°C.

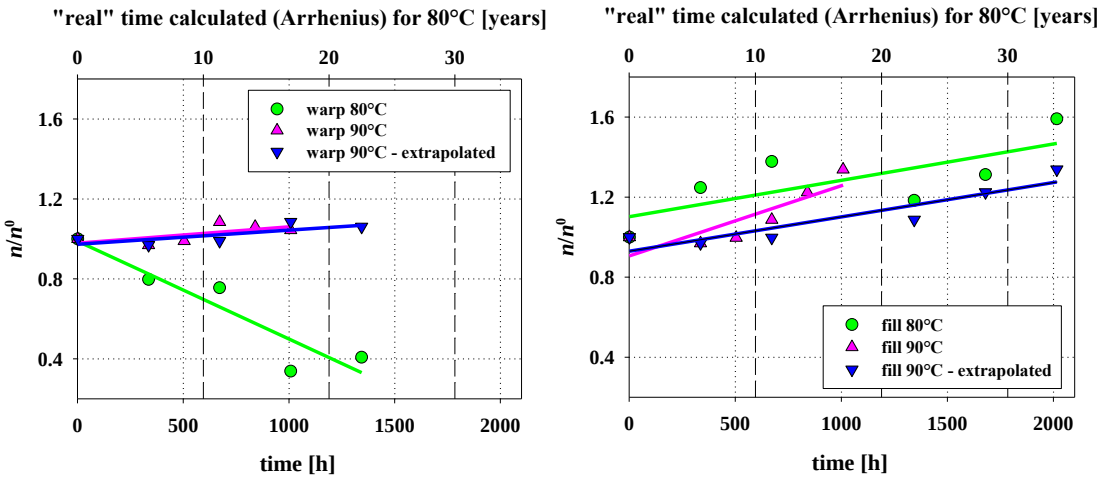

Fig. 6.35C. The Bodner-Partom model parameters (R_0, R_1, m_1, D_1, m_2, n) for the warp and fill direction of the AF9032 fabric for ageing time recalculated according to Arrhenius simplified equation for reference temperature of 8°C and aging temperature of 80°C.

6.4 Summary

The identification of the parameters for the piecewise non-linear, Burgers and Bodner-Partom model has been accomplished successfully. Two ageing types have been investigated: natural and laboratory accelerated. To achieve such a wide database of results a long-lasting experimental testing protocol has been realized.

The analysis of the cyclic load-unload tests has allowed to perform precise exploration of the Bodner-Partom law for the warp and fill direction of the fabric individually, what is a step put forward in comparison with previous achievements in this matter. It has been presented that the evolution of achieved parameters for thermal ageing can be in almost all cases approximated by linear dependency. This finding may be promising in the prediction of the long-term performance of technical fabrics and can be directly used in the numerical calculations of textile structures using the Bodner-Partom model. It has been also shown that evolution of the Bodner-Partom model parameters for the fill direction follows the Arrhenius law. However, more comprehensive study is necessary to confirm this observation.

7 Final summary and conclusions

The presented work considers the investigation on the influence of the ageing phenomenon on the mechanical behavior of polyester reinforced PVC coated fabrics used in civil engineering structures. The study has been stated in the first chapter, where the main aim, range and field of research have been established. Next, the specification of the hanging roofs structures have been presented, with the particular attention paid to the Forest Opera in Sopot (Poland). Due to the reconstruction of this famous amphitheater in 2009-2011 the author had the opportunity to get the material from the canopy that has been used for 20 previous years. It has become the basis of interest on the ageing process of architectural fabrics that this study tries to deal with.

The next chapter includes the presentation of technical fabrics' composite structure and methods of its numerical modelling. More attention is focused on the dense net model that allows the use of different constitutive relations for behavior description of the threads separately for the warp and fill direction of a fabric. The experiments commonly performed on technical fabrics for identification of their mechanical properties are also presented in this chapter.

The state of the art on ageing phenomenon and durability of building materials has been revised in the following chapter. The overview includes the presentation of laboratory equipment and testing methods aimed at the progress evaluation of the natural and artificial ageing. The most widespread and simplest method for the simulation of ageing is the dry heat method. It has been therefore chosen for some experiments performed in this investigation. In the following part, a particular attention has been paid to the ageing of polymers, as from the chemical point of view the technical fabrics components belong there. The main problem with the durability of polymers is related to the phenomenon of the physical ageing. It always occurs below the glass transition temperature and is a particular characteristic known only for polymers. This phenomenon has been as well briefly described. The most popular mathematical formulations dealing with physical ageing has been reported. Time-temperature superposition principle (TTSP) and its upgraded by the Struik form of the time-ageing time superposition principle (TASP) have been given in detail. Finally, the literature overview on ageing of PVC and PET materials has been done. Among reported studies, the ones concerning the ageing of the roofing membranes are of the most significance for the presented investigation. They mainly argue that PVC coated roofing materials keep their initial mechanical properties over many years, reaching even 40 years of service without leakage.

The next chapter comprises the description of three constitutive models selected for analysis of ageing process. It has been decided to assess the ageing phenomenon by the evolution of parameters found for these particular material models. These parameters can be in the future used for the numerical simulations of textile structures and therefore help to predict their life span under service conditions. The author's intention has been to define technical fabrics behavior in

three different ranges of stress-strain relation. Therefore, the non-linear piecewise model (used mainly in elastic modelling), the viscoelastic Burgers and viscoplastic Bodner-Partom models have been chosen. The theoretical foundations, necessary mathematical equations and transformations have been submitted for each constitutive relation thoroughly. The procedure of the parameters identification for each model has been given in detail.

For the identification of the constitutive models presented in the previous chapter the dedicated laboratory tests are required. They have been described in the following chapter that deals with the experimental part of the present study. For a start, the research workshop of two committed laboratories (Gdańsk University of Technology and University of Orleans, PRISME laboratory) have been presented. It should be point out, that the author has been the main designer and coordinator for the manufacturing process of the machine for long-term creep tests that has been used in this study. Succeeding, two different technical fabrics have been taken for investigation towards ageing: the VALMEX fabric from the Forest Opera in Sopot and AF9032 fabric, which initially has been planned to cover the new roof of the rebuilt amphitheater (finally Sheerfill PTFE fabric has been used). Both of them are composed of polyester yarns (acting as reinforcement) and two sides coated with PVC. Additionally, the VALMEX fabric has had two types: the first one used for 20 years on the real roof of the Forest Opera (called the USED) and the second one from the same production part kept for 20 years as spare material for potential repairs of the canopy (called the NOT USED). The experimental program has been then divided in two parts. The first one has covered analysis of the natural ageing and has been based on the comparison between the USED and NOT USED samples. For that reason, both types of the VALMEX membrane have had to undergo the same following tests: uniaxial tensile tests with three different strain rates (necessary for identification of the Bodner-Partom model), biaxial tensile tests, uniaxial load-unload tensile tests and finally creep tests. The AF9032 fabric has been subjected to the accelerated, artificial ageing by the dry heat method. The samples have been maintained in an air-circulated oven at elevated temperatures of 80 and 90°C for up to12 weeks. Every one or two weeks some samples have been withdrawn and undergone uniaxial tensile tests with three different strain rates. To sum up, a wide range of time consuming experiments have been realized. The obtained results have been used for the identification of models material parameters for the VALMEX and AF9032 fabrics.

The material parameters identification is the main subject of the next chapter. All the identifications have been realized separately for the warp and fill direction of both architectural fabrics. At first, the estimations of the elasticity modulus and the yield stress, as well as the strength properties like the ultimate tensile strength and the elongation at break have been presented. For the precise detection of the longitudinal stiffness moduli in the fill direction the cyclic load-unload test have been analyzed. It has occurred, that not the first but the second stiffness modulus identified from the experimental stress-strain curve in the fill direction is

probably the true elastic modulus. This has been then used for shifting the experimental curve to obtain the zero stress value for null strains that has been of the key importance for the forthcoming parameters determination of the Bodner-Partom model. The comparative analysis of the piecewise model parameters between the NOT USED and USED material has revealed that the environmental, in the service ageing of the VALMEX fabric has caused decrease in the UTS for the warp direction and increase of the yield limit for the fill direction. The greatest change, however, has been observed in the growth of PVC coating stiffness (of about 32%). In the case of the biaxial tests, almost all of the strength properties have decreased when comparing the NOT USED and USED material, but the stiffness of PVC has raised again. It seems to be obvious, that outdoor exposure has influenced mostly the coating PVC layer. In the same time the polyester yarns responsible for the mechanical strength of a canopy has been unaffected by the ageing or sufficiently protected by PVC coating from unfavorable environmental conditions.

The identification of the Burgers model parameters has expressed some difficulties. It has been observed that, the ideal approximation of the experimental curve in the whole range of strains is impossible using this model. It has been detected, that the level of the immediate elongation (the theoretical point where the creep of material starts) influences the overall identification results. However, the correlation coefficient between experiment and verifying simulations have always kept high value. It suggests, that Burges model can be used for modelling technical fabrics viscoelastic behavior. The author decided to find differences between the NOT USED and USED fabrics by the juxtaposition of the results, taking into account the influence of the varying immediate elongation. The comparison between materials has shown that ageing has influenced only the parameters related to the linear part of the creep curve (E_1, E_2, η_1). The viscous coefficient η_2 has remained constant throughout the whole identification process. It suggests that it is not susceptible to ageing and can be neglected in further ageing influence analysis. Hence, the investigation on the Burgers model parameters for technical fabrics becomes easier, as the coefficient η_2 has to be determined from the non-linear part of the experimental curve using the least square method. The main differences between the NOT USED and USED fabrics has been noticed for the values of E_2 and η_1 that have been two times greater for the fill than for the warp direction. Once again, it has been proven that the material in the fill direction is more prone to the ageing and service tension than in the warp direction.

The identification of the Bodner-Partom parameters has been successfully accomplished for the warp and fill direction separately. It has been a step put forward in the identification procedure for the fill direction comparing to previous research done on technical fabrics by Kłosowski et al [144]. These authors managed to perform the effective parameters identification only for the warp direction of the fabric and obtained results also applied for description of materials behavior in the fill direction. In present study, it has been possible to conduct the full (for both directions)

parameters identification due to the accurate determination of the longitudinal stiffness moduli in the fill direction and appropriate shifting of the experimental curves as the initial step for further calculations. As a result, two different approaches of the obtained results presentation have been proposed in this study. In the first one, only one the stiffness modulus is taken into account in the linear range of strains and in the second one two moduli values are recognized in the same region. For the inelastic range of deformation the Bodner-Partom law parameters control the curve trajectory in both concepts. The identification outcomes for both approaches have been verified by the numerical simulation of the experimental tests and in all cases high convergence has been reached. This way, it has been proven, that the Bodner-Partom model is suitable for modelling the technical fabrics viscoplastic behavior in both the warp and fill direction of the material. After accomplishing the parameters identification and results verification, the sensitivity analysis of the Bodner-Partom model has been carried out. The parameters m_1 and n have the greatest impact on the overall response of material described by the Bodner-Partom model. With all that data gathered, the comparison between the NOT USED and USED has been conducted. It has revealed that ageing has affected the parameters m_1, m_2 (related to the isotropic and kinematic hardening, respectively) for the warp and fill direction causing their change of about 30%. The greatest increase has been reported for the parameter n, that for the fill direction raised for almost 70 %. The fill direction is generally more subtle to outdoor exposure, as other parameters expressed also more significant changes in comparison to the ones for the warp direction.

The author is aware of the fact, that drawing conclusions about aging effect only from two measuring points in time (the NOT USED and USED) can only be treated as estimation of the observed changes. For confirmation of these conclusions the proposed in this study experimental program must be executed on a set of samples that should be collected from the structure several times during its service life. However, the findings stay in accordance with previously reported researches ([204], [29], [87], [94], [239], [31]), that has proven the statement that PVC coated roofing membranes have kept their initial strength parameters and are in good overall condition after decades of usage. The main reason of their replacement is bad condition of sheet's links or the change of the architecture of the whole roof.

The following identification presented in this chapter has concerned the artificially aged AF9032 fabric. In that case more measuring points have been obtained. Therefore the results have been presented as the evolution of parameters values versus the ageing time (maintenance at elevated temperature of 80°C and 90°C) in the form of the graphs. The observed tendencies of individual parameters can be approximated by the linear functions. Similar trends have been observed before by Bailey et al. [29] for the physical properties like the loss of plasticizer , tensile strength, tear strength, thickness, or specific gravity of PVC membranes aged outdoor. Here, it has been proven that the linear dependency fit also to the evolution of strength and the Bodner-

Partom model's parameters. Some discrepancies between the parameters behavior have been observed for temperature of 80°C and 90°C for the warp direction. For the fill direction for both temperatures the parameters have usually expressed the same increasing or decreasing tendencies. These outcomes have been probably related to the level of temperature. The experiments have been conducted with the temperature level very close to the glass transition temperature of PVC. To sum up, the physical ageing could have affected the samples differently. This effect has been empowered by the fact, that the material in the warp direction has been pretensioned during manufacturing process.

Finally, the results obtained from the accelerated ageing has been recalculated according to the simplified Arrhenius equation. It has stated, that the artificial ageing of the material at temperature of 80°C for 8 weeks equals to the natural ageing of 23 years. The ageing times for two temperature levels (80°C and 90°) and for the warp and fill direction have been recalculated in this manner. Results in the same "real time points "have been compared. This process has revealed that each parameter has followed exactly the Arrhenius law, as some discrepancies between analyzed temperatures have occurred. Therefore for this problem more comprehensive investigation is advisable. After accomplishing the experimental program with the accelerated ageing at additional, third temperature level it will be possible to use the time-temperature superposition principle (TTSP), get the master curve and then check if technical fabrics follow the Arrhenius behavior. It will be a part of future research. Presented here approach is the initial trial to deal with the ageing problem in polyester reinforced PVC architectural membranes.

The main conclusions, which have been finally drawn, are:

- Due to the composite structure of architectural fabrics and their woven reinforcement configuration, the cyclic load-unload tensile tests are necessary to find the longitudinal moduli in both material directions. These moduli are of an important role for many identification processes, like e.g. the appropriate experimental curve shifting before the Bodner-Partom parameters determination.
- The piecewise model is good enough for description of the longitudinal stiffness parameters of the architectural fabrics. It is especially useful in analysis of the fill direction that is characterized by complex material behavior even in the linear range of strains.
- Identification of the Burgers model parameters depends on the level of immediate elongation taken for calculations. The higher this level is, the better simulation fitting of the first non-linear part of creep is possible, but simultaneously worse fitting for the remaining part is obtained.
- It has been proposed to generally conduct Burgers parameters determination in both ways: with special attention paid to the first non-linear part of the creep test or to the

long-lasting linear part. The choice should depend on which part of the creep curve is at the moment more important for engineers.

- The Bodner-Partom constitutive law can be used for modelling the technical fabrics behavior in the viscoplastic domain. The parameters identification has been improved by the appropriate initial shifting of the experimental curve for the fill direction. Consequently, it has been possible to conduct parameters identification separately for the warp and fill direction. The numerical verification has confirmed the correctness of proposed parameters determination in both material directions.
- Two different approaches of the piecewise elastic and Bodner-Partom models results representation have been proposed. In the first one, only one stiffness modulus is taken into account in the linear range of strains and in the second one two moduli are recognized in the same region. For the inelastic range of deformation the Bodner-Partom law parameters control the curve trajectory in both concepts.
- For the technical fabrics the greatest influence on simulation curve of the Bodner-Partom model have the coefficient for isotropic hardening m_1 and the strain rate sensitivity parameter n.
- Comparative analysis of the NOT USED and USED VALMEX fabric has shown very good mechanical performance of the samples exposed outdoor for about 20 years. In the case of uniaxial tensile tests, the ultimate tensile strength (*UTS)* and elongation at break (ε_{ult}) has decreased for 9% and 14% for the warp direction for the USED material. For the fill direction very little change has been detected. In the case of biaxial tests, the same parameters (*UTS,* ε_{ult}*)* have got values of 23% and 14% for the warp direction and 10% and 18% for the fill direction.
- The environmental ageing has influenced mostly the coating material of PVC, as its stiffness has raised for the USED samples for about 32% comparing to the NOT USED ones.
- The stiffness of polyester yarns have stayed unchanged under the environmental ageing for both material directions. It proves that the polyester is either resistant to the ageing or that PVC sufficiently protects the polyester yarns from outdoor unfavorable conditions.
- The environmental ageing has great impact on the parameters E_1, E_2, η_1 of the Burgers model. No ageing influence on the coefficient η_2 has been recognized and therefore it can be neglected in the ageing analysis of the VALMEX fabric.
- The analysis of the artificial ageing of the AF9032 fabric has shown, that the thermal ageing has influenced mostly the behavior of PVC coating, which has become more rigid and brittle over time.

- The technical fabric AF9032 has also shown to be more prone to the accelerated ageing at elevated temperatures for the fill direction than for the warp direction. It stay in accordance with observations made before for the natural ageing of the VALMEX fabric.
- Another interesting observation is that almost all strength parameters for AF9032 fabric change over time with linear dependency for temperatures of 80° and 90°C.
- The development of the Bodner-Partom model parameters identified on samples artificially aged has exposed the same decreasing (or increasing) tendencies for both temperatures of 80° and 90°C for the fill direction. Regarding the warp direction, some discrepancies have been observed. It suggests that behavior in the fill direction of the analyzed fabric is more predictable when subjected to thermal treatment.
- All of the Bodner-Partom parameters evolution over time can be easily approximated by linear functions with very good correlation. This finding can be used for modelling behavior of the fabric material in the numerical calculations for the elasto-viscoplastic range in the form of linear dependence of temperature and time.
- The results of the thermal ageing have been extrapolated for much longer time periods using the Arrhenius methodology. The correctness of this approach has been tested by superposition of the results obtained for temperature of 80° and 90°C. It has been noticed that most of the piecewise and Bodner—Partom model parameters for the fill direction subjected to the thermal ageing follow the Arrhenius relation. In the case of the warp direction none clear tendency can be distinguished. However, in order to draw profound conclusions the more comprehensive investigation is required.
- The low values of the correlation coefficient in some regressions has been caused mainly by the small number of experimental points taken for the identification. Sometimes different type of the approximation function should be considered (this will be the subject of the future research)
- The assumed at the beginning of the research thesis (given in chapter 1.2) has been partially confirmed. The most constitutive parameters are affected by aging. On the other hand there are some parameters which are “rigid” on the aging effect (e.g. η_2 in the Burges model)

8 References

[1] Ageing of composites. Martin R. editor. CRC Press LLC; 2008.

[2] Air, Tent & Tensile Structures, 2013 Fabric Specifier's Guide, *Fabric Architecture* 2013.

[3] Albuquerque AC, Kuruvilla J, Carvalho LH, d'Almeida JRM. Effect of wettability and ageing conditions on the physical and mechanical properties of uniaxially oriented jute-roving-reinforced polyester composites. *Compos. Sci.Technol.* 2000; 60: 833-844.

[4] Allaoui S, Hivet G, Wendling A, Ouagne P, Soulat D. Influence of the dry woven fabrics meso-structure on fabric/fabric contact behaviour. *J Compos Mater* 2012; 46(6): 627–639.

[5] Ambroziak A, Kłosowska D, Kłosowski P. Obliczenia statyczne. Projekt Budowlany. Opera Leśna - Sopot. Tom III A. Konstrukcje Przekrycie Dachowe. Gdańsk; 2005.

[6] Ambroziak A, Kłosowski P. *Constitutive modelling and computation of technical woven fabric using MSC.Marc*. VIII Konferencja Naukowo-Techniczna Programy MES w Komputerowym Wspomaganiu Analizy, Projektowania i Wytwarzania. Rynia-Polska (2003).

[7] Ambroziak A, Kłosowski P. Mechanical properties of polyvinyl chloride-coated fabric under cyclic tests. *J Reinf Plast Compos* 2014, 33:225-234.

[8] Ambroziak A, Kłosowski P. Mechanical properties for preliminary design of structures made from PVC coated fabric. *Constr. Build. Mater.* 2014; 50:74–81.

[9] Ambroziak A, Kłosowski P. Mechanical testing of technical woven fabrics. *J. Reinf. Plast. Compos.* 2013; 32 (10): 726–739.

[10] Ambroziak A, Kłosowski P. Review of constitutive models for technical woven fabrics in finite element analysis. *AATCC Review* 2011; 11(3): 58-67.

[11] Ambroziak A. Geometrycznie nieliniowa analiza membran stosowanych do konstrukcji przekryć wiszących z uwzględnieniem różnych typów związków konstytutywnych. Rozprawa doktorska, 2006, Gdańsk University of Technology

[12] Ambroziak A. Mechanical properties of Precontraint 1202S coated fabric under biaxial tensile test with different load ratios. *Constr. Build. Mater.* 2015; 80: 210–224.

[13] Andersson H. An implicit formulation of the Bodner–Partom constitutive equations. *Comput. Struct.* 2003; 81: 1405–1414.

[14] Andjelković D, Rajaković N. A new accelerated aging procedure for cable life tests. *Electr. Pow. Syst. Res.* 1996; 36: 13-19.

[15] Argyris J, Doltsinis ISt, Silva VD. Constitutive modeling and computation of non-linear viscoelastic solids. Part I: Rheological models and numerical integration techniques. *Comput. Meth Appl. Mech. Eng.* 1992; 98:135–63.

[16] Argyris J, Doltsinis ISt, Silva VD. Constitutive modelling and computation of non-linear viscoelastic solids Part II. Application to orthotropic PCV-coated fabric. *Comput. Meth. Appl. Mech. Eng.* 1992; 98 (7): 159–226.

[17] Arrhenius SA. Über die Dissociationswärme und den Einflusß der Temperatur auf den Dissociationsgrad der Elektrolyte. *Z. Physik. Chem.* 1889; 4: 96–116.

[18] Arrhenius SA. Über die Reaktionsgeschwindigkeit bei der Inversion von Rohrzucker durch Säuren. *Ibid.* 1889. 4: 226–248.

[19] ASTM D1204-14, Standard Test Method for Linear Dimensional Changes of Nonrigid Thermoplastic Sheeting or Film at Elevated Temperature, ASTM International, West Conshohocken, PA; 2014.

[20] ASTM D3746-85(2008), Standard Test Method for Impact Resistance of Bituminous Roofing Systems, ASTM International, West Conshohocken, PA; 2008.

[21] ASTM D-4434. Standard Specification for Polyvinyl Chloride Sheet Roofing. ASTM International; 1985.

[22] ASTM D4533 / D4533M-15, Standard Test Method for Trapezoid Tearing Strength of Geotextiles, ASTM International, West Conshohocken, PA; 2015.

[23] ASTM D570-98(2010)e1, Standard Test Method for Water Absorption of Plastics, ASTM International, West Conshohocken, PA, 2010

[24] ASTM D751-00, Standard Test Methods for Coated Fabrics, ASTM International, West Conshohocken, PA; 2000.

[25] Atkins P, De Paula J. Physical Chemistry (8th ed.). W.H. Freeman and Company; 2006.

[26] Atlas SunSpots, Material Testing Product and Technology News 2010, 40 (88).

[27] Audourin L, Dalle B, Metzger G, Verdu J. Thermal aging of plasticized PVC. I. Weight loss kinetics in the PVC-didecylphthalate system. *J. Appl. Polym. Sci.* 1992; 45: 2091-6.

[28] Audourin L, Dalle B, Metzger G, Verdu J. Thermal aging of plasticized PVC. II. Effect of plasticizer loss on electrical and mechanical properties. *J. Appl. Polym. Sci.* 1992; 45: 2097-103.

[29] Bailey DM, Foltz SD., Rossiter WJ, Lechner JA. Performane of polyvinyl chloride (PVC) roofing: results of ten-year field study. In: Proceedings of the Fourth International Symposium on Roofing Technology, Gaithersburg, USA; 1997.

[30] Bakar M. Własności mechaniczne materiałów polimerowych. Radom: Wydawnictwo Politechniki Radomskiej; 2000.

[31] Beer HR, Delgado AH, Paroli RM, Graveline S. Durability of PVC Roofing Membranes - Proof by Testing After Long Term Field Exposure. 10DBMC International Conference On Durability of Building Materials and Components, Lyon, France; 2005.

[32] Beer HR. Durability of PVC Roof Membranes – Field Investigation and Laboratory Testing After Up to 34 Years Exposure. ICBEST Symposium, Sydney, Australia; 2004

[33] Berdahl P, Akbari H, Levinson R, Miller WA. Weathering of roofing materials – An overview. *Constr. Build. Mater*. 2008; 22: 423–433.

[34] Bernstein R, Derzon DK, Gillen KT. Nylon 6.6 accelerated aging studies: thermal-oxidative degradation and its interaction with hydrolysis. *Polym. Degrad. Stabil.* 2005; 88: 480-488.

[35] Bjork F., Granne F. Roof membranes—The Swedish practice in light of EOTA TB 97/24/9.3.1 PT3. *Mater. Struct.* 2000; 33 (5): 270-277.

[36] Bles G, Nowacki WK, Tourabi A. Experimental study of the cyclic visco-elasto-plastic behaviour of a polyamide fibre strap. *Int. J. Solids Struct.* 2009; 46: 2693–2705.

[37] Bodner SR, Partom Y. Constitutive equations for elastic–viscoplastic strain-hardening materials. *J. Appl. Mech. ASME* 1975; 42: 385–389.

[38] Bodner SR. Evolution Equations for Anisotropic Hardening and damage of Elastic-Viscoplastic Materials. In: Saczak A, Biandsi G, editors. *Plastic Today*, Barking: Elsevier, 1985, p. 471-482.

[39] Bodner SR. Review of a Unified Elastic-Viscoplastic Theory. In Miller K, editor. Unified Constitutive Equations for Creep and Plasticity. *Appl. Sci.* 1987: 273-301.

[40] Bodner SR. Unified Plasticity – an Engineering Approach. Final Report. Faculty of Mechanical Engineering. Technion – Israel Institute of Technology Haifa; 2000.

[41] Bodner, SR, Partom Y. Constitutive equations for elastic–viscoplastic strain-hardening materials. *J. Appl. Mech.* 1985; 42: 385–389.

[42] Boisse P, Borr M, Buet K, Cherouat A. Finite element simulations of textile composite forming including the biaxial fabric behavior. *Compos. Pt. B-Eng*. 1997; 28B: 453–464.

[43] Boisse, P, Buet K, Gasser A, Launay J. Meso/macro-mechanical behavior of textile reinforcements for thin composites. *Compos. Sci. Technol.* 2001; 61(3): 395–401.

[44] Boubaker BB., Haussy B, Ganghoffer JF. Consideration of the yarn–yarn interactions in meso/macro discrete model of fabric Part II: Woven fabric under uniaxial and biaxial extension. *Mech. Res. Commun.* 2007; 34: 371–378.

[45] Boxhammer J. Shorter test times for thermal- and radiation-induced ageing of polymer materials 1: Acceleration by increased irradiance and temperature in artificial weathering tests. *Polym. Test.* 2001; 20: 719–724.

[46] Branicki Cz. *Niektóre zagadnienia statyki siatek cięgnowych*. Praca doktorska, Politechnika Gdańska, 1969.

[47] Branicki Cz., Kłosowski P. *Analiza statyczna wiszących przekryć tekstylnych w zakresie nieliniowym.* Archiwum Inżynierii Lądowej 1983; 3: 189–220.

[48] Brebu M, Vasile C, Antonie SR, Chiriac M, Precup M, Yang J, Roy C. Study of the natural ageing of PVC insulation for electrical cables. *Polym. Degrad. Stabil.* 2000; 67: 209-221.

[49] Bridgens B, Birchall M. Form and function: The significance of material properties in the design of tensile fabric structures. *Eng. Struct.* 2012; 44: 1–12.

[50] Bridgens B, Gosling PD. Direct stress–strain representation for coated woven fabrics *Comput. Struct* 2004; 82: 1913–1927.

[51] Bridgens B. Architectural fabric properties: determination, representation & prediction. PhD Thesis, Newcastle University; 2005.

[52] Brinson LC, Gates TS. Effects of physical aging on long term Creep of polymers and polymer matrix composites. *Inf. J. Solids Struct.* 1995; (32) 617: 827-846.

[53] Brzozowska-Stanuch A, Rabiej S, Sarna E, Maślanka M. Wpływ promieniowania UV na właściwości poliamidu PA6 - metody starzenia materiałów polimerowych. In Wróbel G. editor. Polimery i kompozyty konstrukcyjne. Cieszyn: Logos Press; 2010, p. 48-57.

[54] Buet-Gautier K, Boisse P. Experimental analysis and modelling of biaxial mechanical behaviour of woven composite reinforcements. *Exp. Mech.* 2001; 3: 260–269.

[55] Building materials in civil engineering. Zhang H. editor. Woodhead Publishing Limited and Science Press; 2011.

[56] Bystritskaya EV, Pomerantsev AL, Rodionova OY. Prediction of the aging of polymer materials. *Chemometr. Intell. Lab.* 1999; 47: 175–178.

[57] Cao J, Akkerman R, Boisse P, Chen J, Cheng HS, de Graaf EF, Gorczyca JL et al. Characterization of mechanical behavior of woven fabrics: Experimental methods and benchmark results. *Compos. Pt. A-Appl. Sci. Manuf.* 2008; 39: 1037–1053.

[58] Cash C. Comparative Testing and Rating of Thirteen Thermoplastic Single Ply Roofing Materials, Interface, *Journal of the Roof Consultants Institute* 1999.

[59] Cash G, Bailey DM, Davies AG, Delgado AH, Niles DL, Paroli RM. Predictive Service Life Tests for Roofing Membranes. In: Proceedings of 10DBMC International Conference On Durability of Building Materials and Components Lyon, France, 17-20 April 2005

[60] Chan KS, Bodner SR, Lindholm US. Phenomenological modeling of hardening and thermal recovery in metals. *J. Eng. Mater. Technol.* 1988; 110: 1–8.

[61] Chan KS, Bodner SR, Lindholm US. Phenomenological modeling of hardening and thermal recovery in metals. *J. Eng. Mater.-T. ASME* 1988; 110: 1–8.

[62] Chapra SC, Canale RP. Numerical methods for engineers. New York: McGraw-Hill Inc., 1988.

[63] Chatree H, Thanate R, Wiriya T. Time–temperature and stress dependent behaviors of composites made from recycled polypropylene and rubberwood flour. *Constr. Build. Mater.* 2014; 66: 98–104.

[64] Chazal CF, Pitti RM. An incremental constitutive law for ageing viscoelastic materials: a three-dimensional approach. *C. R. Mec.* 2009; 337 (1): 30-33.

[65] Chen J, Hou H and Chen W. Study on deformation performance of PVC membrane materials under biaxial cyclic tensile loads. *Adv Mater Res* 2012; 479–481: 36–40.

[66] Chen SF., Hu JL, Teng JG. A finite-volume method for contact drape simulation of woven fabrics and garments. *Finite Elem. Anal. Des.* 2001; 37: 513–531.

[67] CIB W080 / RILEM 175 SLM Service Life Methodologies Prediction of Service Life for Buildings and Components. State of the Art Reports. CIB report publication 294; 2004.

[68] CIB W080 WG3 test methods for service life prediction. State of the art report on accelerated laboratory test procedures and correlation between laboratory tests and service life data. Rotterdam: CIB Publication 331; 2010.

[69] Crenshaw VA, Koontz JD. Simulated Hail Damage and Impact Resistance Test Procedures for Roof Coverings and Membranes. *RCI Interface* 2001; 19 (5): 5-10.

[70] Croll SG, Shi X, Fernando BMD. The interplay of physical aging and degradation during weathering for two crosslinked coatings. *Prog. Org. Coat.* 2008; 61: 136–144.

[71] Davies P, Evrard G. Accelerated ageing of polyurethanes for marine applications. *Polym Degrad Stabil* 2007; 92: 1455-1464.

[72] Deflorian F, Rossi S, Fedel M. Organic coatings degradation: Comparison between natural and artificial weathering. *Corros Sci* 2008; 50: 2360–2366.

[73] Deflorian F, Rossi S, Fedrizzi L, Zanella C. Comparison of organic coating accelerated tests and natural weathering considering meteorological data. *Prog. Org. Coat.* 2007*;* 59: 244–250.

[74] DIN16726, 1983-05, Beuth Verlag, Berlin, Germany; 1983.

[75] Drozdov AD. A model for the long-term viscoelastic behavior of aging polymers. *Polymer* 1998; 39 (6-7): 1327-1337.

[76] Durability of Building Materials and Components. Freitas VP, Delgado JMPQ, editors. Springer; 2013

[77] Durability of Building Materials and Components. In: Baker JM, Davies H, Majumdar AJ, Nixon PJ, editors. Proceedings of the Fifth International Conference, Routledge; 2006.

[78] Durability of Building Materials and Components 7. Vol. 2 Testing, Design and Standardization. Sjostrom C, editor. Taylor & Francis; 2006.

[79] Durability of Building Materials and Components. Baker JM, Davies H, Majumdar AJ, Nixon PJ, editors. Taylor & Francis; 1990.

[80] Durability of Building Materials and Components (1980). In: Sereda, PJ, Litvan, GG, editors. ASTM International 1980.

[81] *Dziennik Bałtycki* 2 November 2007.

[82] Elsayed EA. Reliability engineering. Massachusetts: Addison-Wesley; 1996.

[83] Ferhoum R, Aberkane M, Oulai MO. Modelling of thermal ageing effect on elastic-viscoplastic behaviour of semi-cristallin polymers by D.N.L.R approach. *Procedia Engineering* 2011; 10: 1815–1822.

[84] Findley WN, Lai JS, Onaran K, Creep and relaxation of nonlinear viscoelastic materials, North-Holland, Amsterdam-New York-Oxford; 1976.

[85] Fish J, Shek K. Computational plasticity and viscoplasticity for composite materials and structures. . *Compos. Pt. B-Eng.* 1998; 29B: 613–619.

[86] Foley FJ, Koontz JD, Valaltis JK. Aging and Hail Research of PVC Membranes. In 12th International Roofing and Waterproofing Conference Exploring Tomorrow's Technology Today. Orlando, USA; 2002, p. 1-25.

[87] Foltz S, Bailey DM. Polivinyl Chloride (PVC) Roofing: Preliminary Field Test Results. In: ASTM STP 1088, Wallace TJ, Rossiter WJ, editors. Roofing Research and Standards Development: Second Volume, ASTM: 1990; p. 63-81.

[88] Freitas VP, Corvacho H, Quintela M, Delgado JMPQ. Assessing the durability of mortars tiles – A contribution for a prediction model. *Eng. Fail. Anal.* 2014; 44: 36–45.

[89] Gac PY, Saux V, Paris M, Marco Y. Ageing mechanism and mechanical degradation behaviour of polychloroprene rubber in a marine environment: Comparison of accelerated ageing and long term exposure. *Polym. Degrad. Stabil.* 2012; 97: 288-296.

[90] Galliot C, Luchsinger RH. A simple model describing the non-linear biaxial tensile behaviour of PVC-coated polyester fabrics for use in finite element analysis *Compos. Struct.* 2009; 90: 438–447.

[91] Gillen KT, Bernstein R, Derzon DK. Evidence of non-Arrhenius behaviour from laboratory aging and 24-year field aging of polychloroprene rubber materials. *Polym. Degrad. Stabil.* 2005 87: 57-67.

[92] Gillen KT, Celina M, Clough RL, Wise J. Extrapolation of accelerated aging data - Arrhenius or erroneous? *Trends Polym Sci* 1997; 5:250-7.

[93] Gommers, B, Verpoest I, Van Houtte P. Modelling the elastic properties of knitted-fabric-reinforced composites. *Compos. Sci. Technol.* 1996; 56: 685–694.

[94] Graveline S, Beer HR., Paroli RM., Delgado AH. Field Investigation and Laboratory Testing of Exposed Poly(vinyl Chloride) Roof Systems. RCI 20th International Convention and Trade Show, Miami, USA; 2005.

[95] Guedes RM, Morais JJL, Marques AT, Cardon AH. Prediction of long-term behaviour of composite materials. *Comput. Struct.* 2000; 76: 183-194.

[96] Guedes RM. Lifetime predictions of polymer matrix composites under constant or monotonic load", *Compos. Part A-Appl. S* 2006; 37: 703–715.

[97] Guermazi N, Elleuch K, Ayedi HF, Kapsa PH. Aging effect on thermal, mechanical and tribological behaviour of polymeric coatings used for pipeline application. *J. Mater. Process Tech.* 2008; 203: 404–410.

[98] Guermazi N, Elleuch K, Ayedi HF. The effect of time and aging temperature on structural and mechanical properties of pipeline coating. *Mater. Design* 2009; 30: 2006–2010.

[99] Gumargalieva KZ, Ivanov VB, Zaikov GE, Moiseev JV, Pokholok TV. Problems of ageing and stabilization of poly(vinyl chloride). *Polym. Degrad. Stabil.* 1996; 52: 73-79.

[100] Haillant O. Accelerated weathering testing principles to estimate the service life of organic PV modules. *Sol Energ Mat Sol C* 2011; 95:1284–1292.

[101] Hakkarainen M. New PVC materials for medical applications—the release profile of PVC/polycaprolactone–polycarbonate aged in aqueous environments. *Polym. Degrad. Stabil.* 2003; 80: 451–458.

[102] Hamby DM. A review of techniques for parameter sensitivity analysis of environmental models. *Environ. Monit. Assess.* 1994; 32(2): 135-154.

[103] Hassine MB, Naït-Abdelaziz M, Zaïri F, Colin X, Tourcher C, Marque G. Time to failure prediction in rubber components subjected to thermal ageing: A combined approach based upon the intrinsic defect concept and the fracture mechanics. *Mech. Mater.* 2014; 79: 15-24.

[104] Houtman R, M. Orpara, *Bauen mit Textilien* 2000; 4 (3): 27-32.

[105] Howard JB, Gilroy HM. Long-term behaviour of stabilized polyethylene. *Polym. Eng. Sci.* 1975; 15: 268-71.

[106] http://bart.sopot.pl

[107] http://www.architecturalfabrics.com/product-data/9032.php

[108] http://www.instron.com

[109] http://www.mehler-texnologies.com

[110] http://www.webbaviation.co.uk

[111] http://www.zwick.de

[112] htttp://www.britannica.com

[113] Hu H, Sun CT. The characterization of physical aging in polymeric composites. *Compos. Sci. Technol.* 2000; 60: 2693-2698.

[114] Huang S, Khan AS. Modeling the Mechanical Behavior of 1100-0 Aluminum at Different Strain Rates by the Bodner-Partom Model. *Int. J. of Plasticity* 1992, 8: 501-512.

[115] Hukins DWL, Mahomed A, Kukureka SN. Accelerated aging for testing polymeric biomaterials and medical devices. *Med. Eng. Phys.* 2008; 30: 1270–1274.

[116] Hutchinson J. M. Physical aging of polymers. *Prog. Polym. Sci*. 1995; 20: 703-760.

[117] ISO 13934: Textiles - Tensile properties of fabrics - Part 1: Determination of maximum force and elongation at maximum force using the strip method; Part 2: Determination of maximum force using the grab method; 1999.

[118] ISO 13935: 2014. Textiles - Seam tensile properties of fabrics and made-up textile articles - Part 1: Determination of maximum force to seam rupture using the strip method; Part 2: Determination of maximum force to seam rupture using the grab method.

[119] ISO 13937: 2000. Textiles - Tear properties of fabrics - Part 2: Determination of tear force of trouser-shaped test specimens (Single tear method); Part 3: Determination of tear force of wing-shaped test specimens (Single tear method); Part 4: Determination of tear force of tongue-shaped test specimens (Double tear test).

[120] ISO 14040:2006: Environmental management - Life cycle assessment - Principles and framework. 2006

[121] ISO 1421:2001 Fabrics coated with rubber or plastics – determination of breaking strength and elongation at break.

[122] ISO 1421:2001: Fabrics coated with rubber or plastics – determination of breaking strength and elongation at break; 2001.

[123] ISO 15686-2: 2012 Buildings and constructed assets—Service life planning—Part 2: Service life prediction procedures

[124] Ito M, Nagai K. Analysis of degradation mechanism of plasticized PVC under artificial aging conditions. *Polym. Degrad. Stabil.* 200; 92: 260-270.

[125] Ivanov I, Tabiei A. Three–dimensional computational micro–mechanical model for woven fabric composites. *Compos. Struct.* 2001; 54: 489–496.

[126] Ives DJG. Chemical Thermodynamics. University Chemistry: Macdonald Technical and Scientific; 1971.

[127] Jakowluk A. Procesy pełzania i zmęczenia w materiałach. Warszawa: WNT; 1993.

[128] Jakubowicz I Effects of artificial and natural ageing on impact-modified poly(vinyl chloride) (PVC). *Polym. Test.* 2001; 20: 545–551.

[129] Jakubowicz I, Yarahmadi N, Gevert T Effects of accelerated and natural ageing on plasticized polyvinyl chloride (PVC), *Polym Degrad Stabil* 1999; 66: 415-421.

[130] Jelle BP. Accelerated climate ageing of building materials, components and structures in the laboratory. *J. Mater. Sci.* 2012; 47:6475–6496.

[131] Jensen JJ. Eine Statische und Dynamische Unterschung der Seil und Membrantragwerke. Division of Structural Mechanics, The Technical University of Norway; 1970.

[132] Johnson W, Mellor PB. *Engineering plasticity*. London: Van Nostrand Reinhold Co.; 1973.

[133] Kahlen S, Jerabek M, Wallner GM, Lang RW. Characterization of physical and chemical aging of polymeric solar materials by mechanical testing. *Polym. Test* 2010; 29: 72–81.

[134] Karayaka M, Kurath P. Deformation and failure behaviour of woven composite laminates. *J. Eng. Mater. Technol.* 1994; 116: 222–232.

[135] Kato S, Yoshiro T, Minami H. Formulation of constitutive equations for fabric membranes based on the concept of fabric lattice model. *Eng. Struct.* 1999; 21: 691–708.

[136] Kawabata S, Niwa M, Kawai H. The finite deformation theory of plain weave fabrics. Part I: The biaxial deformation theory. *J. Text. Inst.* 1973; 64 (1): 21–46.

[137] Kawabata S, Niwa M, Kawai H. The finite deformation theory of plain weave fabrics. Part III: The shear deformation theory. *J. Text. Inst.* 1973; 64 (2): 62–85.

[138] Kawabata S, Niwa M, Kawai H. The finite deformation theory of plain weave fabrics. Part II: The uniaxial deformation theory. *J. Text. Inst.* 1973; 64 (2): 47–61.

[139] Kazakiewicz MI, Miełaszwili JK,Sułabierdze OG. Aerodynamika dachów wiszących. Warszawa*:* Arkady; 1988.

[140] Kim JK, Yu W-R, Kim SM. Anisotropic creep modeling of coated textile membrane using finite element analysis *Compos. Sci. Technol* 2008; 68: 1688–1696.

[141] King MJ., Jearanaisilawong P, Socrate S. A continuum constitutive model for the mechanical behavior of woven fabrics. *Int. J. Solids Struct.* 2005; 42: 3867–3896.

[142] Kłosowski P, Komar W, Woźnica K. Finite element description of nonlinear viscoelastic behaviour of technical fabric, *Constr. Build. Mater*. 2009; 23: 1133–1140.

[143] Kłosowski P, Woznica K. *Nieliniowe lepkoplastyczne prawa konstytutywne w wybranych zastosowaniach analizy konstrukcji*. Gdańsk: Wydawnictwo Politechniki Gdańskiej; 2007.

[144] Kłosowski P, Zagubień A, Woźnica K. Investigation on rheological properties of technical fabric "Panama". *Arch. Appl. Mech.* 2004; 73: 661-681.

[145] Kłosowski P, Zagubień A, Woźnica K. Investigation on rheological properties of technical fabric Panama. *Arch. Appl. Mech.* 2004; 73: 661-681.

[146] Kłosowski P, Zagubień A. Analysis of Material Properties of Technical Fabric for Hanging Roofs and Pneumatic Shells. *Arch. Civil Eng.* 2003; 3 (3): 277-294.

[147] Kłosowski P. Identyfikacja lepkosprężystego modelu Burgersa dla Poliwęglanu. Nowe kierunki rozwoju mechaniki. Hucisko 2011

[148] Kohlrausch R. Nachtrag tiber die elastische Nachwirkung beim Cocon- und Glasfaden, und die hygroskopische Eigenschaft des Ersteren. *Pogg. Ann. Phys.* 1847; 72(1): 393-425.

[149] Komeili, M, Milani, AS. The effect of meso-level uncertainties on the mechanical response of woven fabric composites under axial loading. *Comput. Struct.* 2012; 90–91: 163–171.

[150] Koontz JD Field evaluation and laboratory testing of PVC roof systems. In: Proceedings of Fourth International Symposium on Roofing Technology, NRCA, Gaithersburg, MD; 1999, p. 22-27.

[151] Kroupa JL, Bartsch M. Influence of viscoplasticity on the residual stress and strength of a titanium matrix composite after thermomechanical fatigue. *Compos. Pt. B-Eng.* 1998; 29B: 633–642

[152] Krzemiński J. Konstrukcje powłokowe. Kształtowanie geometryczne przekryć. Informator Projektanta Przemysłowego nr 45, Warszawa; 1963.

[153] Kuwazuru O, Yoshikawa N. New concept of pseudo-continuum model for plain-weave fabric. Proceedings of the 33rd International SAMPE Technology Conference, Seattle; 2001: p. 564–573.

[154] Kuwazuru O, Yoshikawa N. Theory of Elasticity for Plain-Weave Fabrics. 1st Report, New Concept of Pseudo-Continuum Model. *JSME Int. J.* 2004; A 47: 17–25.

[155] Kuwazuru O., Yoshikawa N.: Theory of Elasticity for Plain-Weave Fabrics (2nd Report, Finite Element Formulation. *JSME Int. J.* 2004; A 47: 26–34.

[156] Lacasse MA. Advances in service life prediction - an overview of durability and methods of service life prediction for non-structural building components. In: Proceedings of the Annual Australasian Corrosion Association Conference. Wellington NZ; 2008, p. 1-13

[157] Laiarinandrasana L, Gaudichet E, Oberti S, Devilliers C. Effects of aging on the creep behaviour and residual lifetime assessment of polyvinyl chloride (PVC) pipes. *Int. J. Pressure Vessels Pip.* 2011; 88: 99-108.

[158] Launay J, Hivet G, Duong AV, Boisse P. Experimental analysis of the influence of tensions on in plane shear behaviour of woven composite reinforcements. *Compos. Sci. Technol.* 2008; 68: 506–515.

[159] Le Gac PY, Le Saux V, Paris M, Marco Y. Ageing mechanism and mechanical degradation behaviour of polychloroprene rubber in a marine environment: Comparison

of accelerated ageing and long term exposure. *Polym. Degrad. Stabil.* 2012; 97: 288-296.

[160] Lemaitre J, Chaboche JL. Mechanics of solid materials. London: Cambridge University Press; 1990.

[161] Lemaitre J. A course on damage mechanics. Berlin: Springer; 1996.

[162] Levenberg K. Method for the Solution of Certain Non-Linear Problems in Least Squares. *Q. Appl. Math.* 1944; 2: 164–168.

[163] Leveque D, Schieffer A, Mavel A, Maire JF. Analysis of how thermal aging affects the long-term mechanical behavior and strength of polymer–matrix composites. *Compos. Sci. Technol.* 2005; 65: 395–401.

[164] Lewin M, Pearce EM. Fiber Chemistry: Handbook of Fiber Science and Technology (IV). Marcel Dekker Inc.; 1985

[165] Linde R, Belder EG, Perera DY. Effect of physical aging and thermal stress on the behavior of polyester/TGIC powder coatings. *Prog. Org. Coat* 2000; 40: 215–224.

[166] Lodi PC, Bueno BS, Vilar OM, Correia NS. Weathering degradation of polyester and polypropylene geotextiles. In: Geosynthetics in Civil and Environmental Engineering. Springer Berlin Heidelberg; 2009, p 35-39.

[167] Lounis Z, Lacasse MA, Vanier DJ, Kyle BR. Towards standardization of service life prediction of roofing membranes. In: Wallace TJ, Rossiter WJ, editors. Roofing Research and Standards Development. 4th Vol. ASTM; 1998.

[168] Marquardt D. An Algorithm for Least-Squares Estimation of Nonlinear Parameters. *SIAM J. Appl. Math.* 1963; 11 (2): 431–441.

[169] Martienssen W, Warlimont H. Handbook of Condensed Matter and Materials Data. Berlin: Springer; 2005.

[170] Mazza E, Papes O, Rubin MR, Bodner SR, Binur NS. Nonlinear Elastic-Viscoplastic Constitutive Equations for Aging Facial Tissues. *Biomech. Model. Mechanobiol*. 2005, 4 (2–3): 178–189.

[171] McCullough RL. Micro-models for composite materials: continuous fiber composites. In: Carlsson LA, Gillespie JW, editors. Delaware Composites Design Encyclopedia, vol. 2. Lancaster: Technomic Publishing Company, 1990; p. 49-90.

[172] Mehler Texnologies. Advertising catalogue 2012.

[173] Mercier J, Bunsell A, Castaing P, Renard J. Characterisation and modelling of aging of composites. *Compos Part A-Appl* 2008; 39: 428–438.

[174] Mora EP. Life cycle, sustainability and the transcendent quality of building materials. *Build. Environ*. 2007; 42: 1329–1334.

[175] Moreno V, Jordan EH. Prediction of material thermomechanical response with a unified viscoplastic constitutive model. *Int J Plasticity* 1986; 2: 223–45.

[176] Morland, LW, Lee EH. Stress analysis for linear viscoelastic materials with temperature variation. *Trans. Sot. Rheol.*1960; IV: 233-263.

[177] Mouzakis DE, Zoga H, Galiotis C. Accelerated environmental ageing study of polyester/glass fiber reinforced composites (GFRPCs). *Compos. Pt. B-Eng* 2008; 39: 467–475.

[178] NFPA 701 (2015): Standard Methods of Fire Tests for Flame Propagation of Textiles and Films.

[179] Ng S, Tse P, Lau K. Numerical and experimental determination of the in-plane elastic properties of 2/2 Twill weave fabric composites. *Compos. Pt. B-Eng*. 1998; 29B: 735–744.

[180] Nguyen-Tri P, El Aidani R, Leborgne E, Pham T, Vu-Khanh T. Chemical ageing of a polyester nonwoven membrane used in aerosol and drainage filter. *Polym. Degrad. Stabil.* 2014; 101: 71-80

[181] Ni J, Luo R-A, Chen Y-L, et al. Characteristics of architectural membrane materials under biaxial tensile loads. *Gongcheng Lixue*/*Eng. Mech.* 2009; 26: 100–104.

[182] Nordtest Method NT Build 495. 2000. Building materials and components in the vertical position: exposure to accelerated climatic strains.

[183] Nowacki W. Teoria pełzania. Warszawa: Arkady; 1963.

[184] Otto F. Dachy wiszące. Kształtowanie i konstrukcja. Warszawa: Arkady; 1959.

[185] Pargana JB, Lloyd-Smith D, Izzuddin BA. Advanced material model for coated fabrics used in tensioned fabric structures. *Eng. Struct.* 2007; 29: 1323–1336

[186] Paroli RM, Smith TL, Whelan BJ. Shattering of Unreinforced PVC Roofing Membranes: Problem Phenomenon, Causes and Prevention. In: Proceedings of the 10th Conference on Roofing Technology, National Roofing Contractors Association, Rosemont, USA; 1993.

[187] Peirce FT. The geometry of cloth structure. *J. Text. Inst.* 1937; 28 (3): 45–96.

[188] Peng X, Cao J. *A* Dual homogenization and finite element approach for material characterization of textile composites. *Compos. Pt. B-Eng*. 2002 33: 45–56.

[189] POLNAM Zakłady Konfekcji Technicznej. Raport parametry wytrzymałościowe tkaniny VALMEX FR 1000 Hallentype III Universal. Częstochowa; 1989.

[190] Potluri P, Thammandra VS. Influence of uniaxial and biaxial tension on meso-scale geometry and strain fields in a woven composite. *Compos. Struct.* 2007; 77: 405–418.

[191] Pyrz M, Zaïri F. Identification of viscoplastic parameters of phenomenological constitutive equations for polymers by deterministic and evolutionary approach. *Modell. Simul. Mater. Sci. Eng.* 2007, 15 (2): 85-103.

[192] Rabinovitch EB, Summers JW, Northcott WE. Changes in Properties of Rigid PVC During Weathering. *J Vinyl Technol.* 1993, 15 (4): 214-218.

[193] Rahouadj R, Cunat C. Physical Aging and glass transition of polymers. In: Handbook of Materials and Behavior models. Burlington: Academic Press; 2001.

[194] Rattensperger H, Eberhardsteiner J, Mang HA. Numerical investigation of high pressure hydraulic hoses with steel wire braid. In: IUTAM Symposium on Computational Mechanics of Solid Materials at Large Strains; 2003, p. 407–416.

[195] Raun X, Chou T. Experimental and theoretical studies of the elastic behavior of knitted fabric composites. *Compos. Sci. Technol. 1995;* 56: 1391–1403.

[196] Razak HA., Chua CS, Toyoda H. Weatherability of coated fabrics as roofing material in tropical environment. *Build. Environ. 2*004; 39: 87–92.

[197] Read BE, Dean GD, Tomlins PE, Lesniarek-Hamid JL. Physical aging and creep in PVC. *Polymers* 1992; 33(13): 2689-2698.

[198] Read BE, Tomlins PE, Dean GD. Physical aging and short-term creep in amorphous and semi-crystalline polymers. *Polymers* 1990; 31: 1204-15.

[199] Read BE. Creep of glassy polymers in the alpha- and beta-retardation region. Physical aging and nonlinear behaviour. *J. Rheol.* 1992; 36: 1719-1736.

[200] Real LP, Gardette JL. Ageing and characterisation of PVC-based compounds utilised for exterior applications in the building construction field 1: Thermal ageing. *Polym. Test.* 2001; 20: 779–787.

[201] Realff ML, Boyce MC, Backer S. A micromechanical model of the tensile behavior of woven fabric. *Text. Res. J.* 1997; 67 (6): 445–459.

[202] Rojek M. Metodologia badań diagnostycznych warstwowych materiałów kompozytowych o osnowie polimerowej. *Open Access Librar*y 2011; 2: 11-31.

[203] Rosato DV, Rosato MV. Plastic product material and process selection handbook. Kidlington, Oxford, UK: Elsevier; 2004.

[204] Rosenfiled MJ, Wilcoski J. Experimental Polivinyl Chloride (PVC) Roofing: Field Tests Results, TR M-87/04/ADA178193, USACERL; 1987.

[205] Rubin MB, Bodner SR. A three-dimensional nonlinear model for dissipative response of soft tissue. *Int. J. Solids Struct.* 2002; 39 (19): 5081-5099.

[206] Sagar TV, Potluri P, Hearle JWS. Mesoscale modelling of interlaced fibre assemblies using energy method. *Comput. Mater. Sci.* 2003; 28: 49–62.

[207] Saltelli A, Ratto M, Andres T, Campolongo F, Cariboni J, Gatelli D. et al. Global Sensitivity Analysis. The Primer. John Wiley & Sons; 2008.

[208] Sands CM. Rapid implementation of material models within finite element analysis. *Comput. Mater. Sci.* 2009; 47: 286–296.

[209] Sawant S, Muliana A. A thermo-mechanical viscoelastic analysis of orthotropic materials. *Compos. Struct.* 2008; 83: 61–72.

[210] Schapery RA. Correspondence principles and a generalized J integral for large deformation and fracture-analysis of viscoelastic media. *Int. J. Fract.* 1984; 25(3):195–223.

[211] Schapery RA. On the characterization of nonlinear viscolelastic materials. *Polym. Eng. Sci* 1969; 9(4):295–310.

[212] Schieffer A, Mairea JF, Leveque D. A coupled analysis of mechanical behaviour and ageing for polymer-matrix composites. *Compos. Sci. Technol.* 2002; 62: 543–549.

[213] Schwarzl F, Staverman AJ. Time-temperature dependence of linear viscoelastic behaviour. *J. Appl. Phys*. 1952; 23(8): 838-43.

[214] Scida D, Aboura Z, Benzeggagh ML. The effect of ageing on the damage events in woven-fibre composite materials under different loading conditions. *Compos. Sci. Technol.* 2002; 62: 551–557.

[215] Seaman RN, Bradenburg F. Utilization of vinyl-coated polyester fabrics for architectural applications. - Part 1. *Fabric Architecture* 2000.

[216] Seaman RN, Bradenburg F. Utilization of vinyl-coated polyester fabrics for architectural applications. - Part 1. *Fabric Architecture*, 2000.

[217] Shi D, Yang X, Wang Y. Improvement on the Modeling of Rate-Dependent Plasticity and Cyclic Hardening by Bodner-Partom Model. *Chin. J. Aeronaut.* 2005; 18 (1): 83-89.

[218] Shockey, DA, Elrich DC, Simons JW. Improved Barriers to Turbine Engine Fragments. Final Annual Report; 2002.

[219] SIA V280, 1986-12, Switzerland; 1986.

[220] Siginer, DA. Stability of non-linear constitutive formulations for viscoelastic fluids. New York: Springer; 2014.

[221] Sleiman M, Kirchstetter TW., Berdahl P, Gilbert HE, Quelen S, Marlot L et al. Soiling of building envelope surfaces and its effect on solar reflectance – Part II: Development of an accelerated aging method for roofing materials. *Sol Energ Mat Sol C* 2014; 122: 271–281.

[222] Sobotka Z. *Zavešenie střechy – konstrukce a navrhováni*. Praga; 1962.

[223] Song S-C, Duan Z-P, Tan D-W. The application of B-P constitutive equations in finite element analysis of high velocity impact. *Int. J. Solids Struct.* 2001; 38: 5215-5222.

[224] Stanuszek M. Computer Modelling of Cable Reinforced Membranes. *Comput. Assist. Mech. Eng. Sci. 2002;* 9: 223-237.

[225] Stanuszek M. FE analysis of large deformations of membranes with wrinkling. *Finite Elem. Anal. Des.* 2003; 39: 599– 618.

[226] Struik LCE. Physical Aging in Amorphous Polymers and Other Materials, Amsterdam: Elsevier Scientific Publications Co.; 1978.

[227] Sullivan, JL. Creep and physical aging of composites. *Comput. Sri. Tech.* 1990; 39: 207-232.

[228] Tabiei A, Ivanov I. Materially and geometrically non-linear woven composite micro-mechanical model with failure for finite element simulations. *Int. J. Non-Linear Mech.* 2004; 39: 175–188.

[229] Tabiei A, Jiang Y: Woven fabric composite model with material nonlinearity for nonlinear finite element simulation. *Int. J. Solids Struct.* 1999; 18: 2757–2771.

[230] Tanov RR, Brueggert M. Finite element modelling of non-orthogonal loosely woven fabrics in advanced occupant restraint systems. *Finite Elem. Anal. Des.* 2003; 39: 357–367.

[231] Tawfik SY, Asaad JN, Sabaa MW. Thermal and mechanical behaviour of flexible poly(vinyl chloride) mixed with some saturated polyesters", *Polym. Degrad. Stabil.* 2006; 91: 385-392.

[232] Taylor JR.: *Wstęp do analizy błędu pomiarowego.* Warszawa: Wydawnictwo Naukowe PWN; 1999.

[233] Villa KM, Krasny JF. Small-Scale Vertical Flammability Testing for Fabrics. *Fire Saf. J.* 1990; 6: 229-241.

[234] Vitruvius P, Morgan MH. Vitruvius: The ten books on architecture. New York: Dover Publications;1960.

[235] Wang JZ, Parvatareddy H, Chang T, Yyengar N, Dillart DA, Reifsnider KL. Physical aging behavior of high-performance composites. *Compos. Sci. Technol.* 1995; 54: 405-415.

[236] Wang Y, Meng J, Zhao Q, Qi S. Accelerated Ageing Tests for Evaluations of a Durability Performance of Glass-fiber Reinforcement Polyester Composites. *J. Mater. Sci. Technol.* 2010; 26(6): 572-576.

[237] Warren W. The large deformation elastic response of woven kevlar fabric. *Polym. Compos.* 1992, 13 (4): 278–284.

[238] Wei YT, Nasdala L, Rothert H, Xie Z. Experimental investigations on the dynamic mechanical properties of aged rubbers. *Polym. Test.* 2004; 23: 447–453.

[239] Whelan BJ, Graveline S, Delgado AH, Paroli RM. Field Investigation and Laboratory Testing of Exposed Poly(vinyl Chloride) Roof Systems. CIB World Building Congress, "Building for the Future", Toronto, Canada; 2004.

[240] White JR. Polymer ageing: physics, chemistry or engineering? Time to reflect. C. R. Chim. 2006; 9: 1396–1408.

[241] Wilczyński AP. Polimerowe kompozyty włókniste. Warszawa: WNT; 1996.

[242] Wilkes CE, Summers JW, Daniels CA, Berard MT in PVC Handbook. Hanser Verlag; 2005.

[243] Williams ML, Landel RF, Ferry JD. The temperature dependence of relaxation mechanism in amorphous polymers and other glass-liquids. *J. Am. Chem. Soc.* 1955; 77: 370.

[244] Wise J, Gillen KT, Clough RL. An ultrasensitive technique for testing the Arrhenius extrapolation assumption for thermally aged elastomers. *Polym. Degrad. Stabil.* 1995; 49: 403-418.

[245] Woźnica K, Kłosowski P. Evaluation of viscoplastic parameters and its application for dynamic behaviour of plates. *Arch. App. Mech.* 2000*;* 70: 561-570.

[246] Xing L, Taylor TJ. Correlating Accelerated Laboratory, Field, and Thermal Aging TPO Membranes. *J. ASTM Int.* 2011; 8 (8).

[247] Xu Y, Wu Q, Lei Y, Yao F. Creep behavior of bagasse fiber reinforced polymer composites. *Bioresour. Technol.* 2010; 101: 3280–3286.

[248] Xue P, Peng X, Cao J. A non-orthogonal constitutive model for characterizing woven composites *Compos. Pt. A-Appl. Sci. Manuf.* 2003; 34: 183–193.

[249] Yang TC, Wu JH, Noguchi T, Isshiki M. Methodology of accelerated weathering test through physicochemical analysis for polymeric materials in building construction. In: Materials Research Innovation, vol 18, suppl. 3, W.S. Maney&Son Ltd.; 2014.

[250] Yarahmadi N, Jakubowicz I, Gevert T. Determination of the potential for recycling of polymeric products found in buildings from the 1960s and 70's - a case study. *Int. J. Low Energy Sustain. Build.* 1999; 1.

[251] Yarahmadi N, Jakubowicz I, Martinsson L. PVC floorings as post-consumer products for mechanical recycling and energy recovery. *Polym. Degrad. Stabil.* 2003; 79: 439–448.

[252] Zagubień A. Badania laboratoryjne i identyfikacja niesprężystych właściwości materiałowych tkaniny powlekanej typu "PANAMA". Rozprawa doktorska, Politechnika Koszalińska; 2002.

[253] Zaïri F, Naït-Abdelaziz M, Woźnica K, Gloaguen J-M. Constitutive equations for the viscoplastic-damage behaviour of a rubber-modified polymer. *Eur. J. Mech. A-Solids* 2005; 24: 169–182.

[254] Żerdzicki K, Kłosowski P, Woźnica K. Application of the Bodner-Partom constitutive equations for modelling the technical fabric Valmex used for the hanging roof of the Forest Opera in Sopot. In: Pietraszkiewicz W, Gorski J, editors. *Shell structures: Theory and Applications*, Taylor & Francis; 2014, p. 579–582.

[255] Żerdzicki K, Woźnica K, Kłosowski P. Experimental research on technical fabric of the Forest Opera roof in Sopot. *Mach. Dyn. Res.* 2012, 36 (2): 136–145.

[256] Żerdzicki K. Właściwości mechaniczne poliwęglanu w różnych temperaturach. In A. Buchacz, editor. Badania i analizy wybranych zagadnień z budownictwa, Gliwice: Wydawnictwo Politechniki Śląskiej; 2011, p. 423-430.

[257] Zhang L, Ernst LJ, Brouwer HR. A study of nonlinear viscoelasticity of an unsaturated polyester resin. Part 1. Uniaxial model. *Mech. Mater*. 1997; 26: 141-166.

[258] Zhou Z, He Y, Hu H, Zhao F, Zhang X. Creep performance of PVC aged at temperature relatively close to glass transition temperature. *Appl. Math. Mech.* 2012; 33(9): 1129–1136.

[259] Żyliński T. *Metrologia włókiennicza, Tom I.* Warszawa: Wydawnictwo Przemysłu Lekkiego i Spożywczego; 1967.